Nanoscopic Materials

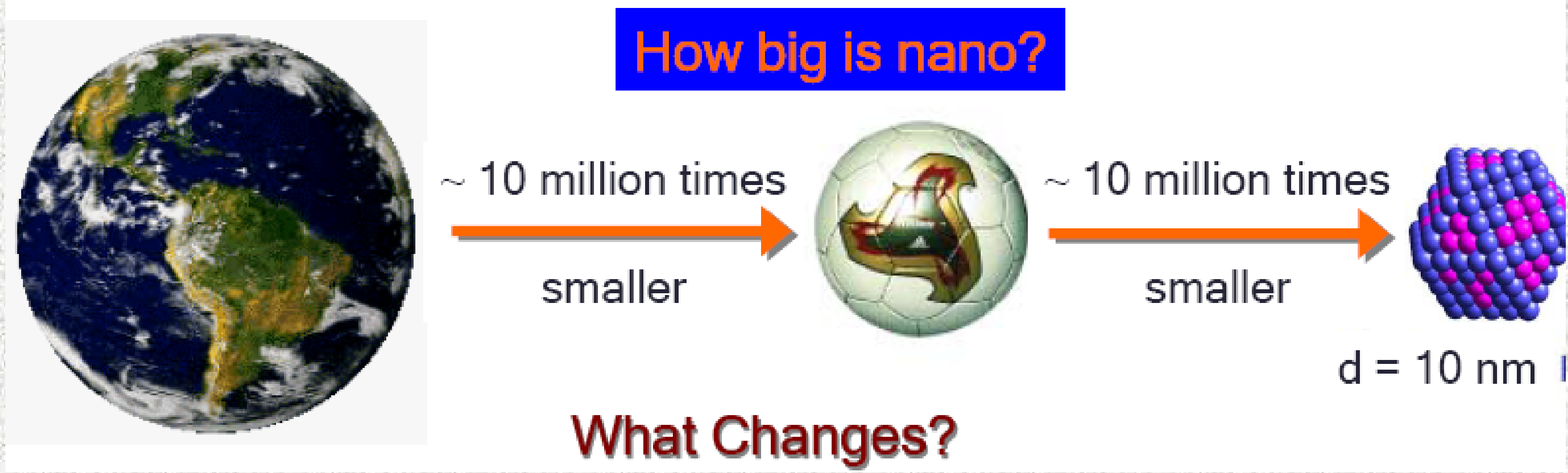

- **Chemical methods to change physical and chemical properties – composition, substituents,….**
- **Size is another variable to change physical and chemical properties for constant chemical composition**
- **Each physical property or fenomenon has a characteristic length**
- **When particle size is comparable to the characteristic length, property start to depend on the size**

Nanoscopic Materials

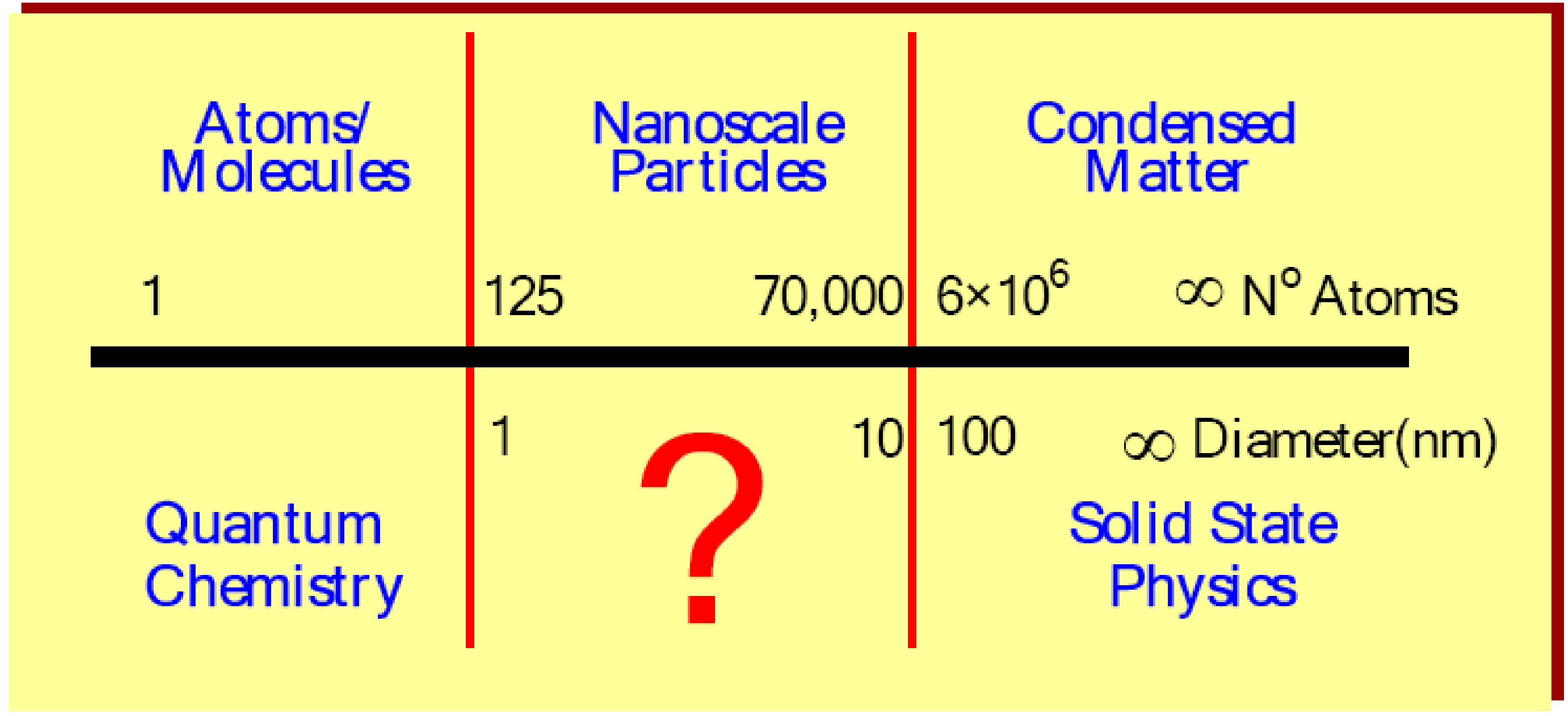

Atoms/ Molecules	Nanoscale Particles		Condensed Matter		
1	125	70,000	6×10^6	∞	N° Atoms
	1	10	100	∞	Diameter(nm)
Quantum Chemistry	?		Solid State Physics		

Nanoscopic Materials

Nanoparticles 1 – 100 nm

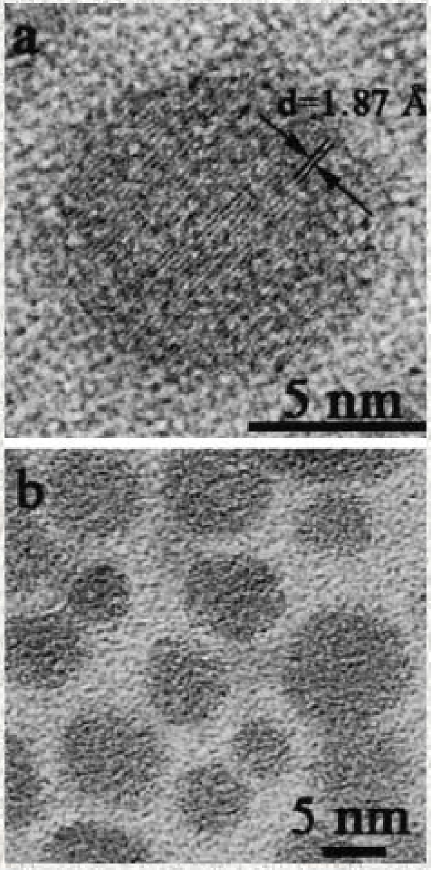

1 nm = 10^{-9} m

1 nm = 10 Å

Traditional materials > 1 µm

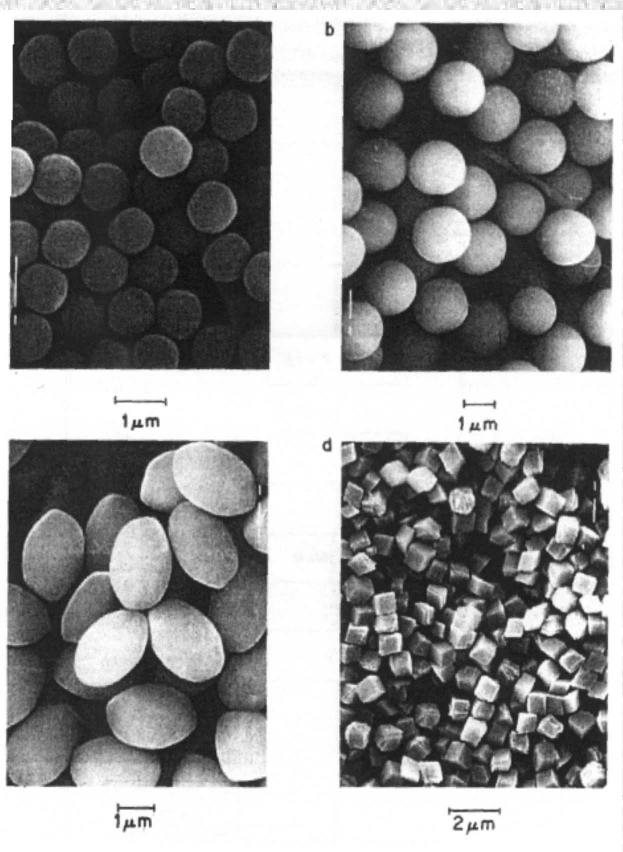

Nanoscopic Materials

Size 1 – 100 nm

EU definition (2011):

A natural, incidental or manufactured material containing particles, in an unbound state or as an aggregate or as an agglomerate and where, for 50% or more of the particles in the number size distribution, one or more external dimensions is in the size range 1 nm – 100 nm.

http://ec.europa.eu/environment/chemicals/nanotech/faq/definition_en.htm

Nanoscopic Materials

Nanoscale regime
Size 1 – 100 nm (traditional materials > 1 μm)

Physical and chemical properties depend on the size !!

Natural examples:
- ☯ **Human teeth, 1-2 nm fibrils of hydroxyapatite $Ca_5(PO_4)_3(OH)$ + collagen**
- ☯ **Asbestos, opals, calcedon**
- ☯ **Primitive meteorites, 5 nm C or SiC, early age of the Solar system**

Nanoscale objects have been around us, but only now we can observe them, manipulate and synthesize them.

Nanostructural Materials

“Prey”, the latest novel by Michael Crichton, author of “Jurassic Park”.

The horrible beasties threatening humanity in this new thriller are not giant dinosaurs, but swarms of minute “nanobots” that can invade and take control of human bodies.

Last summer, a report issued by a Canadian environmental body called the action group on erosion, technology and concentration took a swipe at nanotechnology. It urged a ban on the manufacture of new nanomaterials until their environmental impact had been assessed. The group is better known for successfully campaigning against biotechnology, and especially against genetically modified crops.

The research, led by a group at the National Aeronautics and Space Administration's Johnson Space Centre in Houston, has found in preliminary studies that inhaling vast amounts of nanotubes is dangerous. Since they are, in essence, a form of soot, this is not surprising. But as most applications embed nanotubes in other materials, they pose little risk in reality.

Room at the Bottom

What I want to talk about is the problem of manipulating and controlling things on a small scale …

As soon as I mention this, people tell me about miniaturization, and how far it has progressed today. They tell me about electric motors that are the size of the nail on your small finger. And there is a device on the market, they tell me, by which you can write the Lord's Prayer on the head of a pin. But that's nothing; that's the most primitive, halting step in the direction I intend to discuss. It's a staggeringly small world that is below. In the year 2000, when they look back at this age, they will wonder why it was not until the year 1960 that anybody began seriously to move in this direction……

Prof. Richard Feynman in "There's plenty of room at the bottom", lecture delivered at the annual meeting of the APS, Caltech, 29 December, 1959.

Nanoscale Writing

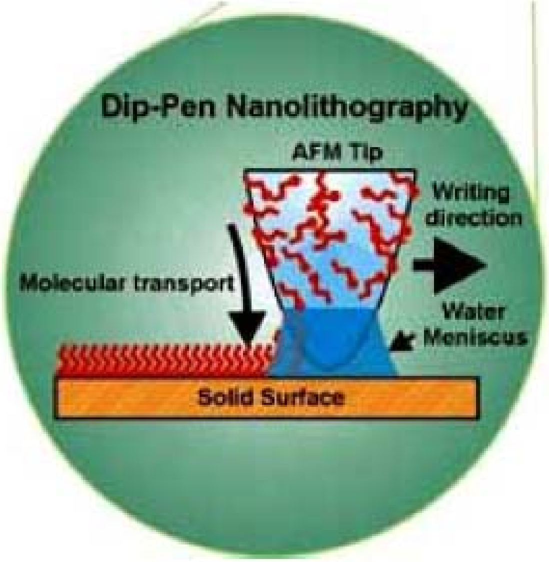

Nanoscale writing with an AFM (Mirkin et al.)

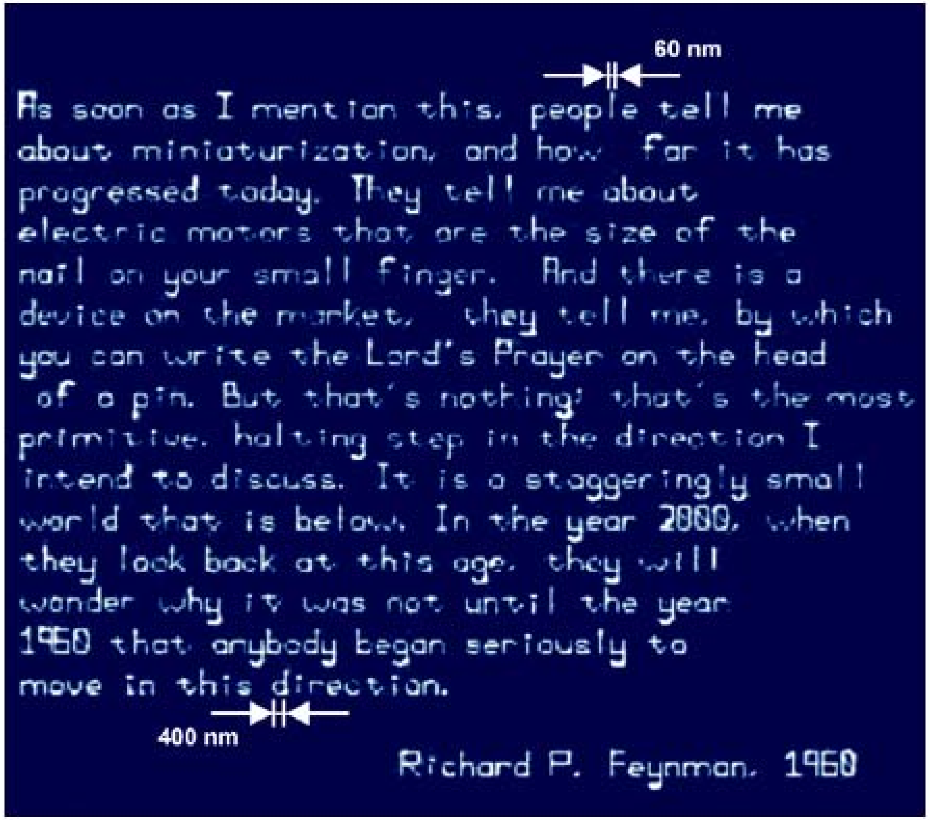

As soon as I mention this, people tell me about miniaturization, and how far it has progressed today. They tell me about electric motors that are the size of the nail on your small finger. And there is a device on the market, they tell me, by which you can write the Lord's Prayer on the head of a pin. But that's nothing; that's the most primitive, halting step in the direction I intend to discuss. It is a staggeringly small world that is below. In the year 2000, when they look back at this age, they will wonder why it was not until the year 1960 that anybody began seriously to move in this direction.

Richard P. Feynman, 1960

STM

Scanning Tunelling Microscopy

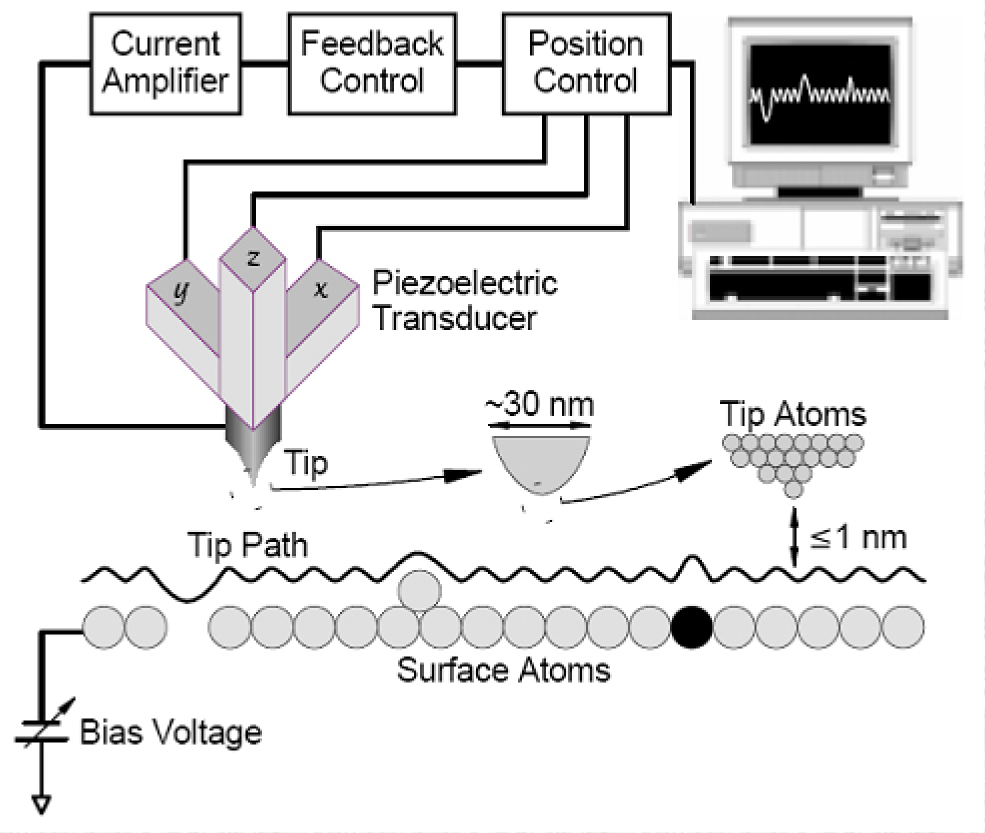

Binning and Rohrer
Nobel 1986

Nanoscale Writing

STM positioned Xe atoms on Ni crystal, 5 nm letters

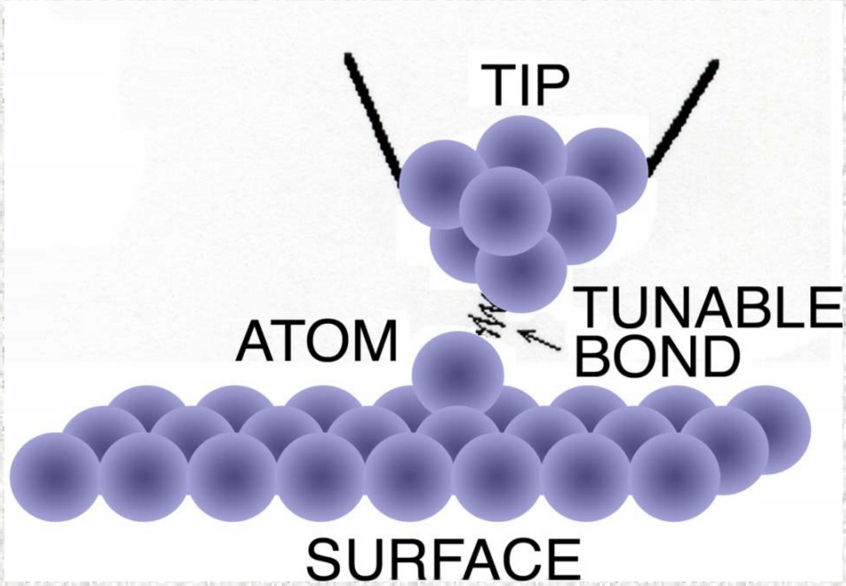

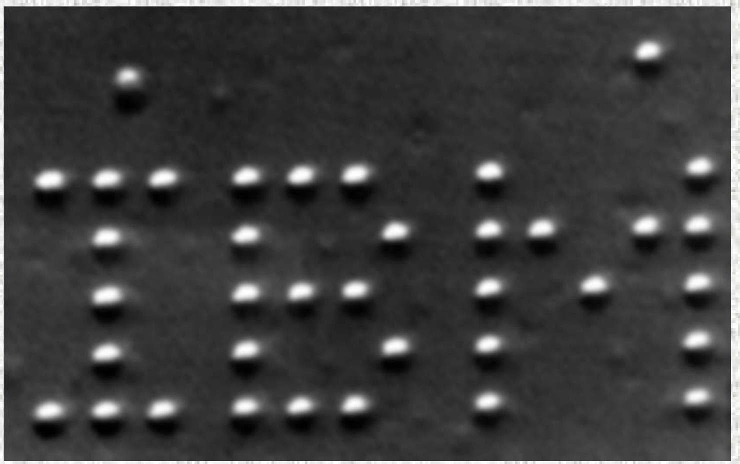

Nanoscopic Materials

Negligible light scattering - New optics

Quantum size effects - Information technology, Storage media

High surface area - Catalysts, Adsorbents

Large interfacial area - New composites

Surface modifications - Targeted drug delivery

Nanoscopic Size

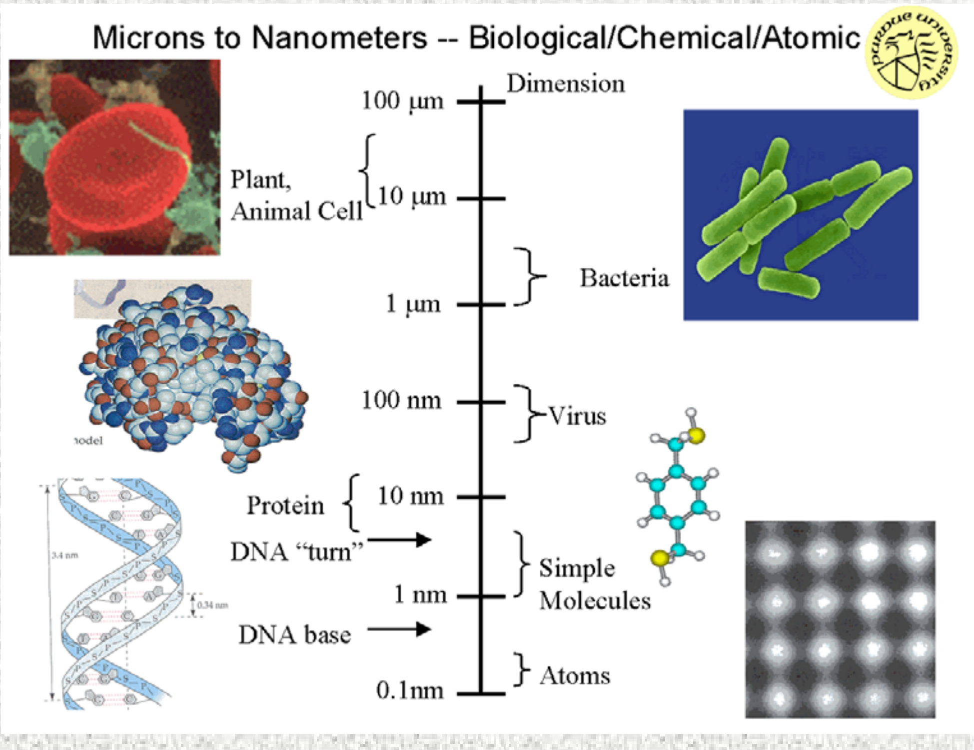

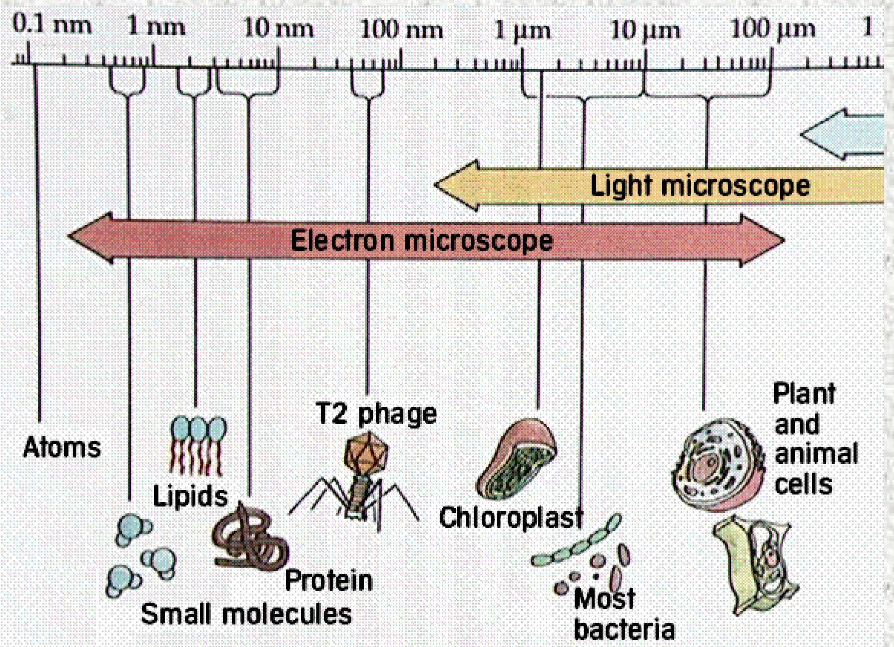

The largest known bacterium - Thiomargarita namibiensis - 100-750 microns

The Nano-Family

At least one dimension is between 1 - 100 nm

0-D structures (3-D confinement):

- **Quantum dots**
- **Nanoparticles**

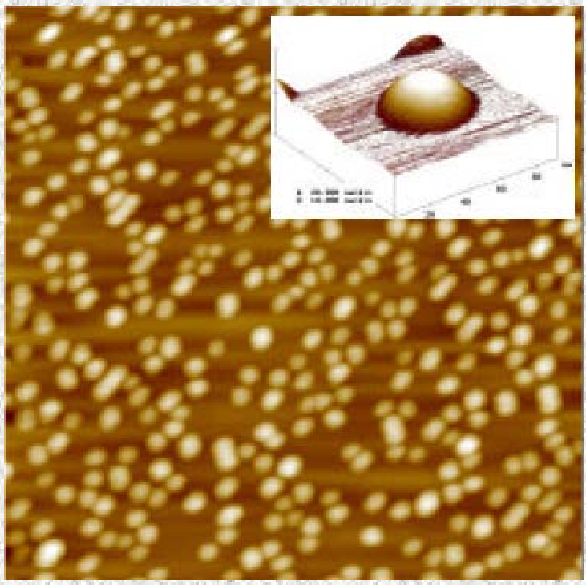

AFM 1 µm x 1 µm
InAs on GaAs/InP

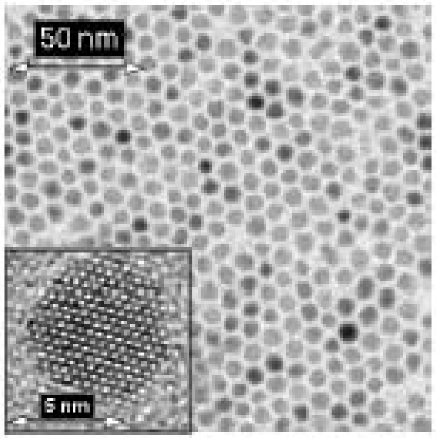

CdTe nanoparticles

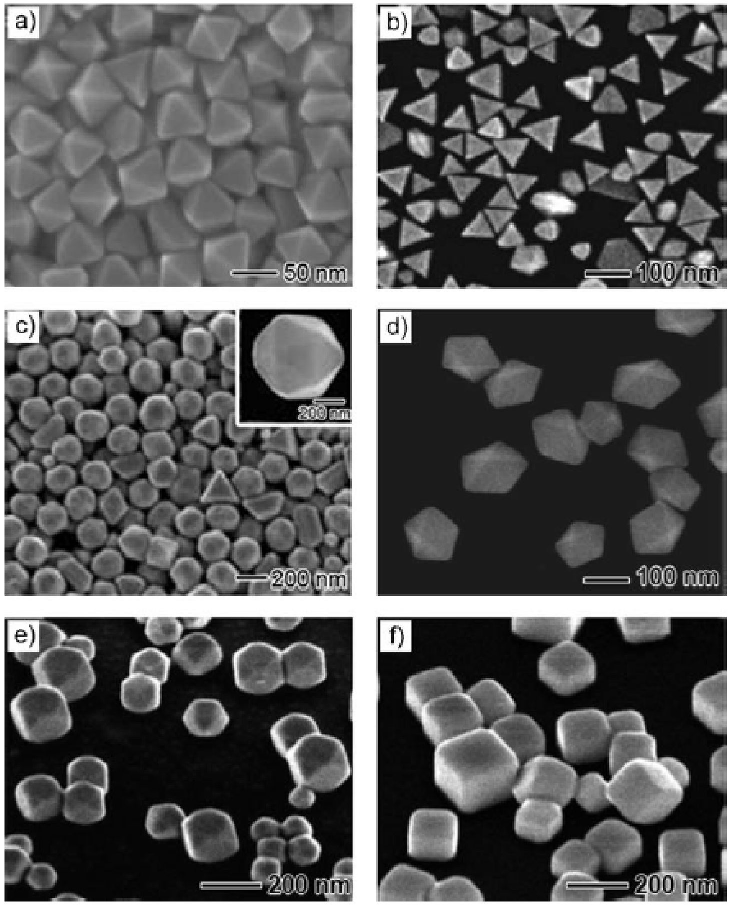

Au nanoparticles

The Nano-Family

1-D structures (2-D confinement):

- Nanowires
- Nanorods
- Nanotubes
- Nanofibers

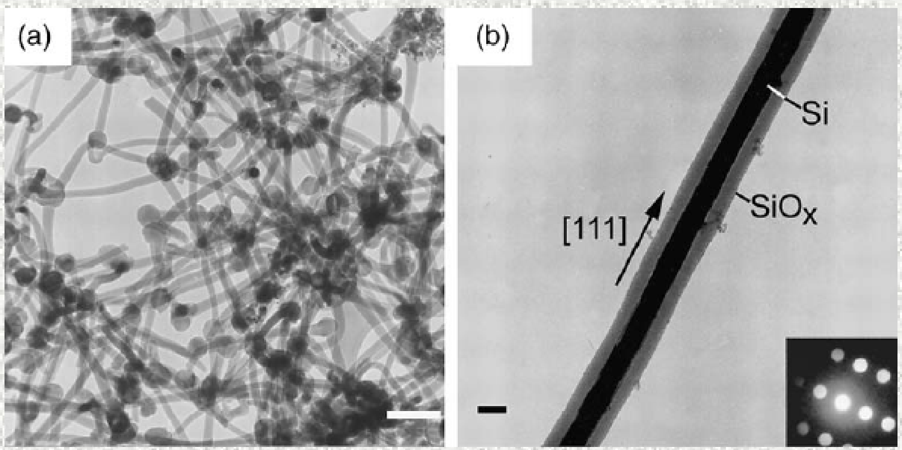

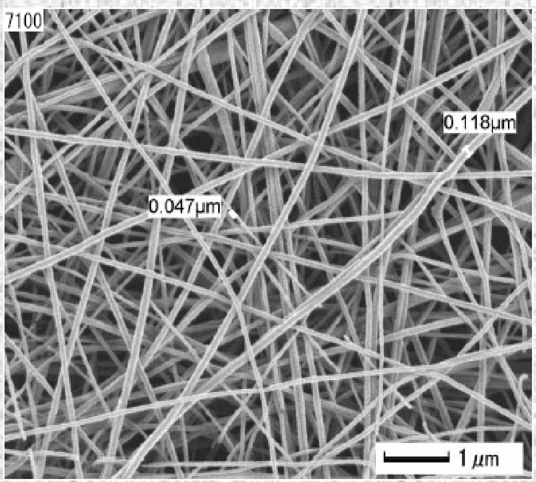

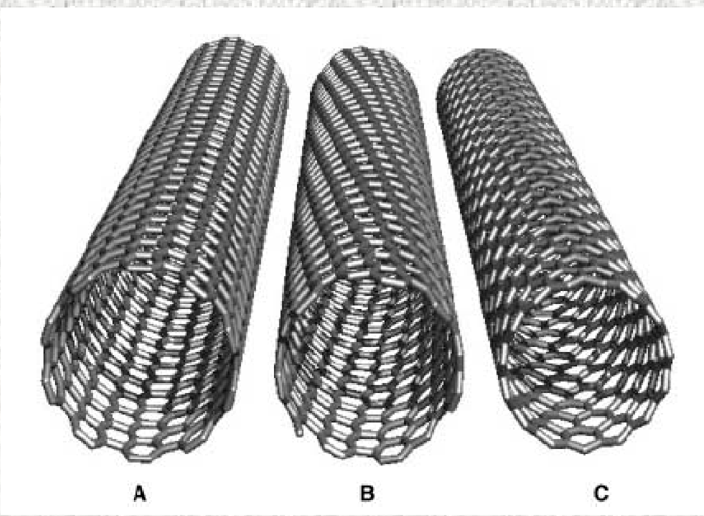

Electrospinning

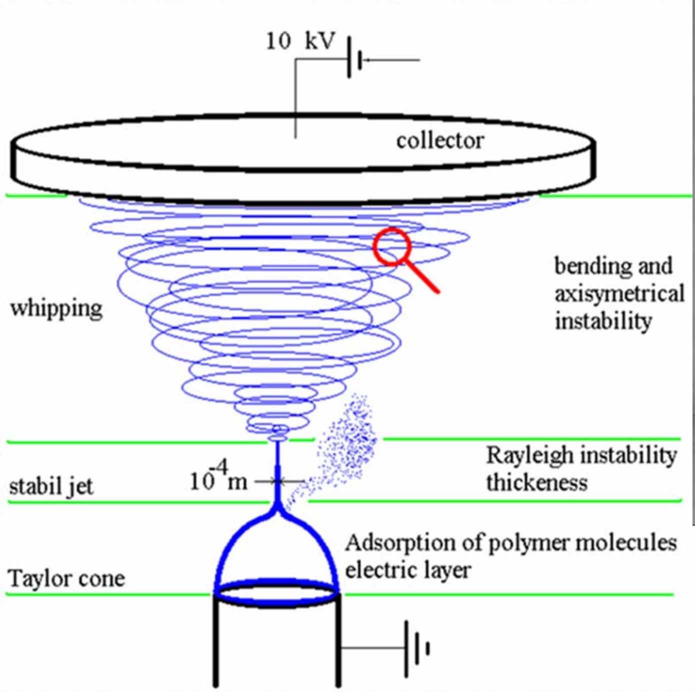

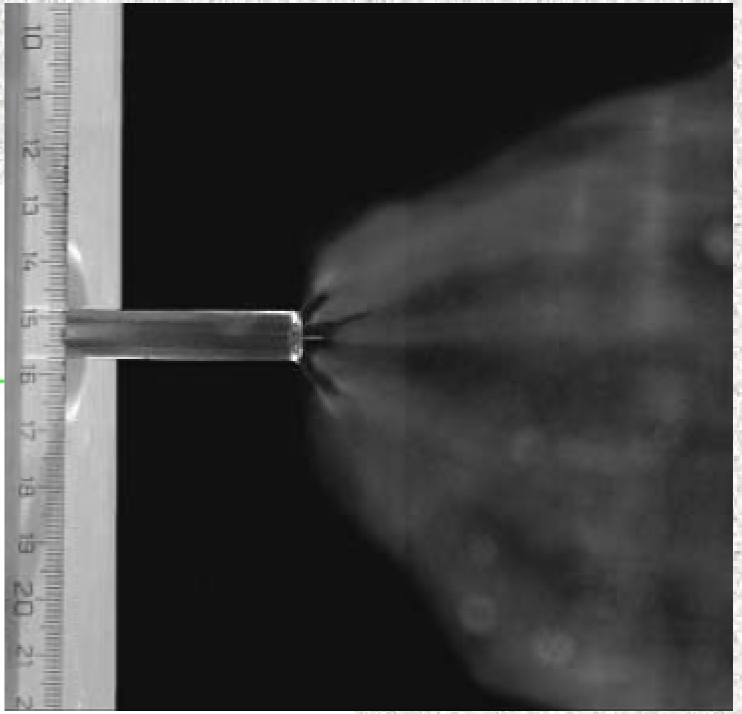

The Nano-Family

2-D structures (1-D confinement):

- **Thin films**
- **Planar quantum wells**
- **Superlattices**
- **Graphene**
- **SAM**

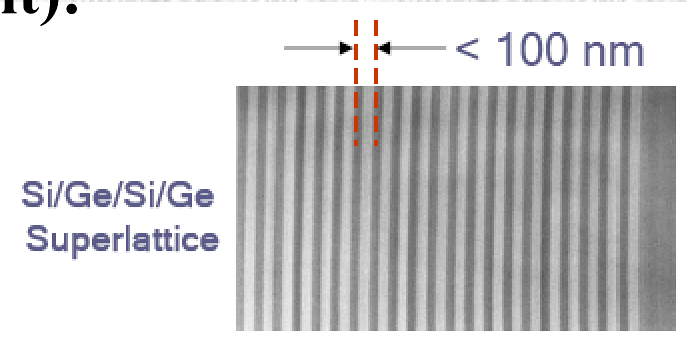

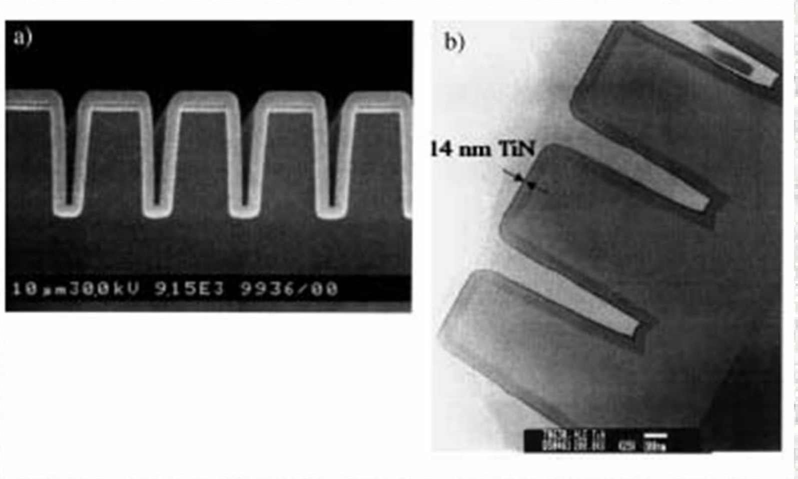

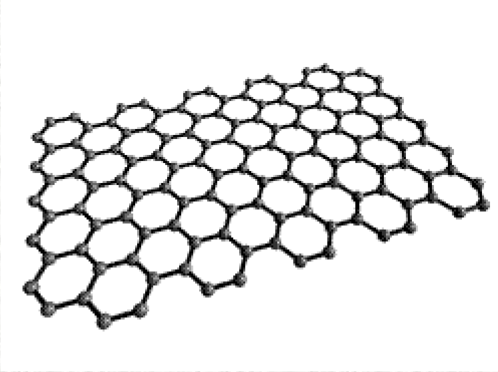

Coherence Length, *d*

Scherrer equation

$$d = \frac{k\lambda}{\beta \cos\theta}$$

k = 0.89, λ = wavelength,
β = full width at half-maximum of a standard (Si)

XRD patterns of iron oxide nanocrystals of 4, 6, 8, 9, 10, 11, 12, 13, and 15 nm

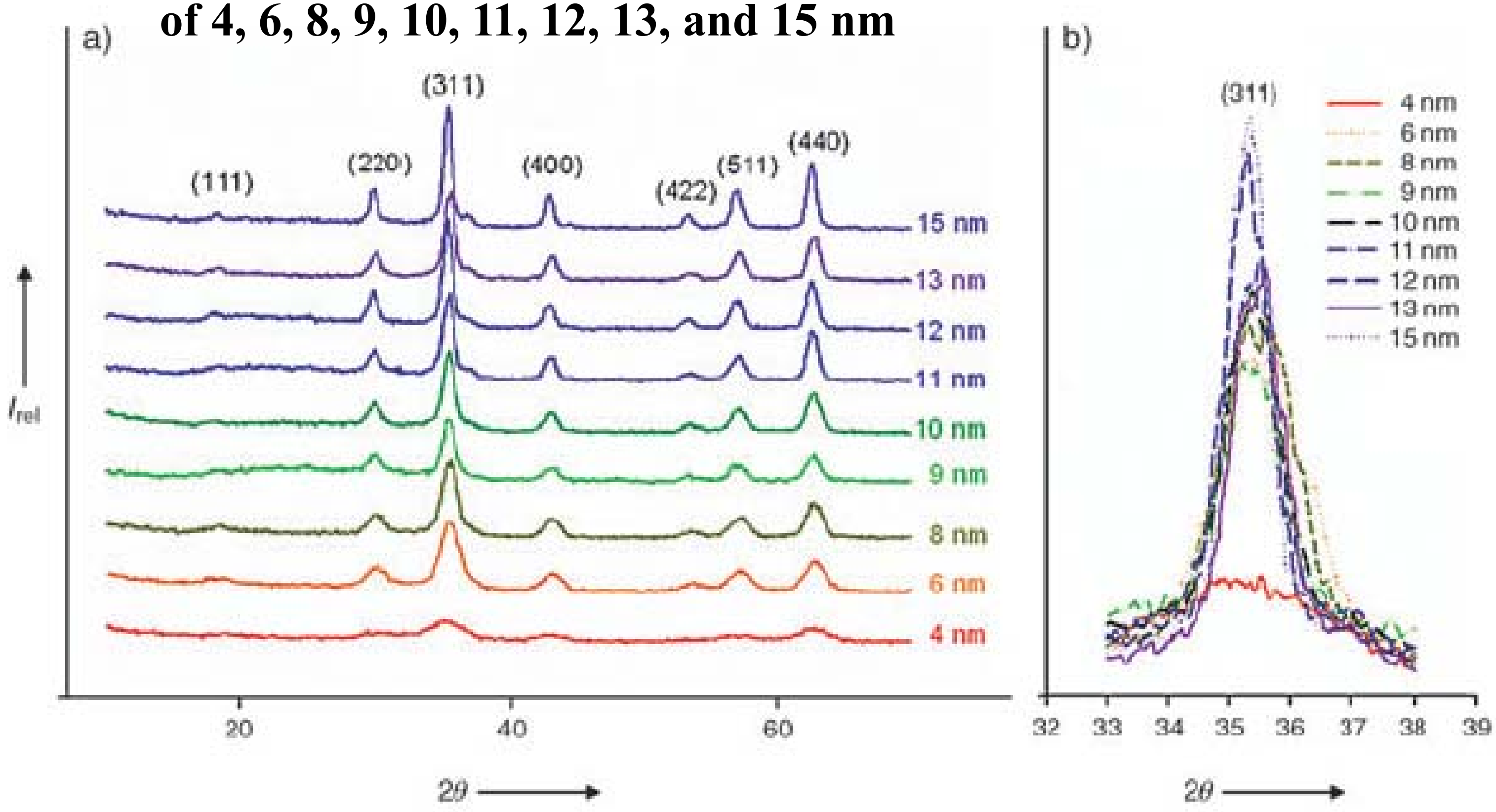

Surface Effects

Decreasing grain size = Increasing volume fraction of grain boundaries (50% for 3 nm particles)

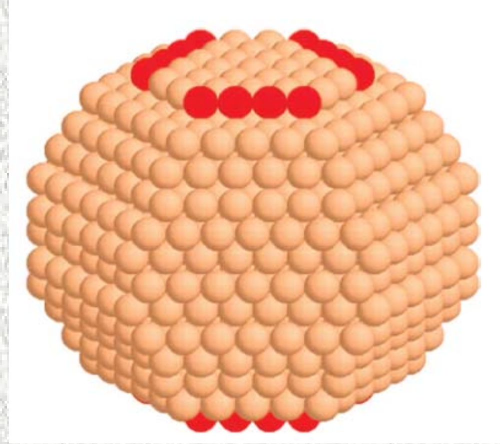

Ru particle diameter 2.9 nm

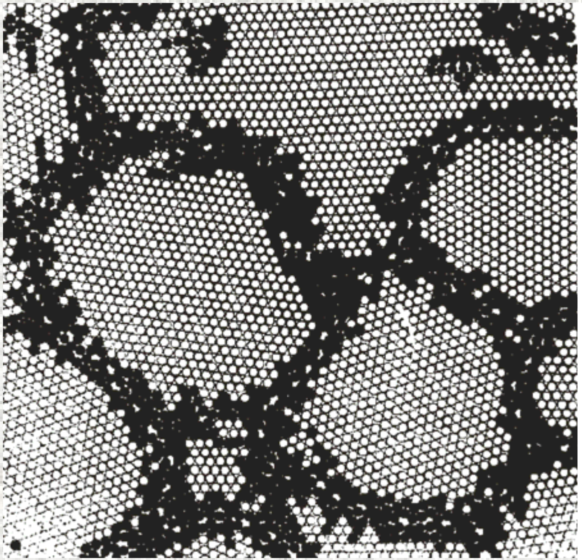

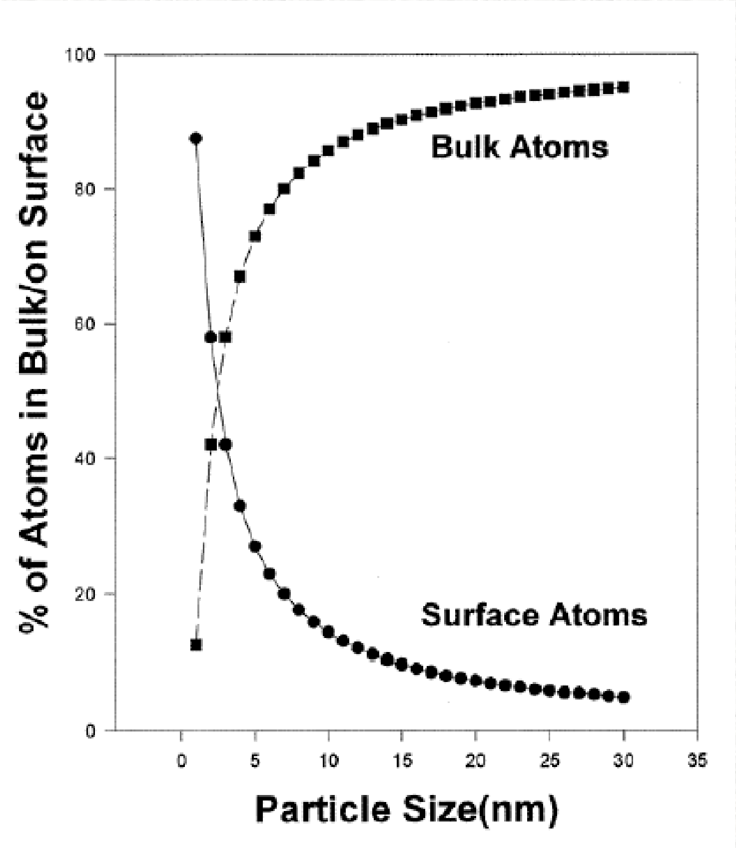

Surface Effects

Dispersion F = the fraction of atoms at the surface

F is proportional to surface area divided by volume

N = total number of atoms

V ~ r^3 ~ N

$$F \approx \frac{r^2}{r^3} \approx \frac{1}{r} \approx \frac{1}{\sqrt[3]{N}}$$

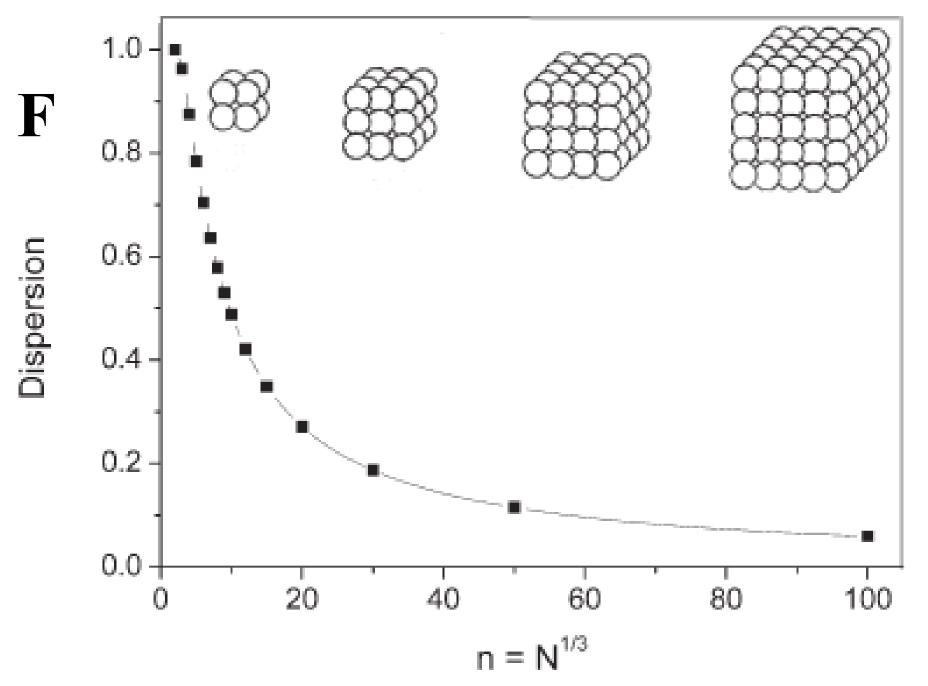

n = number of atoms at the cube edge

Surface Effects

Properties of grain boundaries

- Lower coordination number of atoms
- Reduced atomic density (by 10 – 30 %)
- Broad spectrum of interatomic distances

Experimental evidence

- HREM
- EXAFS, reduced number of nearest and next-nearest neighbors
- Raman spectroscopy
- Mössbauer spectroscopy, quadrupole splitting distribution broadened
- Diffusivity enhanced by up to 20 orders of magnitude !!
- Solute solubility in the boundary region

Ag (fcc) and Fe (bcc) immiscible in (s) or (l), but do form solid solution as nanocrystalline alloy

- EPR, nano-Si gives a sharp signal

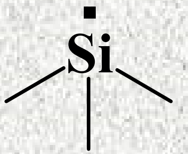

Surface Effects

Atoms at surfaces
- **fewer neighbors than atoms in the bulk = lower coordination number**
- **stronger and shorter bonds**
- **unsatisfied bonds**
- **surface atoms are less stabilized than bulk atoms**

The smaller a particle the larger the fraction of atoms at the surface, and the higher the average binding energy per atom

The melting and other phase transition temperatures scale with surface-to-volume ratio and with the inverse size

Example: the melting point depression in nanocrystals

2.5 nm Au particles 930 K **bulk Au 1336 K**

Surface Effects

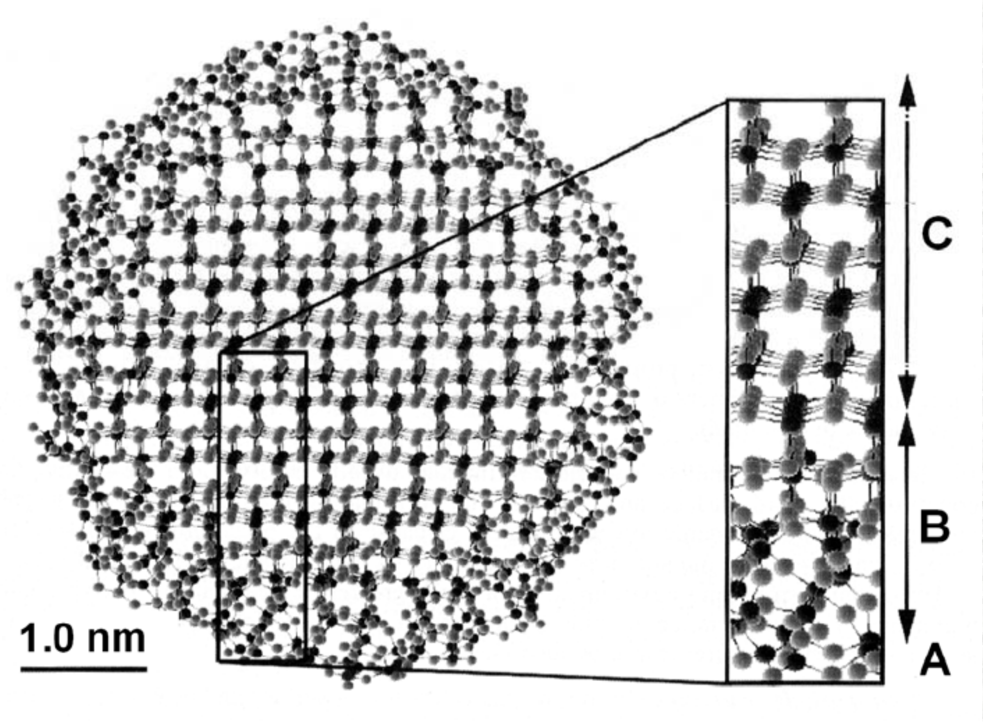

A = Atoms at surfaces (one layer) – fewer neighbours, lower coordination, unsatisfied (dangling) bonds

B = Atoms close to surface (several layers) – deformation of coordination sphere, distorted bond distances and angles

C = Bulk atoms – not present in particles below 2 nm

Graphite shells

Surface Effects

coordination number

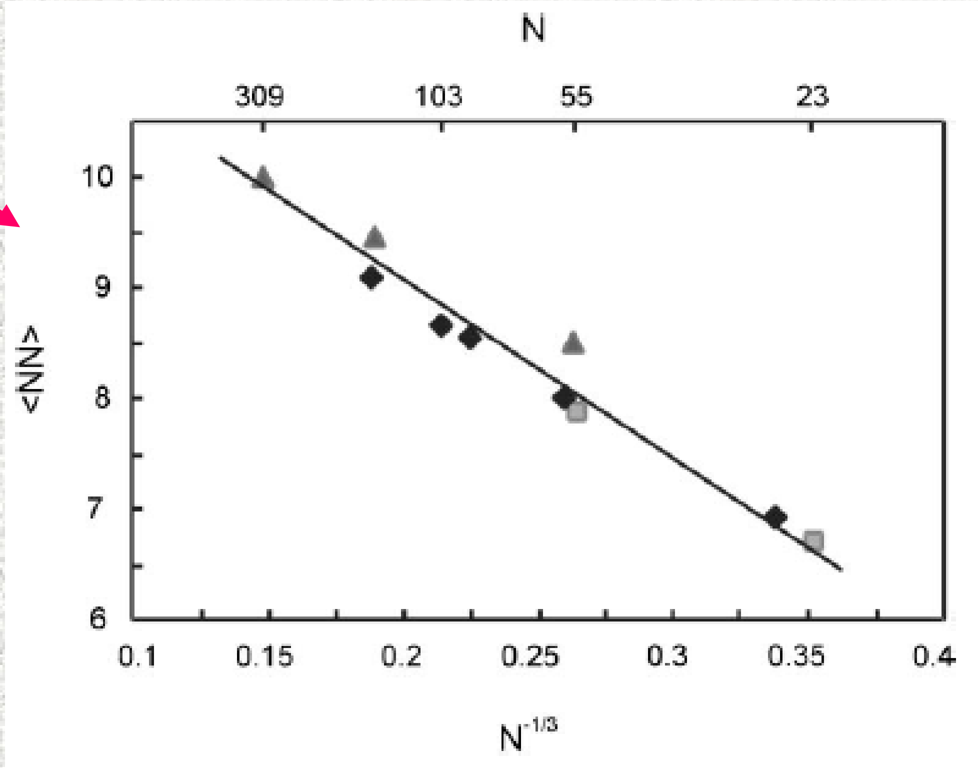

Calculated mean coordination number <NN> as a function of inverse radius, represented by $N^{-1/3}$ for Mg clusters (triangles = icosahedra, squares = decahedra, diamonds = hcp

Surface Effects

Atom binding (vaporization) energies lower in nanoparticles, fewer neighbors to keep atoms from escaping

Plasticity of nanocrystalline ceramics

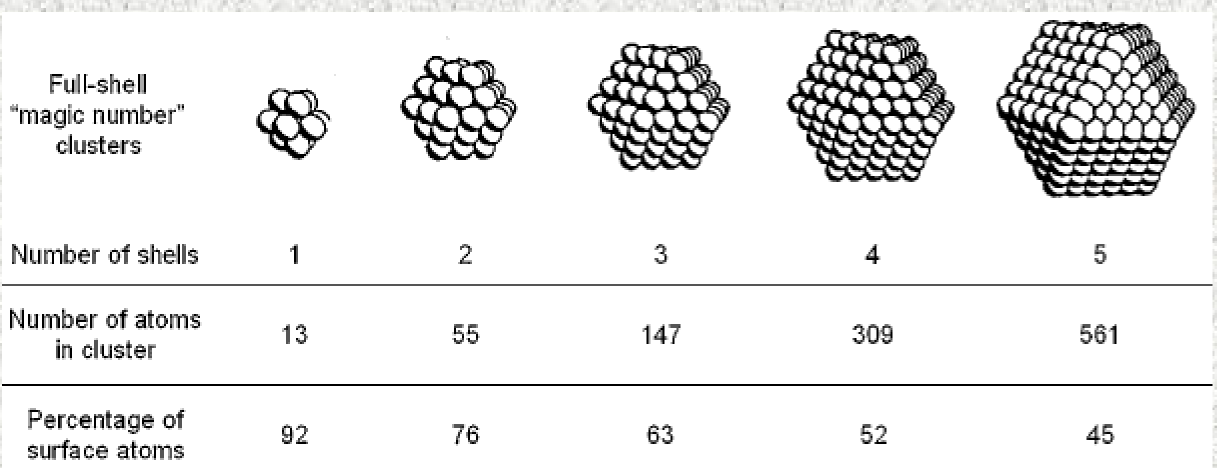

Full-shell "magic number" clusters					
Number of shells	1	2	3	4	5
Number of atoms in cluster	13	55	147	309	561
Percentage of surface atoms	92	76	63	52	45

Surface Effects

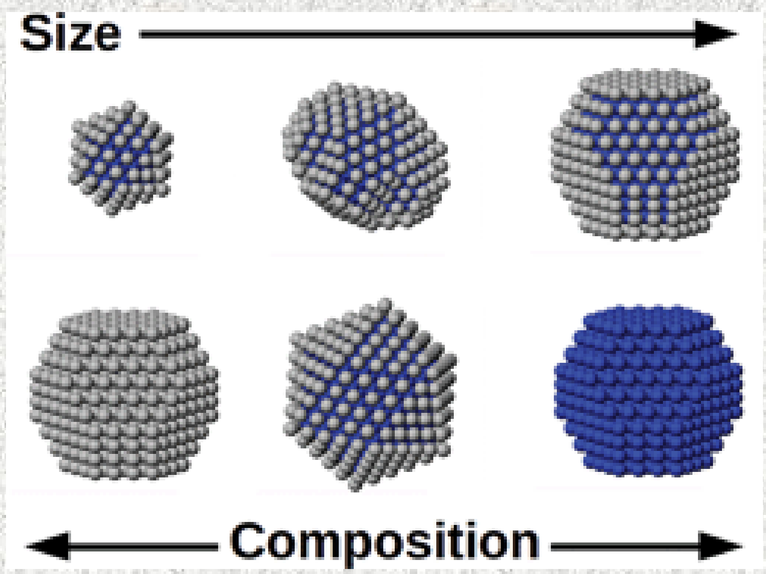

Alloys:
Core-shell
Janus
Random mixture

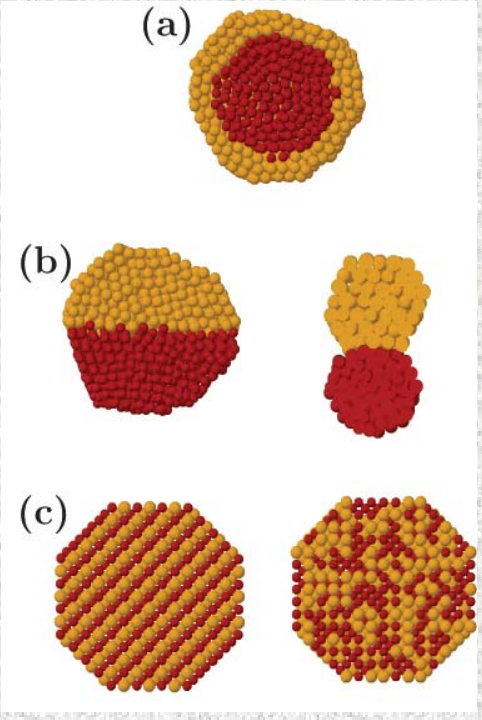

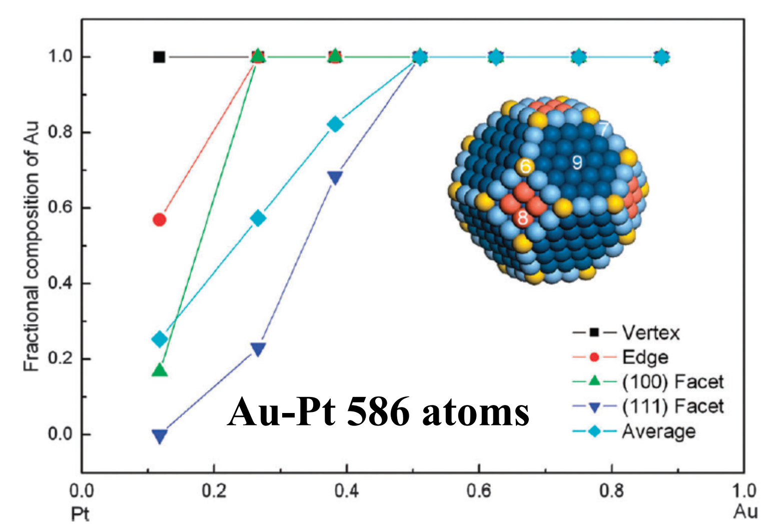

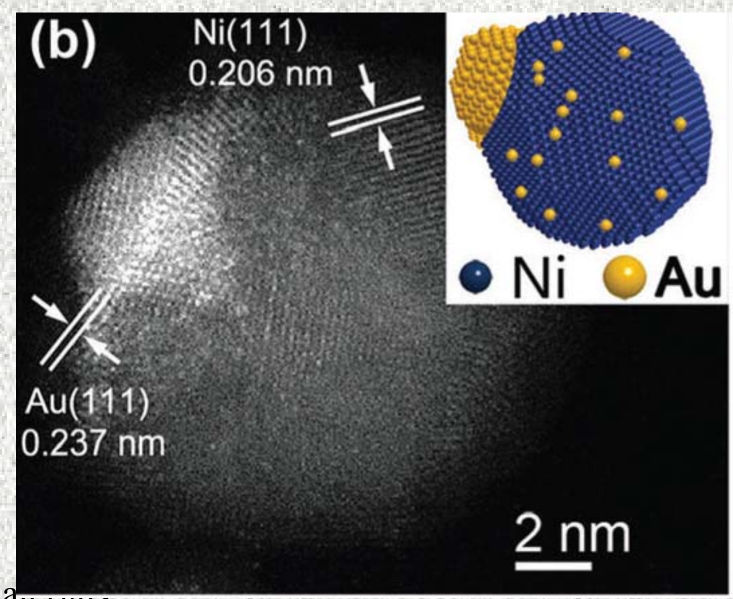

Melting Point Depression

povrchové atomy v pevné látce jsou vázány menším počtem kratších a pevnějších vazeb, což v případě malých částic s velkým podílem povrchových atomů vede ke snížení průměrné hodnoty kohezní energie částice, zvýšení průměrné amplitudy tepelných vibrací atomů a k zvýšení „průměrného“ tlaku uvnitř částic

mají společný důsledek – snížení t

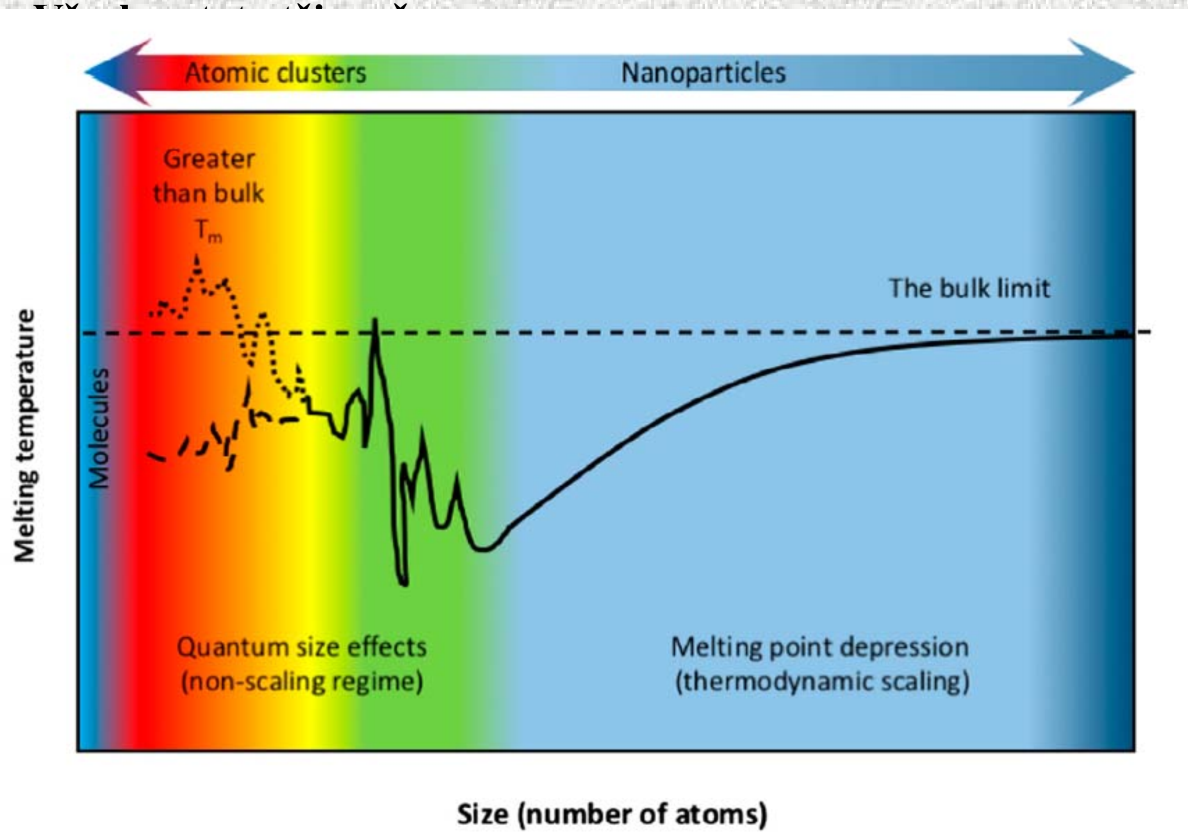

Melting Point and Enthalpy Depression

Nanocalorimetry of Sn nanoparticles

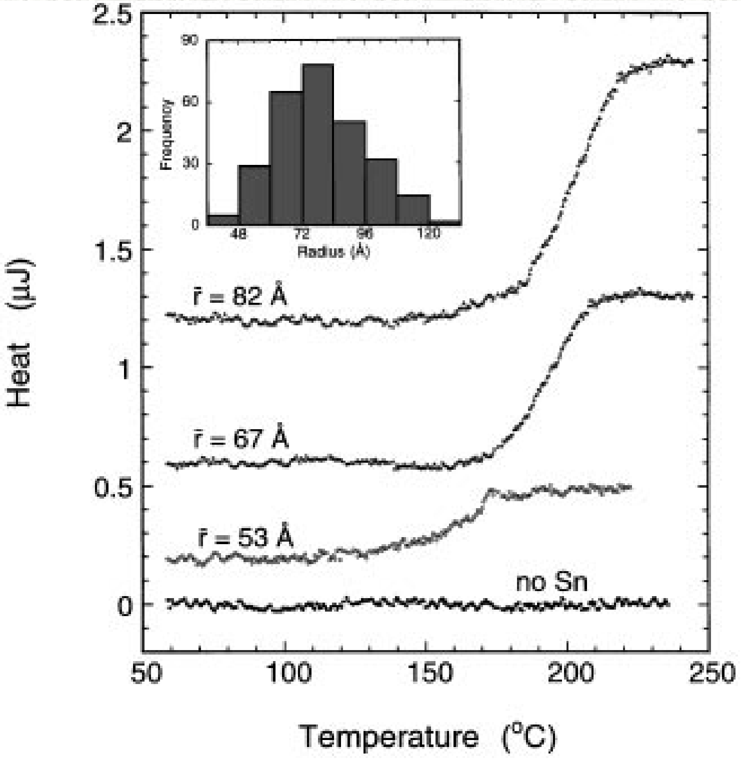

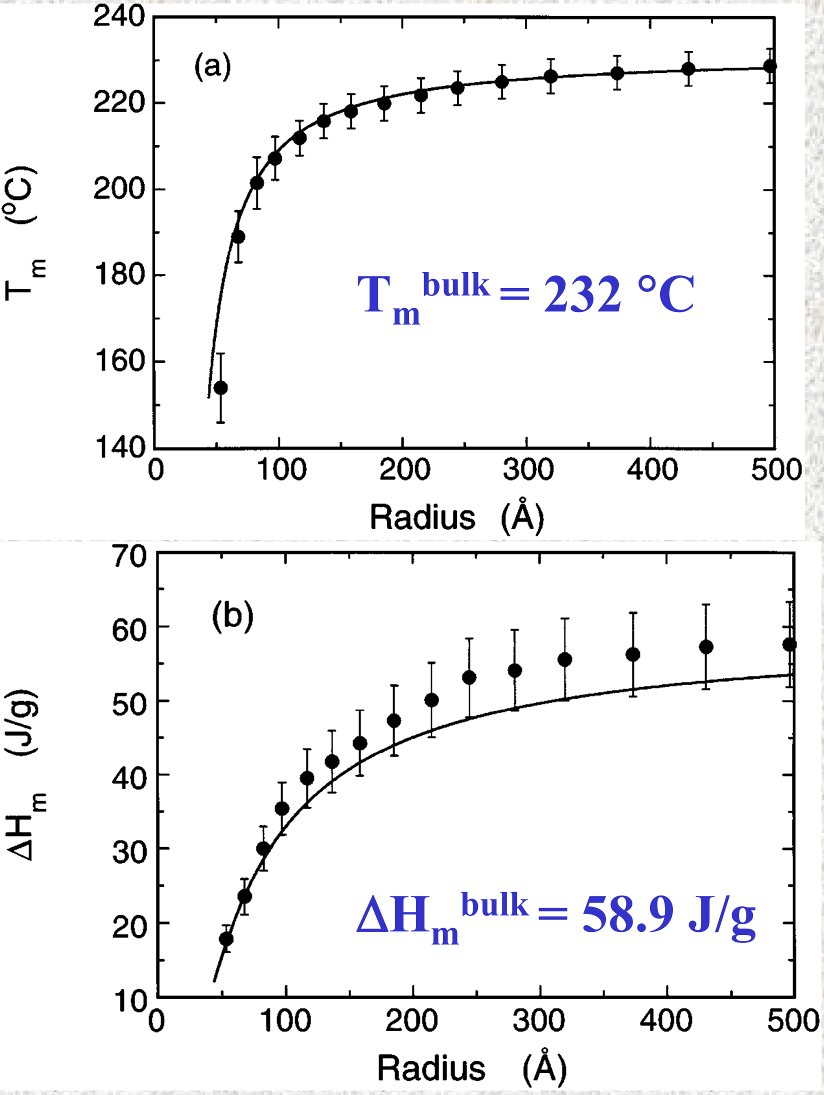

$T_m^{bulk} = 232$ °C

$\Delta H_m^{bulk} = 58.9$ J/g

Melting Point and Enthalpy Depression

Nanocalorimetry of
Sn nanoparticles

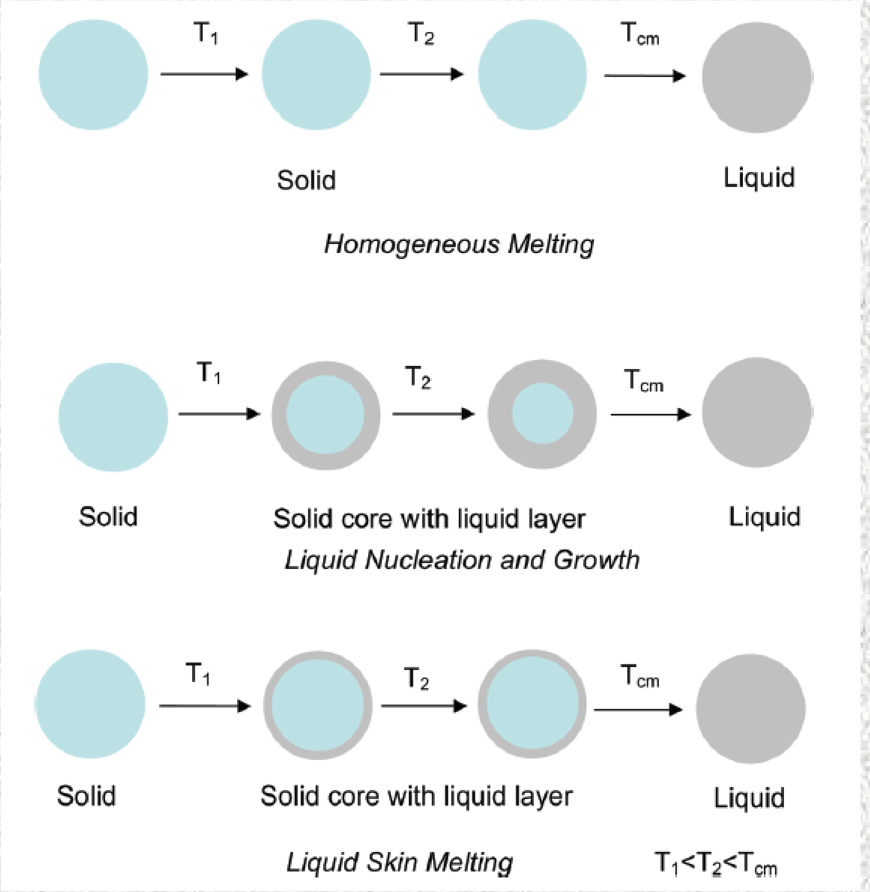

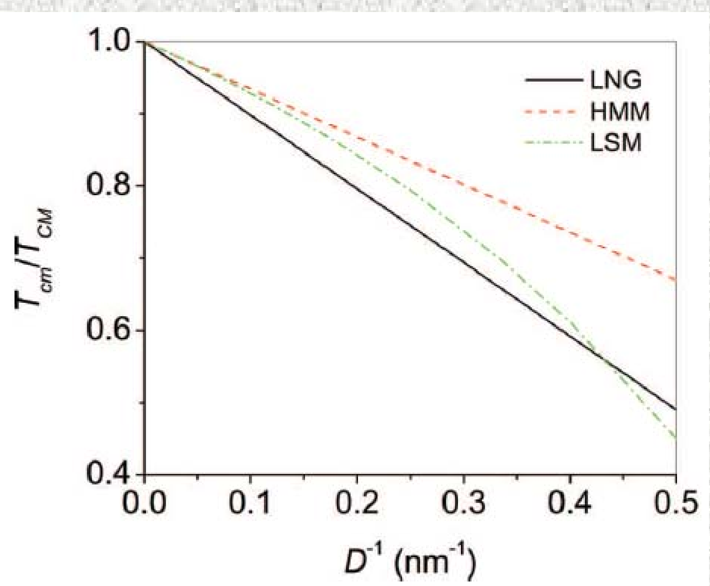

Melting Point Depression

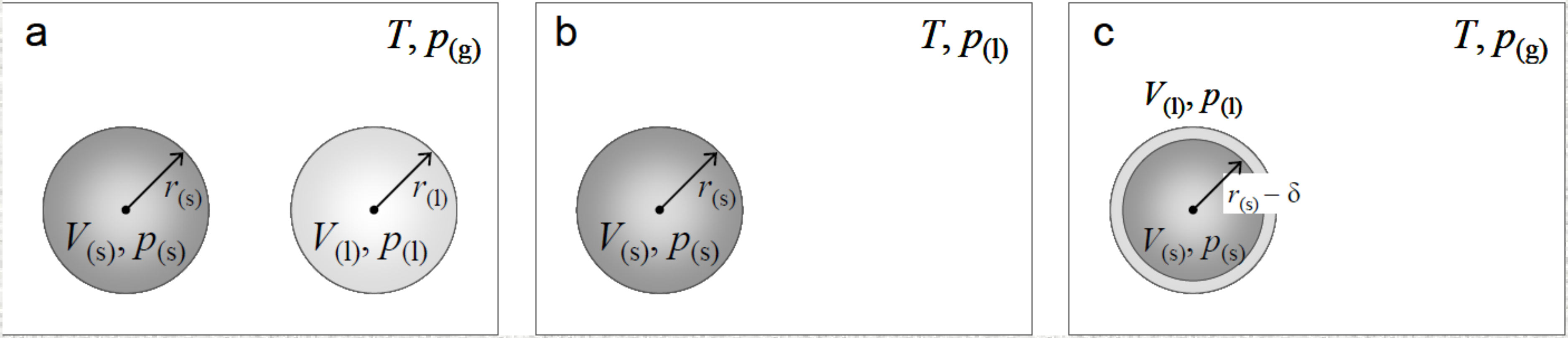

Homogeneous melting model

Triple point of coexisting solid and liquid nanoparticles of the same mass surrounded by vapor

$$\frac{T_r^{\mathrm{F}}}{T_\infty^{\mathrm{F}}} = 1 - \frac{2M}{\Delta H_{\mathrm{m}}^{\mathrm{F}} \rho_{(\mathrm{s})} r_{(\mathrm{s})}} \left[\gamma_{(\mathrm{sg})} - \gamma_{(\mathrm{lg})} \left(\frac{\rho_{(\mathrm{s})}}{\rho_{(\mathrm{l})}} \right)^{2/3} \right]$$

Continuous Liquid Meling

Melting particle is surrounded by liquid

$$\frac{T_r^{\mathrm{F}}}{T_\infty^{\mathrm{F}}} = 1 - \frac{2M}{\Delta H_{\mathrm{m}}^{\mathrm{F}} \rho_{(\mathrm{s})} r_{(\mathrm{s})}} \gamma_{(\mathrm{sl})}$$

Liquid Skin Melting

Thin melted layer of a constant thickness δ coexisting with solid core and vapor

$$\frac{T_r^{\mathrm{F}}}{T_\infty^{\mathrm{F}}} = 1 - \frac{2M}{\Delta H_{\mathrm{m}}^{\mathrm{F}} \rho_{(\mathrm{s})} r_{(\mathrm{s})}} \left[\frac{\gamma_{(\mathrm{sl})}}{1 - \delta / r_{(\mathrm{s})}} + \gamma_{(\mathrm{lg})} \left(1 - \frac{\rho_{(\mathrm{s})}}{\rho_{(\mathrm{l})}} \right) \right]$$

Melting Point Depression

$$T_m(r) = T_m(\text{bulk}) - \frac{2T_m(\text{bulk})\text{M}}{\Delta H_m^{bulk}\rho_s r}\left[\gamma_{sg} - \gamma_{lg}\left(\frac{\rho_s}{\rho_l}\right)^{\frac{2}{3}}\right]$$

Sn **–** 4wt%**Ag** **–** 0.5wt%**Cu** Nano alloy particles

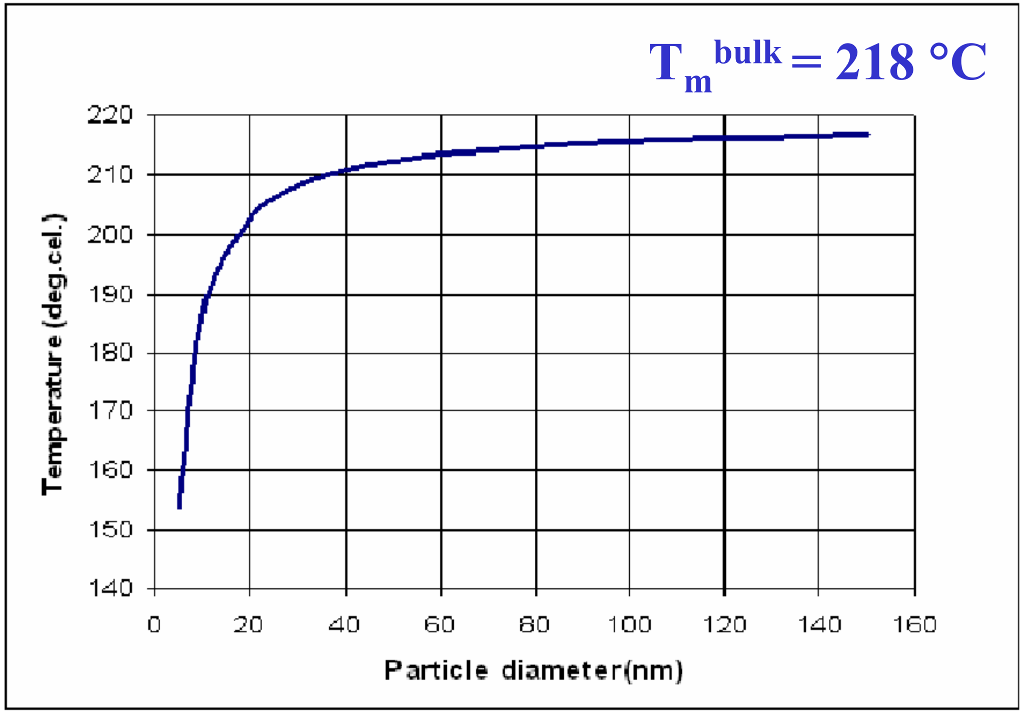

$T_m^{bulk} = 218$ °C

Homogeneous melting model:

$T_m(r)$ = mp of the cluster with radius r

T_m^{bulk} = mp of the bulk material

γ_{sg} = the interfacial energies between the s and g phases

γ_{lg} = the interfacial energies between the l and g phases

ρ_s and ρ_l = solid and liquid phase densities

M = molar mass

ΔH_m^{bulk} = the bulk latent heat of melting

Gibbs–Thomson Equation

for $\rho_s \sim \rho_l$

$\gamma_{sl} = \gamma_{sg} - \gamma_{lg}$ **Continuous Liquid Meling**

$$\frac{T_m(r)-T_m^{bulk}}{T_m^{bulk}} = -\frac{2V_{mol}^{l}\gamma_{sl}}{\Delta H_m r}$$

$T_m(r)$ = mp of the nanoparticle with radius r

T_m^{bulk} = mp of the bulk material

V_{mol}^{l} = the molar volume of the liquid = M/ρ_s solid?

γ_{sl} = the interfacial tension between the s and l surface

ΔH_m^{bulk} = the bulk molar enthalpy of melting, endothermic

In nanoparticles confined in pores

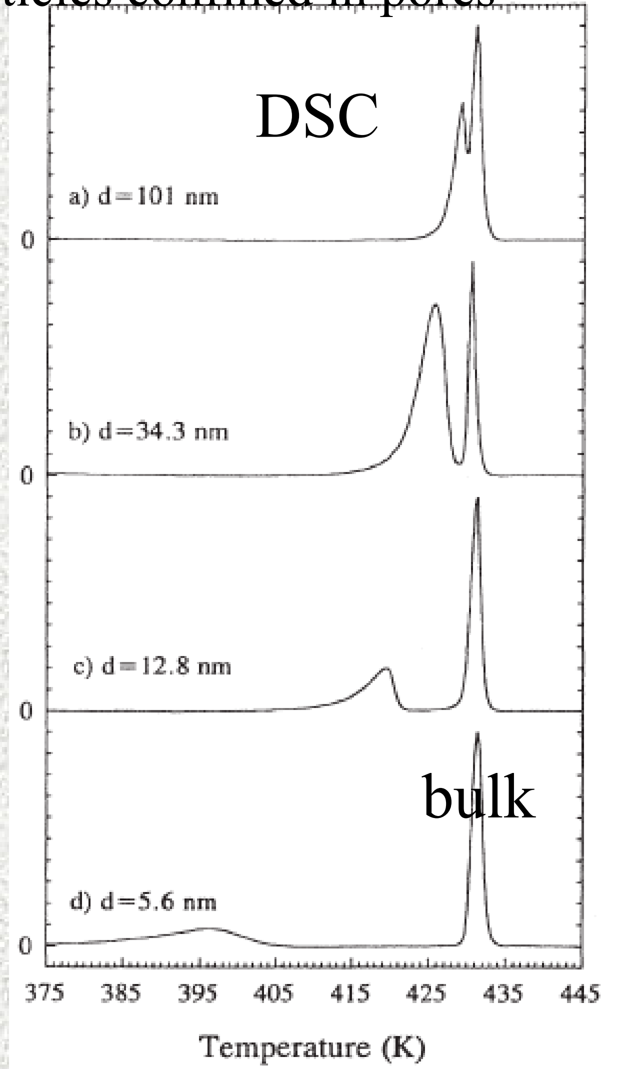

Phase Transitions

Phase transitions = collective phenomena

With a lower number of atoms in a cluster a phase transition is less well defined and broadened

Small clusters behave more like molecules than as bulk matter

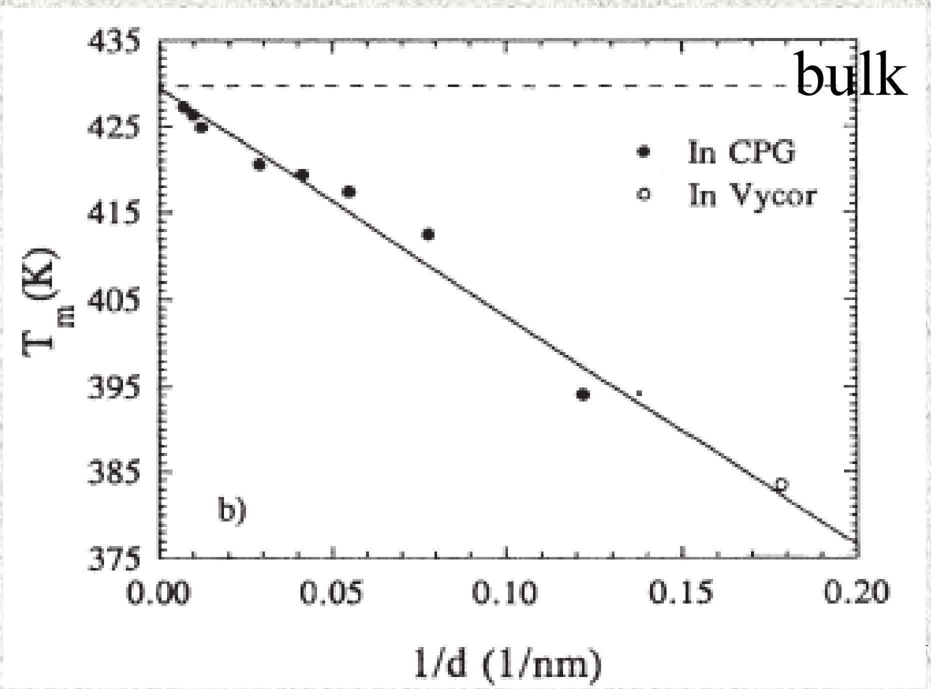

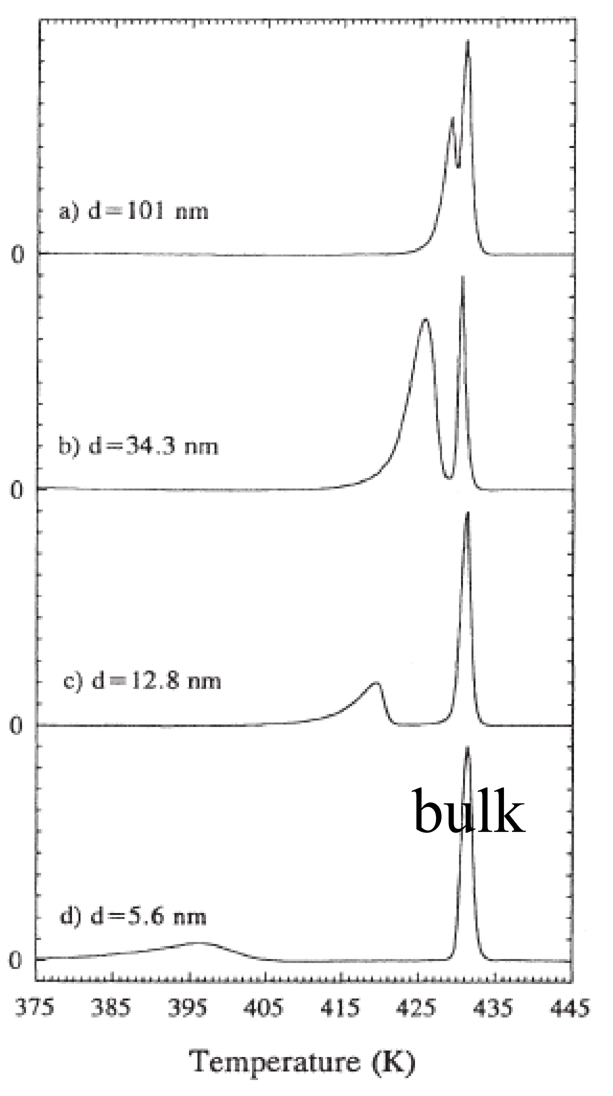

First-Order Phase Transitions

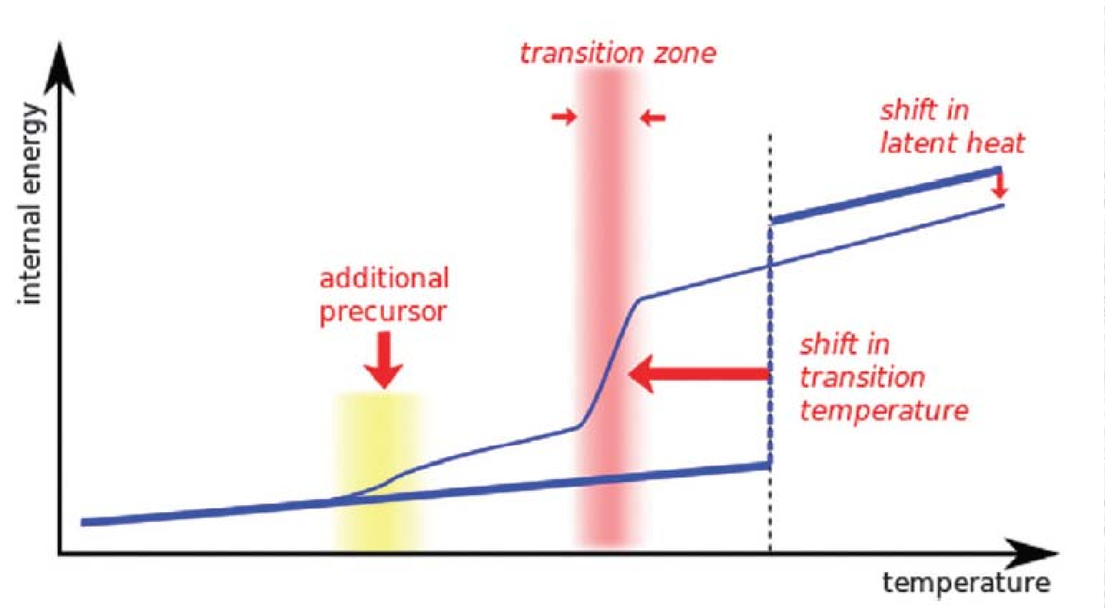

3 main consequences of a size decrease on caloric curve:

*** The transition is shifted, usually to a lower temperature (surface atoms are less coordinated and less bound than interior atoms)**
*** The transition temp. is no longer sharp but becomes smooth and takes place over a finite range (fluctuations in TD quantities)**
*** The latent heat is lower than in the bulk limit**

Surface Effects

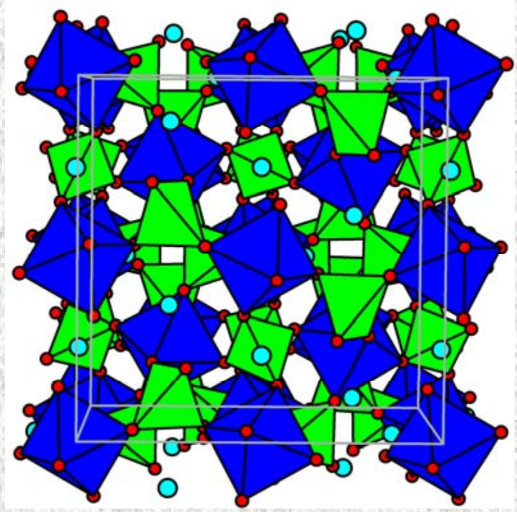

Reduction in particle size

- metal particles usually exhibit a lattice contraction
- oxide particles exhibit a lattice expansion

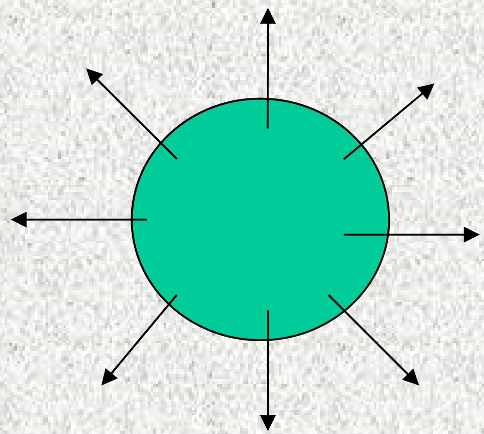

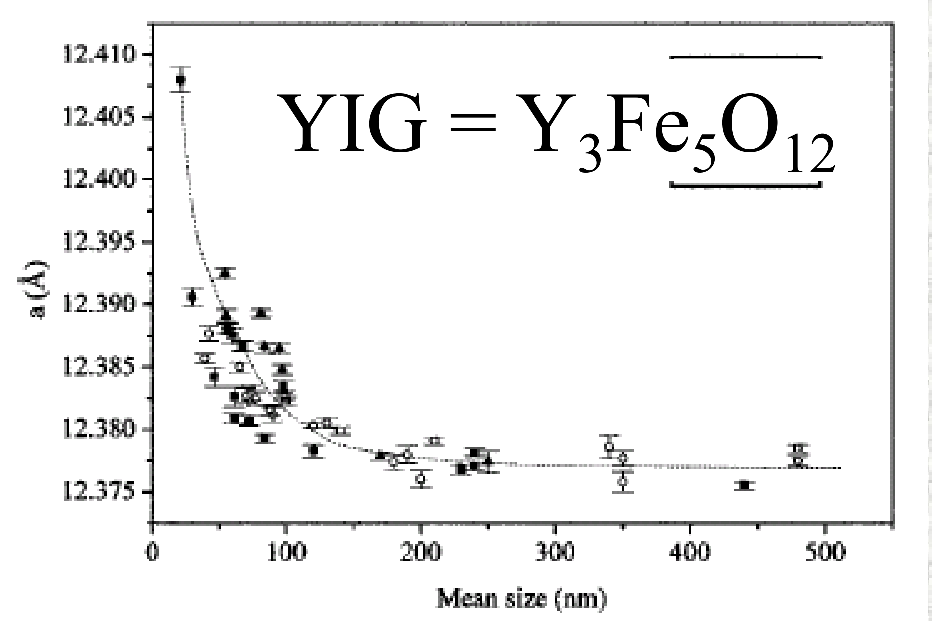

YIG = $Y_3Fe_5O_{12}$

Surface Effects

Correlation between the unit-cell volume (cubic) and the XRD particle size in γ-Fe_2O_3 nanoparticles

The smaller the particle size the larger the unit cell volume.

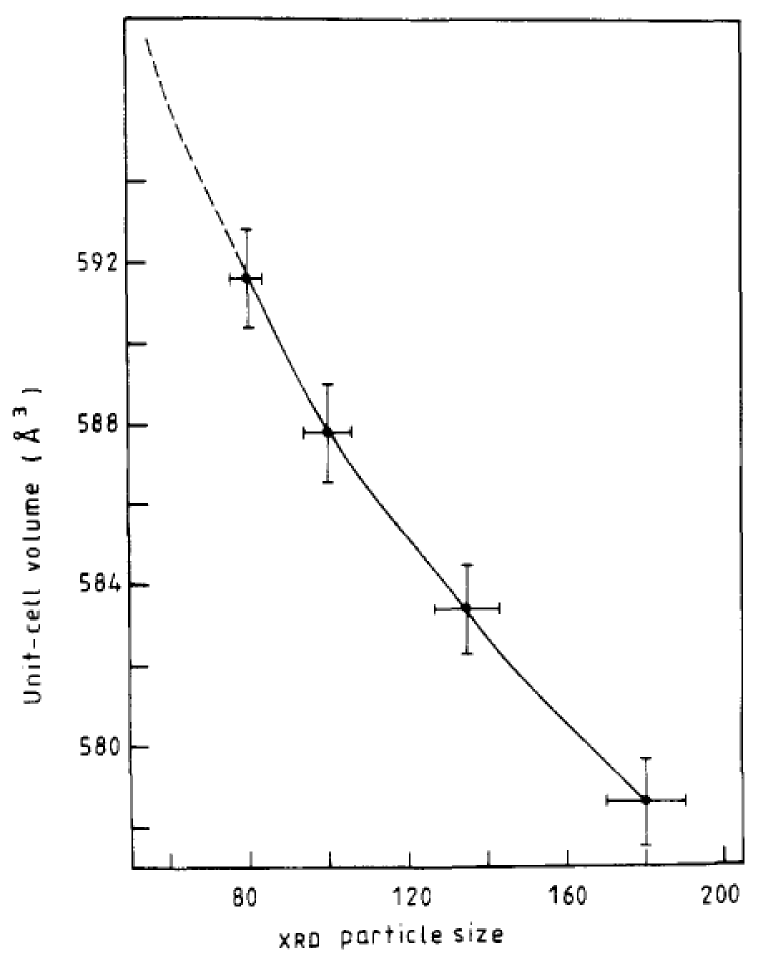

Surface Effects

The inter-ionic bonding in nanoparticles has a directional character ions in the outermost layer of unit cells possess unpaired electronic orbitals

Associated electric dipole moments, aligned roughly parallel to each other point outwards from the surface

The repulsive dipolar interactions increase in smaller particles reduced by allowing unit cell volume to increase

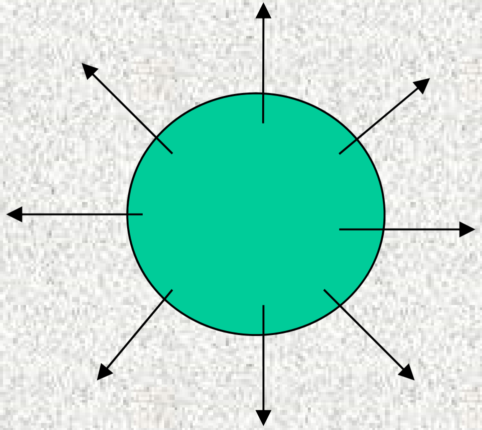

Quantum Confinement Effects

Physical and chemical properties depend on the size !!

ⓘ Finite-size effects
MO to Band transition

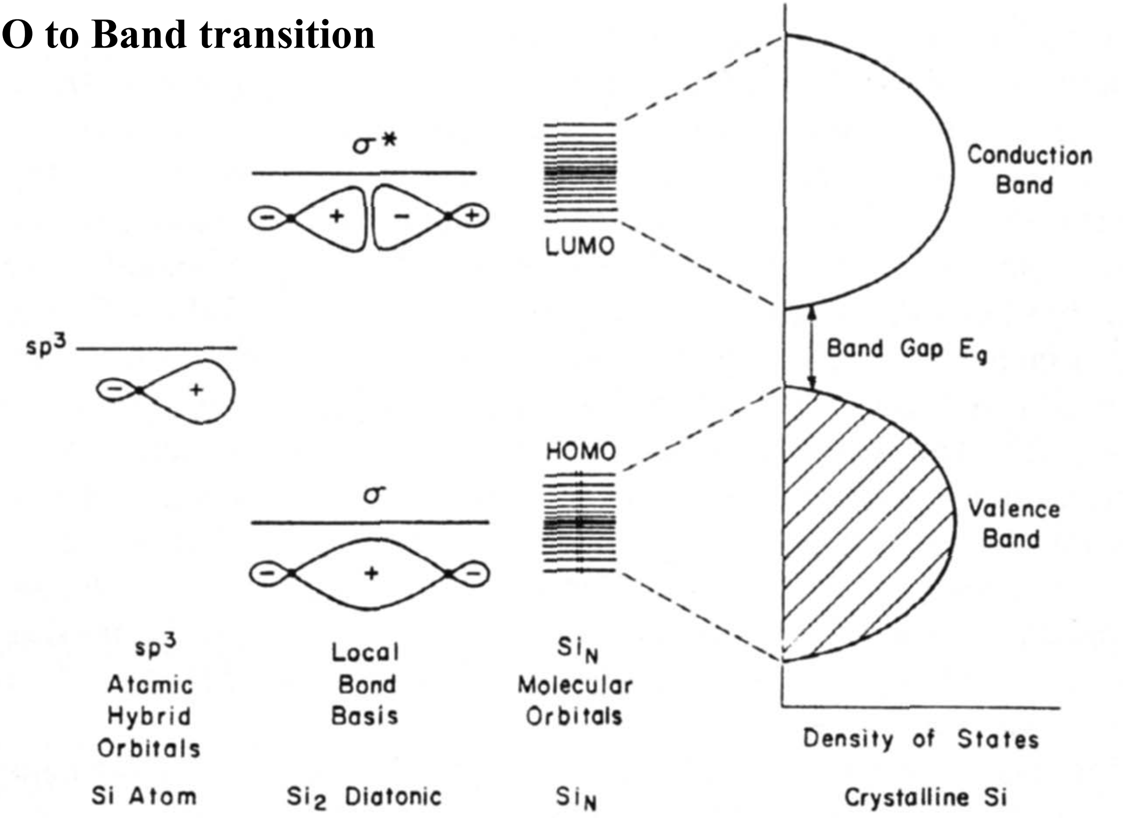

Quantum Size Effects

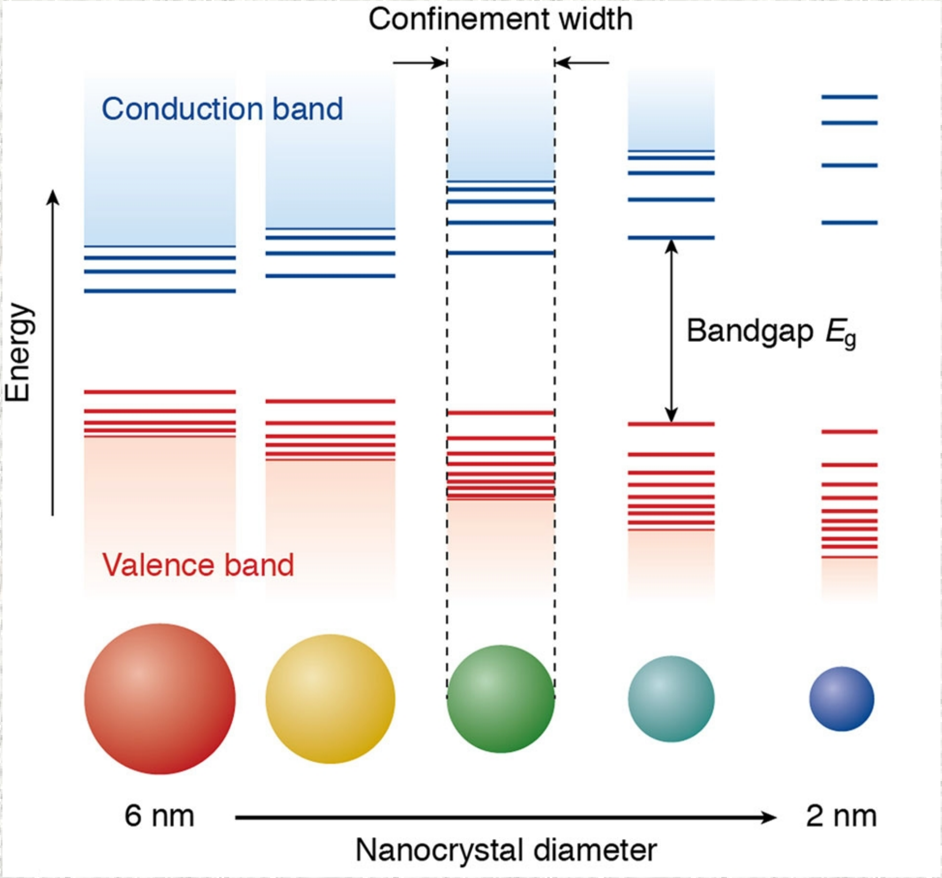

Band gap dependency on the nanoparticle size

Metal-to-Insulator Transition

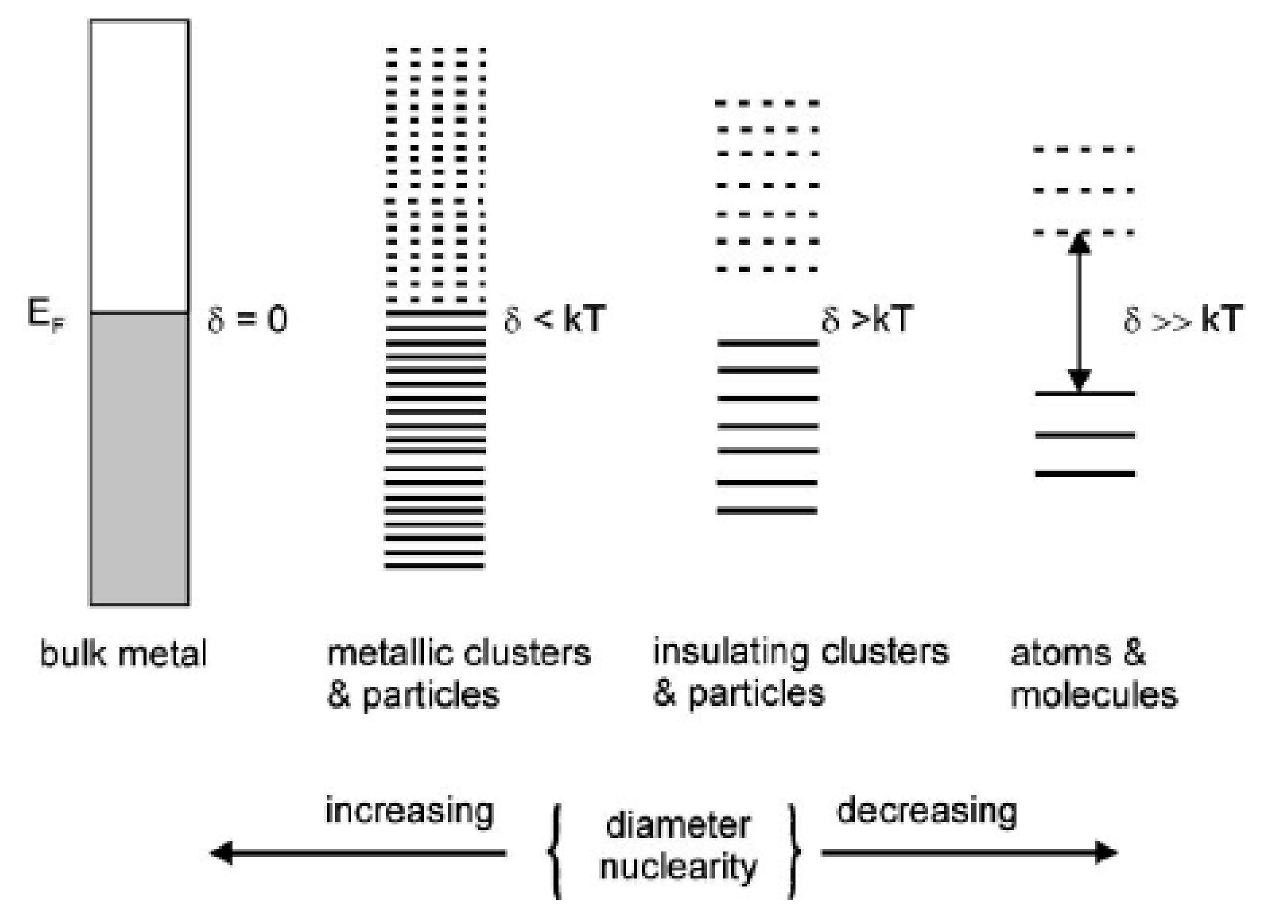

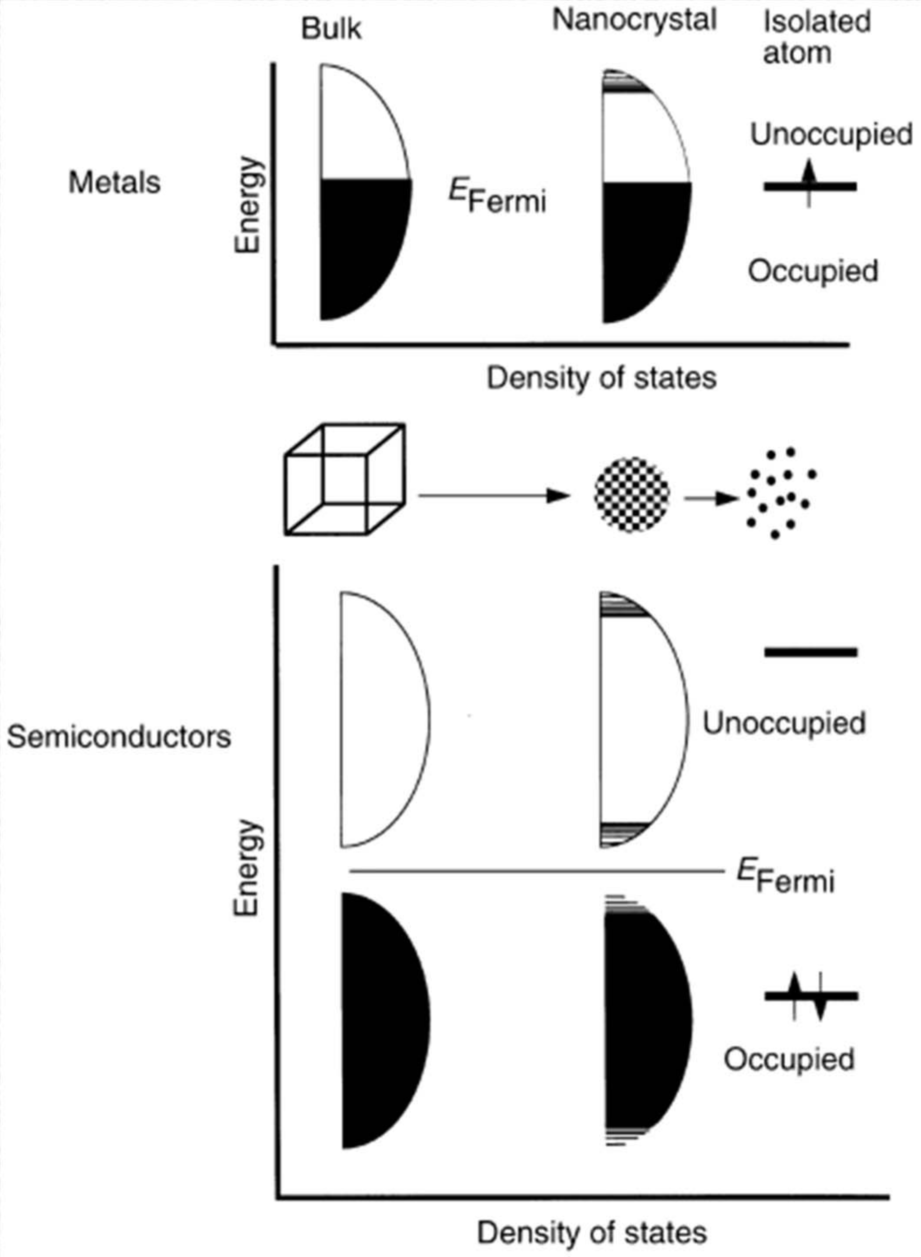
Bulk
Nanocrystal
Isolated atom
Metals
Energy
Unoccupied
E_{Fermi}
Occupied
Density of states
Semiconductors
Energy
Unoccupied
E_{Fermi}
Occupied
Density of states

Metal-to-Insulator Transition

Band gap increases with decreasing size

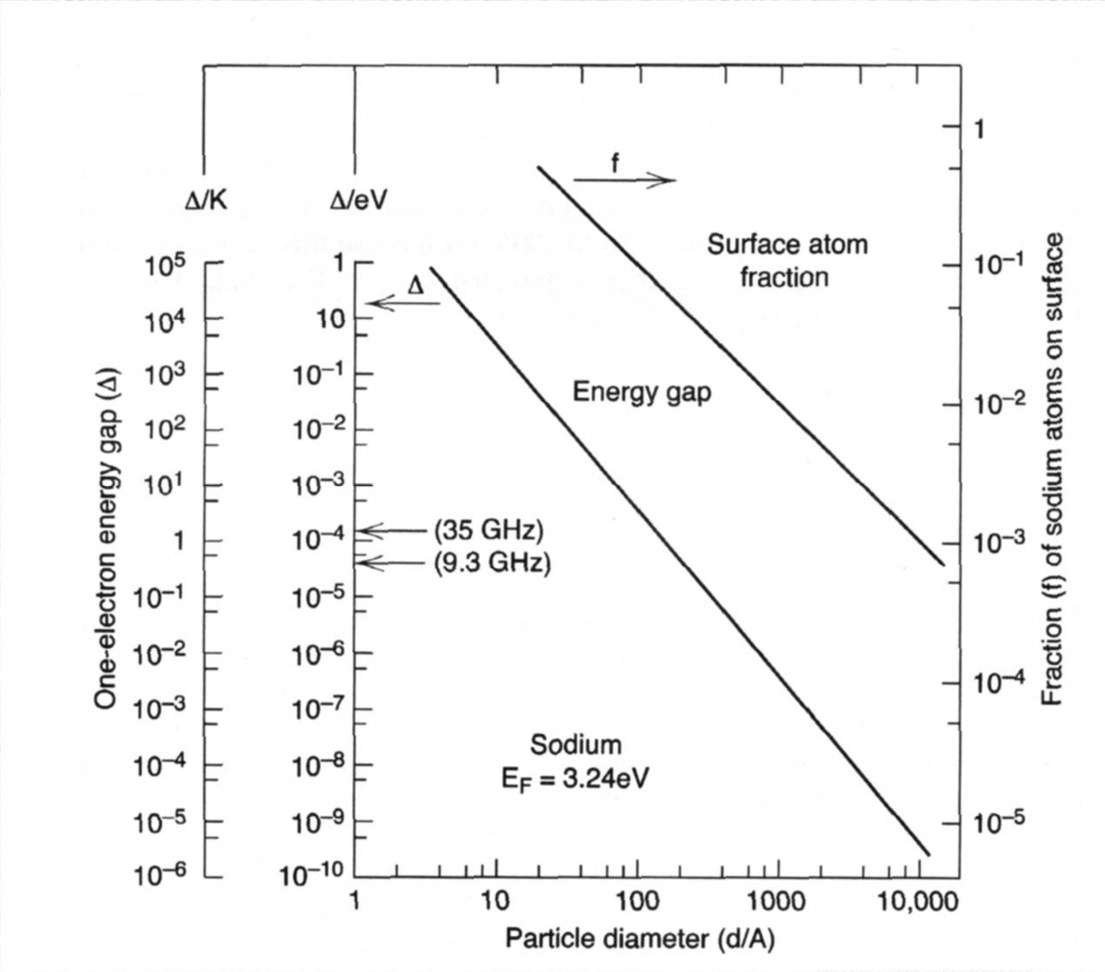

Metallic behavior
Single atom cannot behave as a metal
nonmetal to metal transition
100-1000 atoms

Magnetic behavior
Single domain particles
large coercive field

Metal-to-Insulator Transition

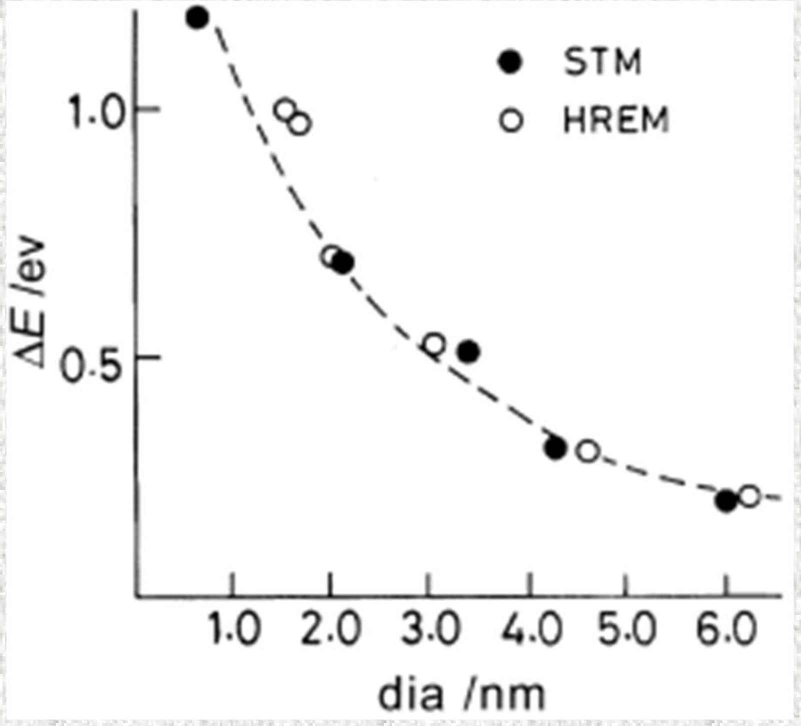

The increase in the core-level binding energy in small particles
poor screening of the core charge

the size-induced metal-nonmetal transition in nanocrystals

Variation of the shift, Δ*E*, in the core-level binding energy (relative to the bulk metal value) of Pd with the nanoparticle diameter

Electrical Conductivity

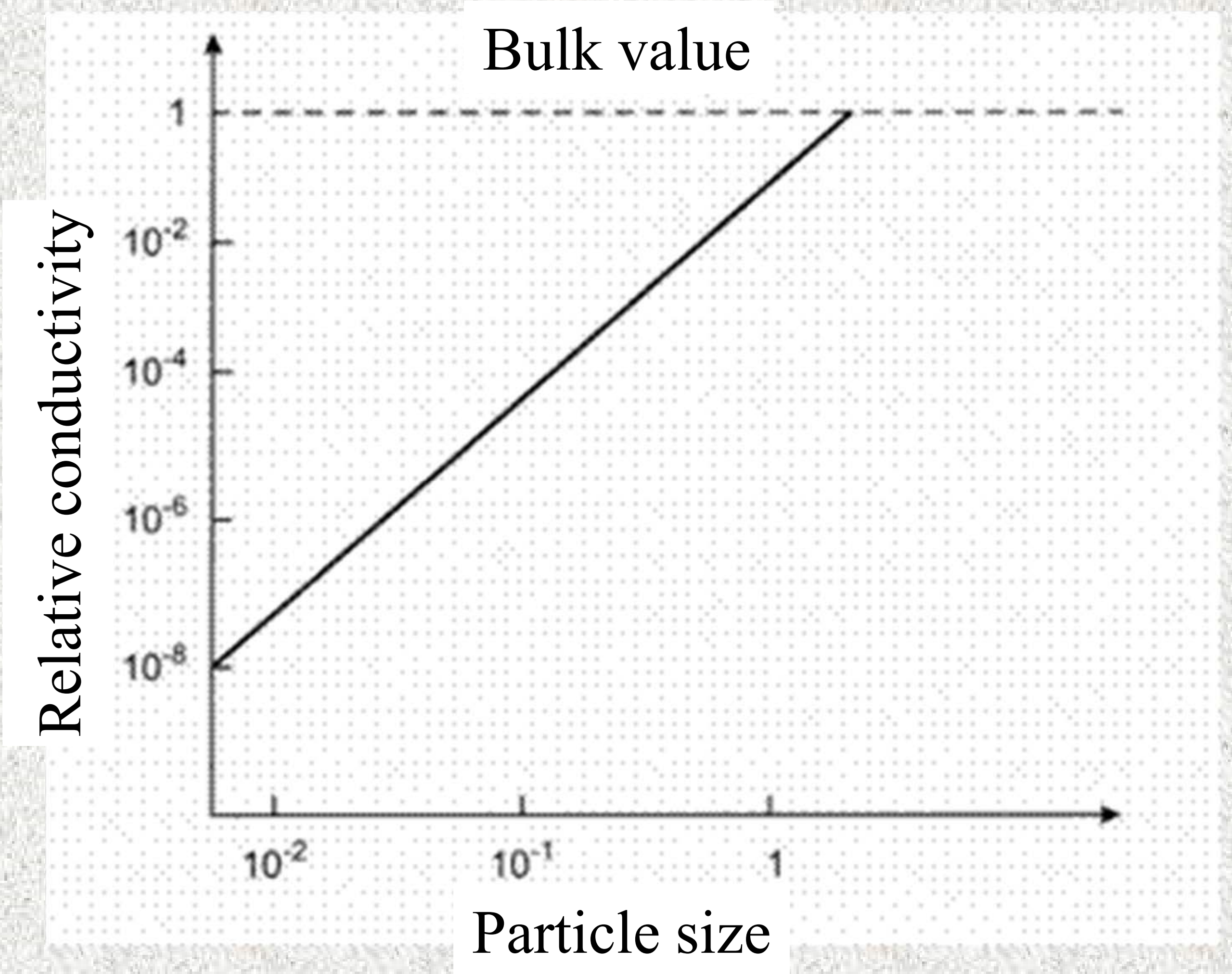

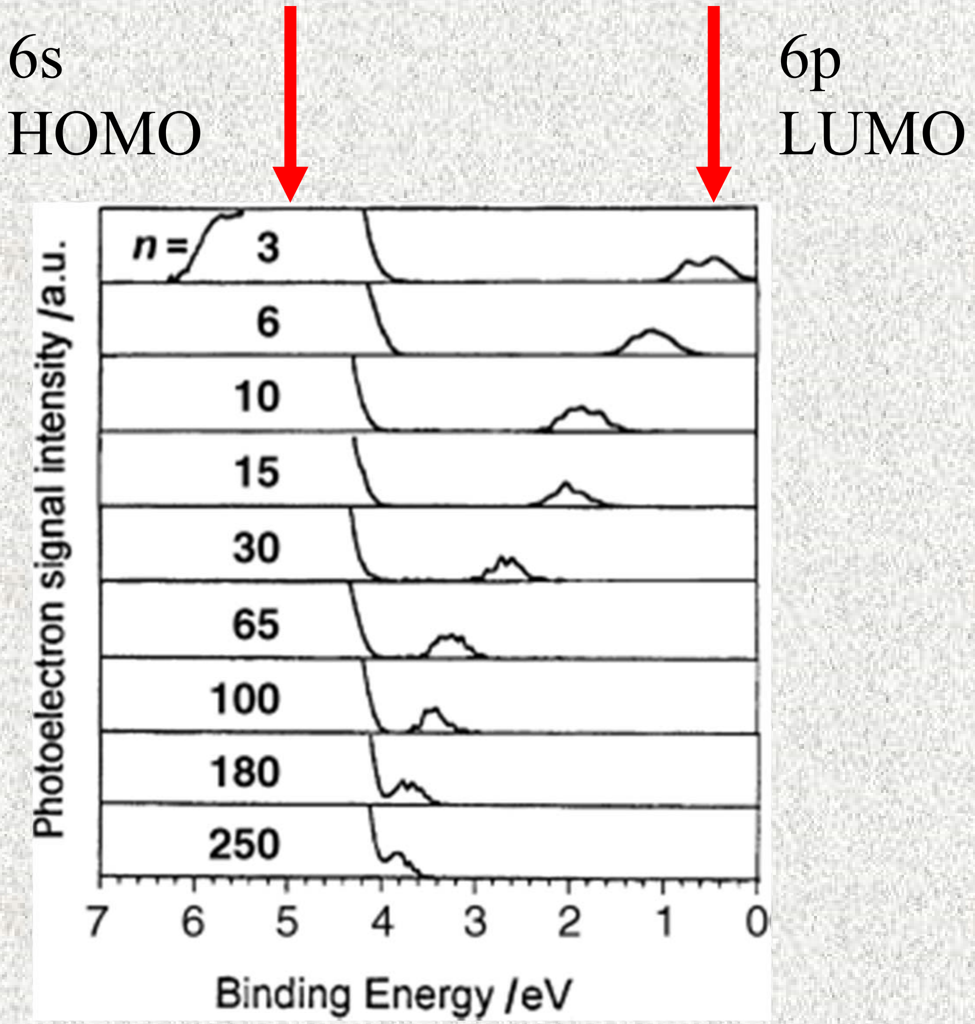

Photoelectron spectra of Hg clusters of nuclearity n
The 6p peak moves gradually towards the Fermi level
the band gap shrinks with increase in cluster size

a) Absorption spectra of CdSe nanocrystals (at 10 K) of various diameters

b) Wavelength of the absorption threshold and band gap as a function of the particle diameter for various semiconductors. The energy gap in the bulk state in parenthesis

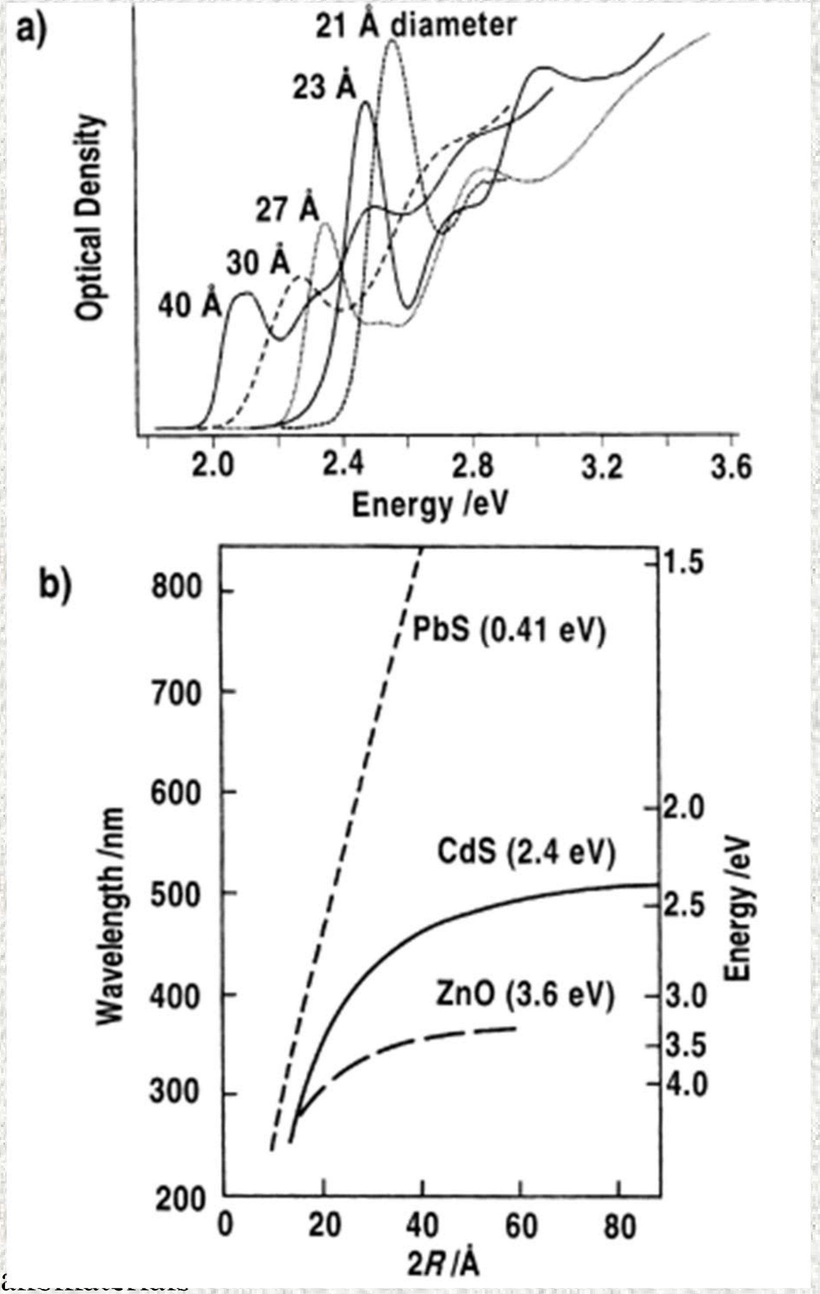

Quantum Confinement Effects

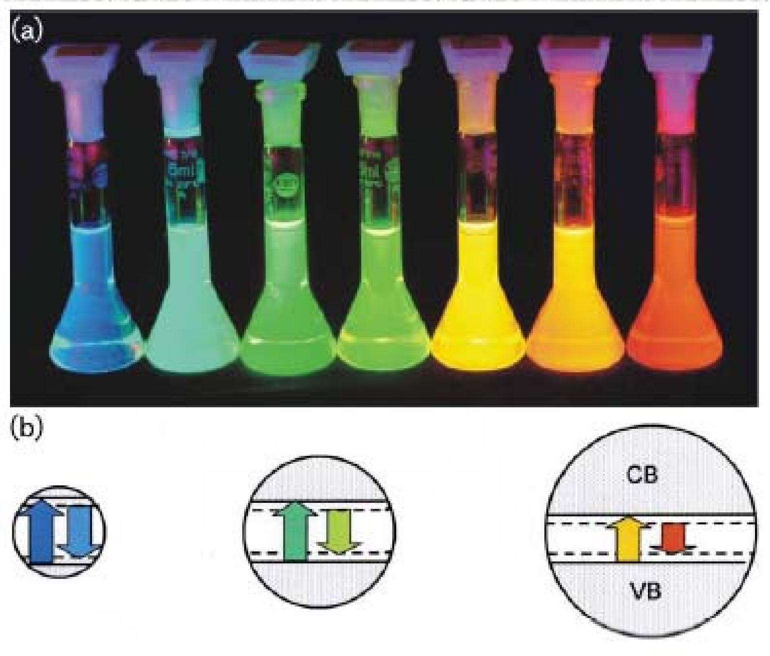

Fluorescence of CdSe–CdS core–shell nanoparticles with a diameter of 1.7 nm (blue) up to 6 nm (red)

Smaller particles have a wider band gap

Bohr Radii

Quantum confinement - particles must be smaller than the Bohr radius of the electron-hole pair

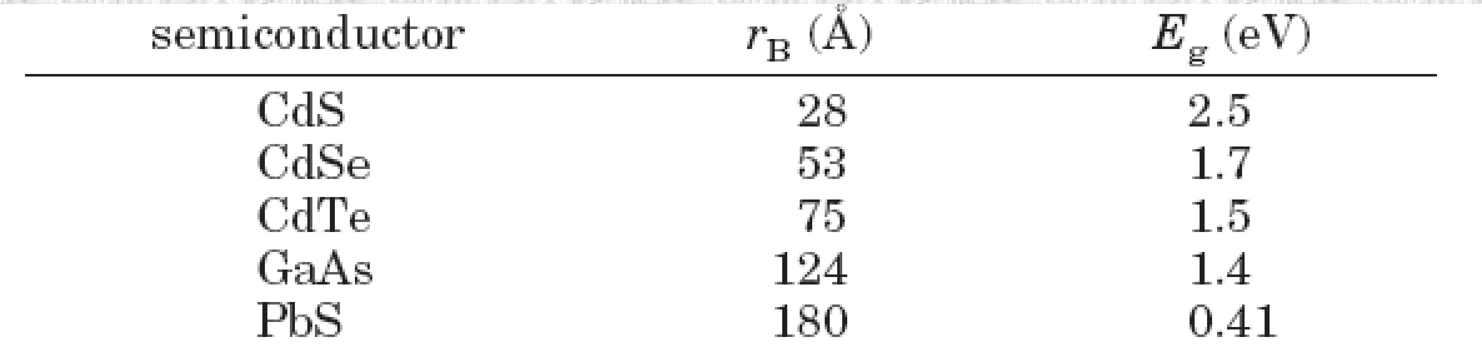

semiconductor	r_B (Å)	E_g (eV)
CdS	28	2.5
CdSe	53	1.7
CdTe	75	1.5
GaAs	124	1.4
PbS	180	0.41

Quantum Confinement Effects

Ⓟ Optical properties
nc-TiO_2 is transparent

Blue shift in optical spectra of nanoparticles

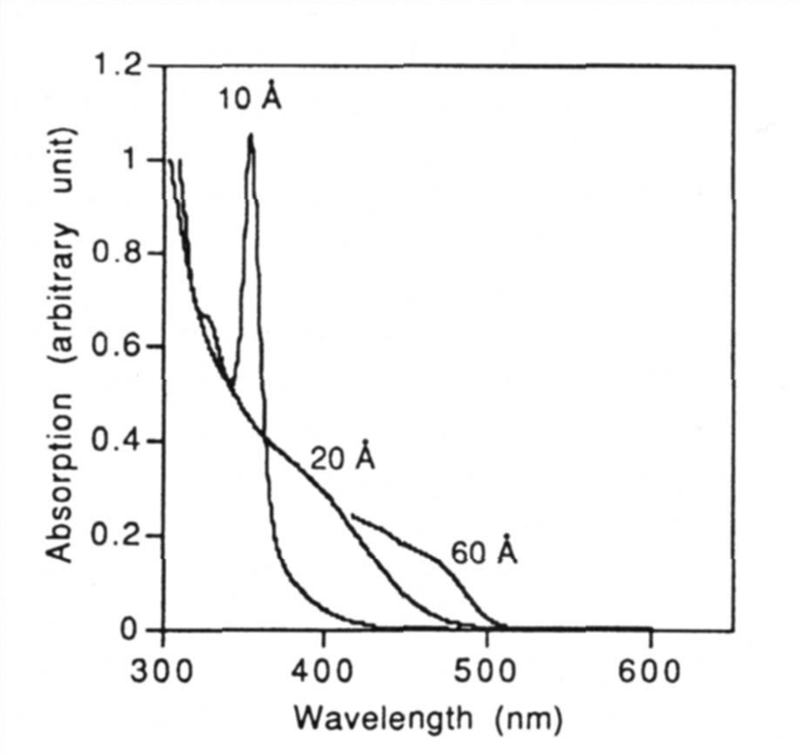

a) Variation of the nonmetallic band gap with nanocrystal size

b) in CdS nanocrystals

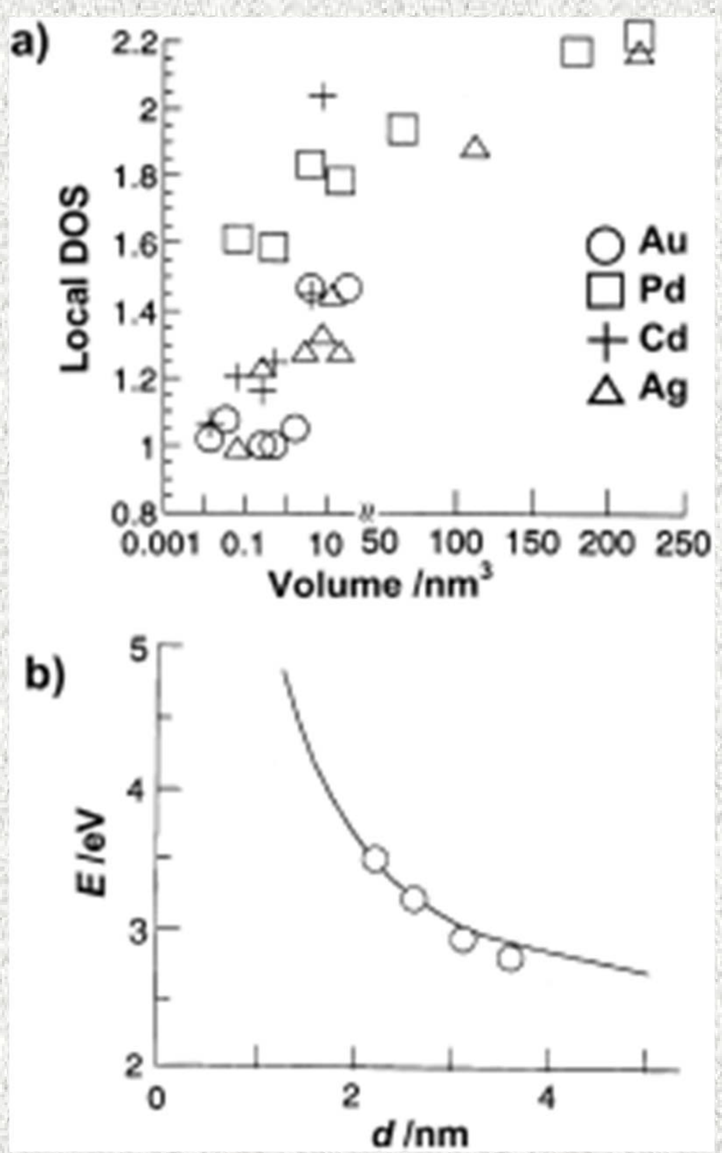

Nanoscopic Materials

NANO -particles, crystals, powders
-films, patterned films
-wires, rods, tubes
-dots

Nanostructured materials = nonequilibrium character

- ➢good sinterability
- ➢high catalytic activity
- ➢difficult handling
- ➢adsorption of gases and impurities
- ➢poor compressibility

PREPARATION METHODS

Top-down: from bulk to nanoparticles
Bottom-up: from atoms to nanoparticles

Preparation Methods

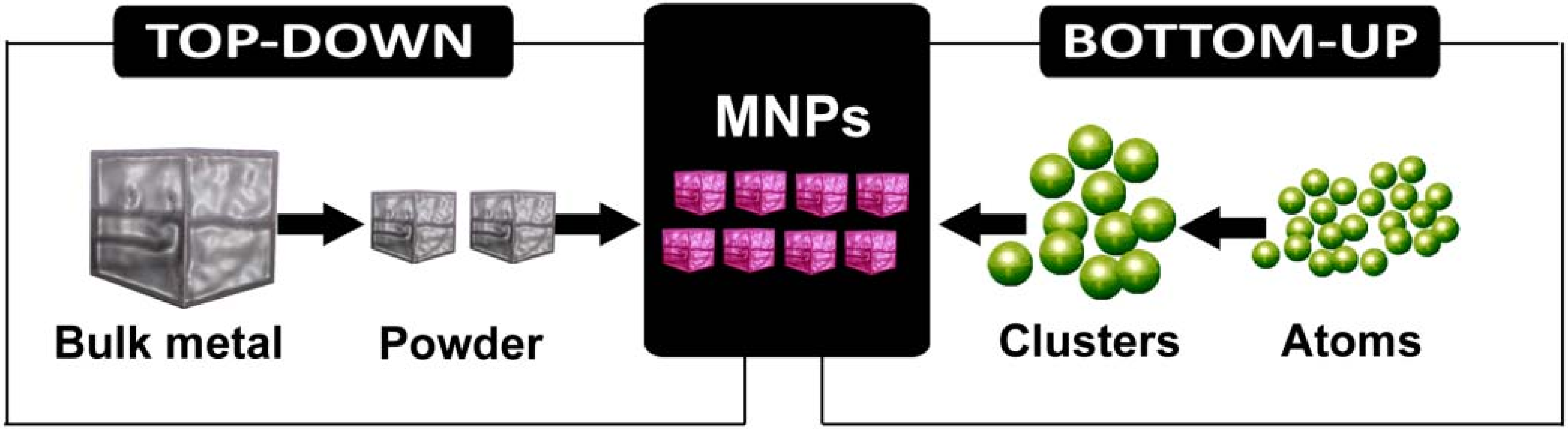

Top-down: from bulk to nanoparticles

Bottom-up: from atoms to nanoparticles

Bottom-up Synthesis: Atom Up

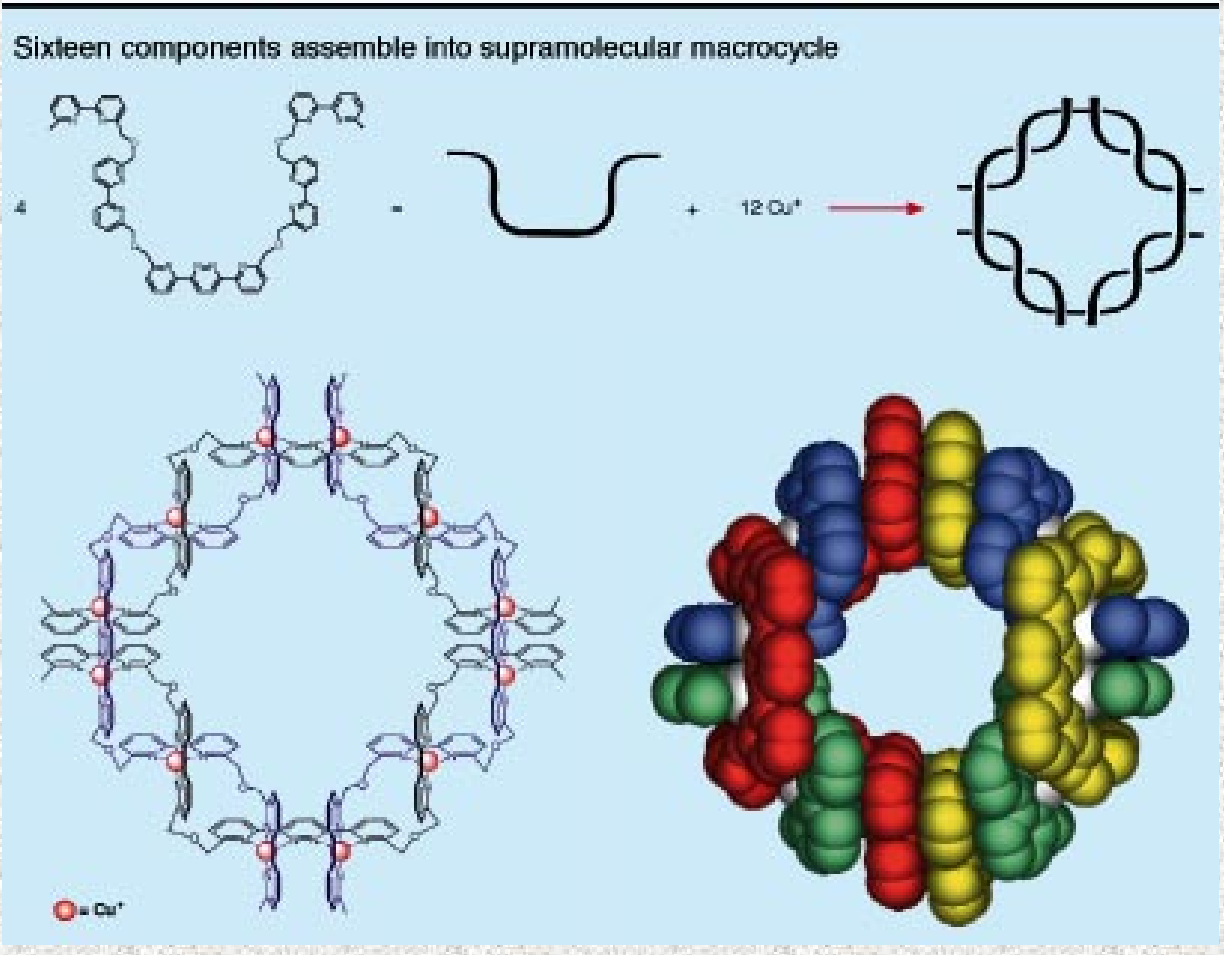
Sixteen components assemble into supramolecular macrocycle

NANOSTRUCTURAL MATERIALS

Bottom-up Synthesis

🛠 **Atom Aggregation Method**

GEM – gas evaporation method

- ✧ **evaporation by heating – resistive, laser, plasma, electron beam, arc discharge**
- ✧ **the vapor nucleates homogeneously owing to collisions with the cold gas atoms**
- ✧ **condensation**
  - **in an inert gas (He, Ar, 1kPa) on a cold finger, walls - metals, intermetallics, alloys, SiC, C_{60}**

in a reactive gas	**O_2**	**TiO_2, MgO, Al_2O_3, Cu_2O**
	N_2, NH_3	**nitrides**

in an organic solvent matrix

NANOSTRUCTURAL MATERIALS

Bottom-up Synthesis

SMAD – the solvated metal atom dispersion
1 – 2 g of a metal, 100 g of solvent, cooled with liquid N_2
more polar solvent (more strongly ligating) gives smaller particles
Ni powder: THF < toluene < pentane = hexane

Carbide formation

$$\text{Ni(g)} + \text{pentane} \xrightarrow{\text{77 to 300 K}} \text{Ni}_x\text{C}_y\text{H}_z \xrightarrow{\text{180 °C, octane}} \text{Ni}_3\text{C}$$

NANOSTRUCTURAL MATERIALS

Bottom-up Synthesis

- **Thermal or Sonocative Decomposition of Precursors**

$Fe(CO)_5 \longrightarrow$ nc-Fe + 5 CO sono

$[Co(en)_3]WO_4 \longrightarrow$ nc-WC – 23% Co

$PhSi(OEt)_3 + Si(OEt)_4 + H_2O \longrightarrow gel \xrightarrow{\text{Ar, 1500 °C}} \beta\text{-SiC}$

$(CH_3SiHNH)_n\,(l) \longrightarrow Si_3N_4 + SiC$ laser

$M(BH_4)_4\,(g) \xrightarrow{300\text{-}400°C}$ borides MB_{2+x} (M = Ti, Zr, Hf)

$Si(OEt)_4 + Ag^+ \text{ or } Cu^{2+} + H_2O \longrightarrow SiO_2/Ag^+/Cu^{2+}$

$\xrightarrow{H_2,\ 550\ °C} SiO_2/Ag/Cu$

NANOSTRUCTURAL MATERIALS

Bottom-up Synthesis

🛠 **Reduction of Metal Ions**

Borohydride Reduction - Manhattan Project

Aqueous, under Ar

$2\ Co^{2+} + 4\ BH_4^- + 9\ H_2O \longrightarrow Co_2B + 12.5\ H_2 + 3\ B(OH)_3$

Under air

$4\ Co_2B + 3\ O_2 \longrightarrow 8\ Co + 2\ B_2O_3$

Nonaqueous

$Co^{2+} + BH_4^- + \text{diglyme} \longrightarrow Co + H_2 + B_2H_6$

$TiCl_4 + 2\ NaBH_4 \longrightarrow TiB_2 + 2\ NaCl + 2\ HCl + H_2$

$MX_n + n\ NR_4[BEt_3H] \longrightarrow M + NR_4X + n\ BEt_3 + n/2\ H_2$

M = group 6 to 11; n = 2,3; X = Cl, Br

mixed-metal particles

NANOSTRUCTURAL MATERIALS

Bottom-up Synthesis

Au colloidal particles

$HAuCl_4$ + $NaBH_4$ in toluene/H_2O system, TOABr as a phase transfer agent, Au particles in the toluene layer, their surface covered with Br, addition of RSH gives stable Au colloid

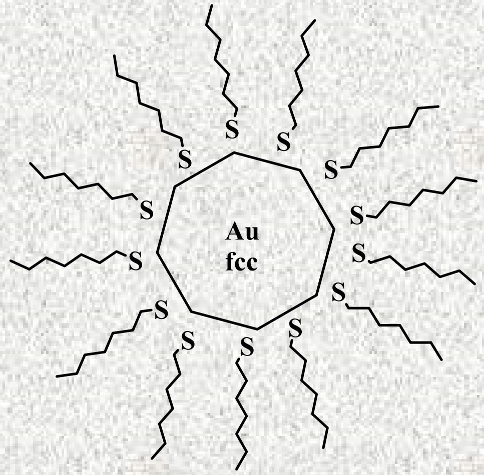

Bottom-up Synthesis

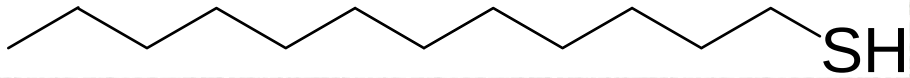

Two-dimensional array of thiol-derivatised Au particles (mean diam 4.2 nm)

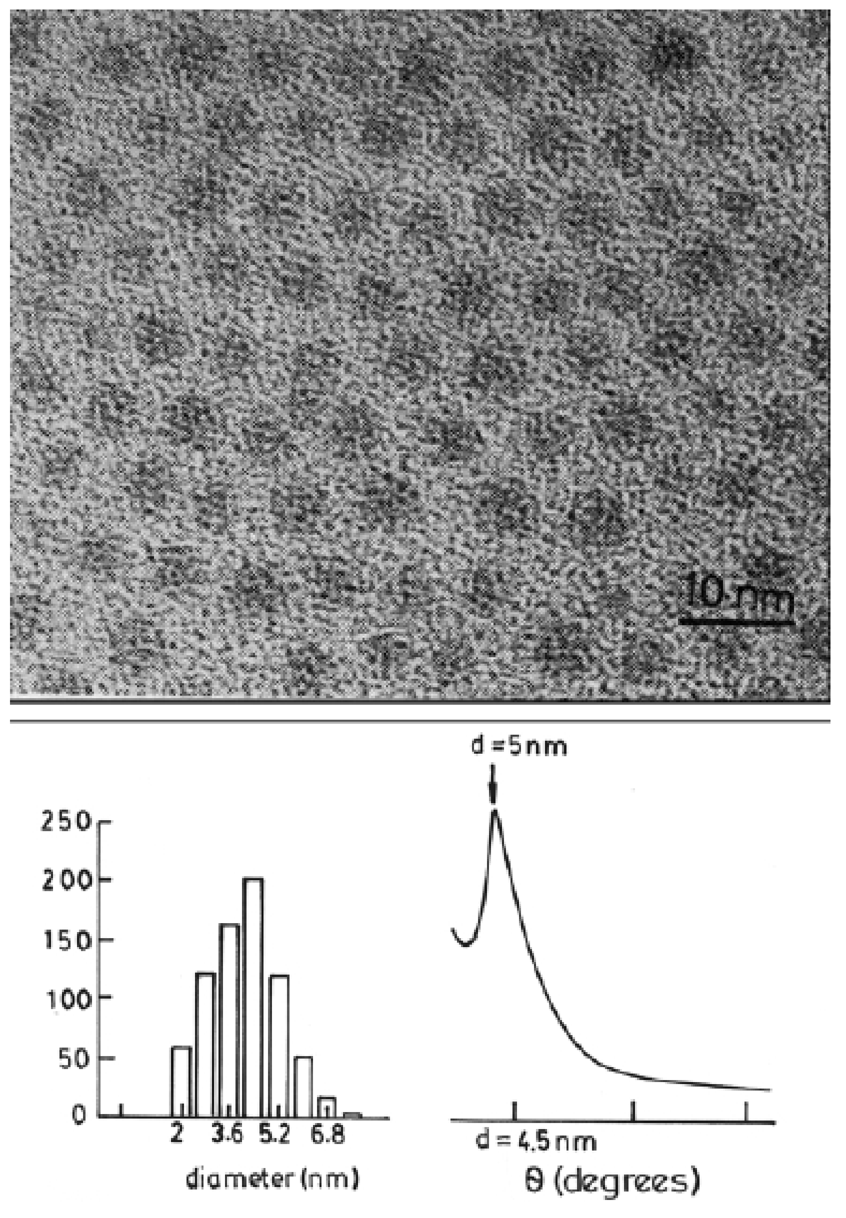

TEM micrograph of hexagonal arrays of thiolized Pd nanocrystals:

a) 2.5 nm, octane thiol

b) 3.2 nm, octane thiol

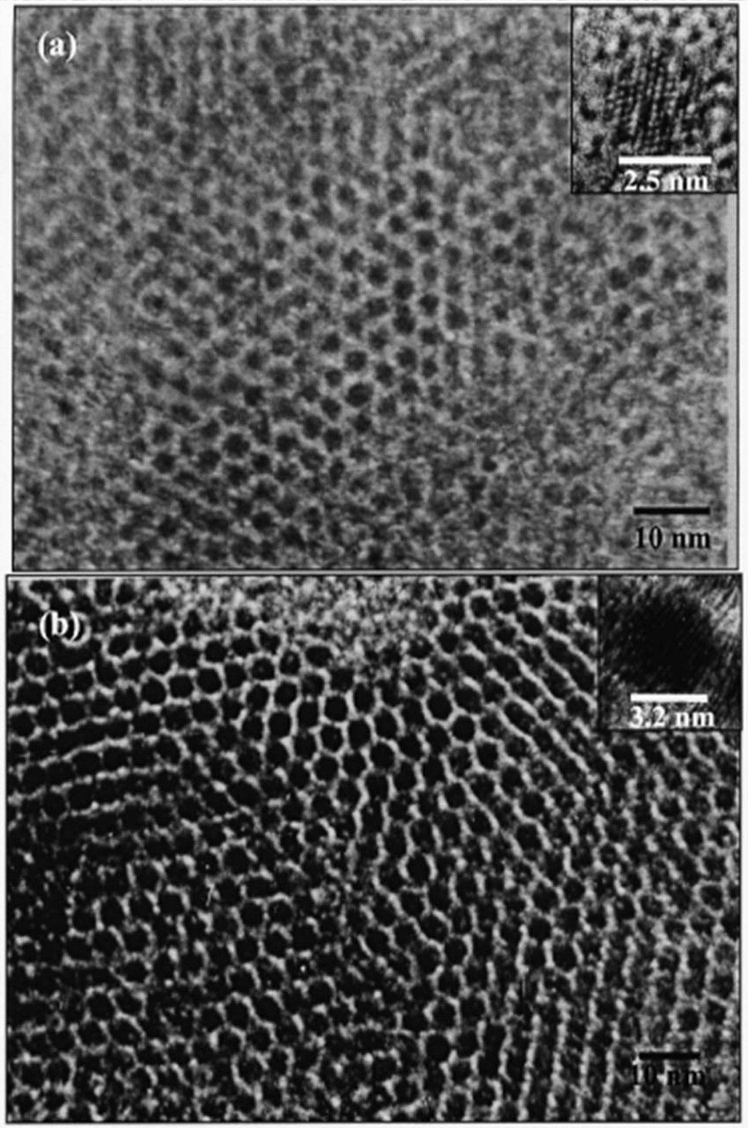

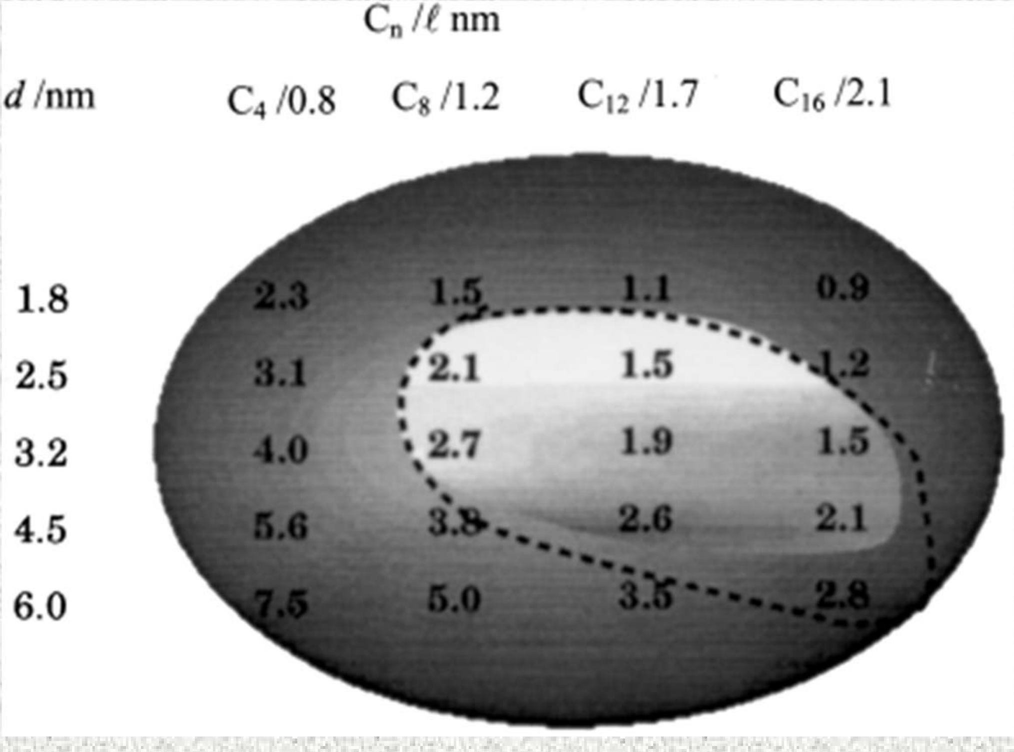

	C_n /ℓ nm			
d /nm	C_4 /0.8	C_8 /1.2	C_{12} /1.7	C_{16} /2.1
1.8	2.3	1.5	1.1	0.9
2.5	3.1	2.1	1.5	1.2
3.2	4.0	2.7	1.9	1.5
4.5	5.6	3.8	2.6	2.1
6.0	7.5	5.0	3.5	2.8

The *d-l* phase diagram for Pd nanocrystals thiolized with different alkane thiols.

The mean diameter, *d*, obtained by TEM.
The length of the thiol, *l*, estimated by assuming an all-*trans* conformation of the alkane chain.
The thiol is indicated by the number of carbon atoms, C_n.

The bright area in the middle encompasses systems which form close-paced organizations of nanocrystals. The surrounding darker area includes disordered or low-order arrangements of nanocrystals. The area enclosed by the dashed line is derived from calculations from the soft sphere model

NANOSTRUCTURAL MATERIALS

Alkali Metal Reduction

in dry anaerobic diglyme, THF, ethers, xylene

$NiCl_2 + 2\,K \rightarrow Ni + 2\,KCl$

$AlCl_3 + 3\,K \rightarrow Al + 3\,KCl$

Reduction by Glycols or Hydrazine

“Organically solvated metals”

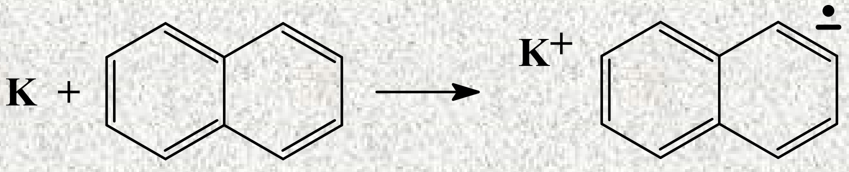

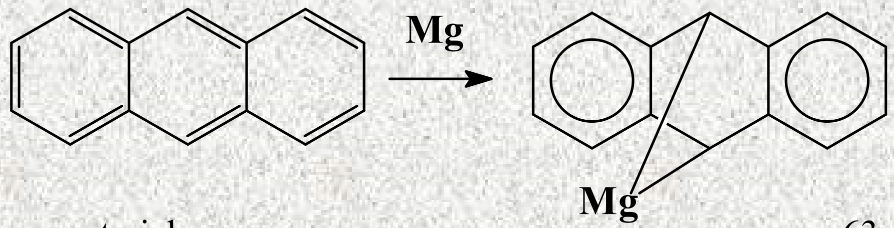

Alkalide Reduction

$13\ K^+(15\text{-crown-}5)_2Na^- + 6\ FeCl_3 + 2CBr_4$

THF $\Big\downarrow$ –30 °C

$2\ Fe_3C$ (nano) $+ 13\ K(15\text{-crown-}5)_2Cl_{0.43}Br_{0.57} + 13\ NaCl$

Anealed at 950 °C / 4 h

Fe_3C: 2 – 15 nm

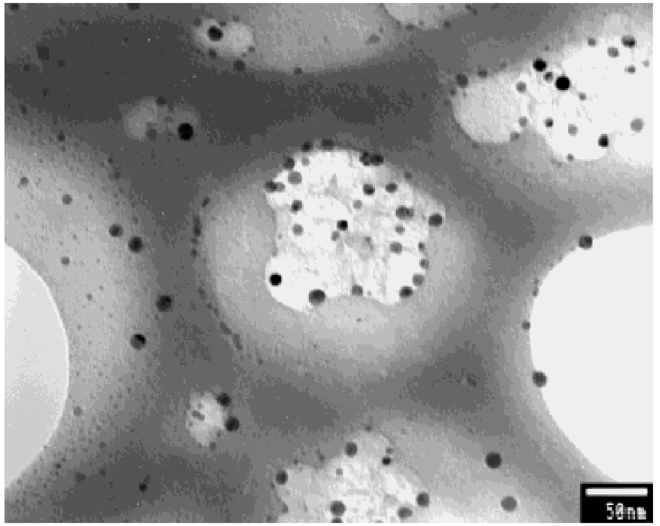

NANOSTRUCTURAL MATERIALS

Bottom-up Synthesis

🛠 **Reactions in Porous Solids – Zeolites, Mesoporous materials**

Ion exchange in solution, reaction with a gaseous reagent inside the cavities

$M^{2+} + H_2E \longrightarrow ME$ M = Cd, Pb; E = S, Se

Ship-in-the-Bottle Synthesis

Ru^{3+} + Na-Y $\longrightarrow$ Ru(III)-Y
Ru(III)-Y + 3 bpy $\longrightarrow$ $Ru(bpy)_3^{2+}$ reduction of Ru(III)

Conducting carbon wires
Acrylonitrile introduced into MCM-41 (3 nm diam. channels)
Radical polymerization
Pyrolysis gives carbon filaments

NANOSTRUCTURAL MATERIALS

Bottom-up Synthesis

- **Gel or Polymer Matrices**

- **Sol-Gel Method**

Aerogels, supercritical drying

- **Aerosol Spray Pyrolysis**

Aqueous solution, nebulization, droplet flow, solvent evaporation, chemical reaction, particle consolidation, up to 800 °C

$$3Gd(NO_3)_3 + 5\ Fe(NO_3)_3 \longrightarrow Ga_3Fe_5O_{12} + 6\ O_2 + 24\ NO_2$$

$$MnCl_2 + 2\ FeCl_3 + 4\ H_2O \longrightarrow MnFe_2O_4 + 8\ HCl$$

$Mn(NO_3)_2 + Fe(NO_3)_3$ **no go, why?**

$$2\ MCl_n\ (g) + n\ H_2 \xrightarrow{850\text{-}900\ °C} \underset{3\text{-}11\ \mathrm{nm}}{M^0} + 2n\ HCl$$

NANOSTRUCTURAL MATERIALS

Bottom-up Synthesis

- Inverse Micelles

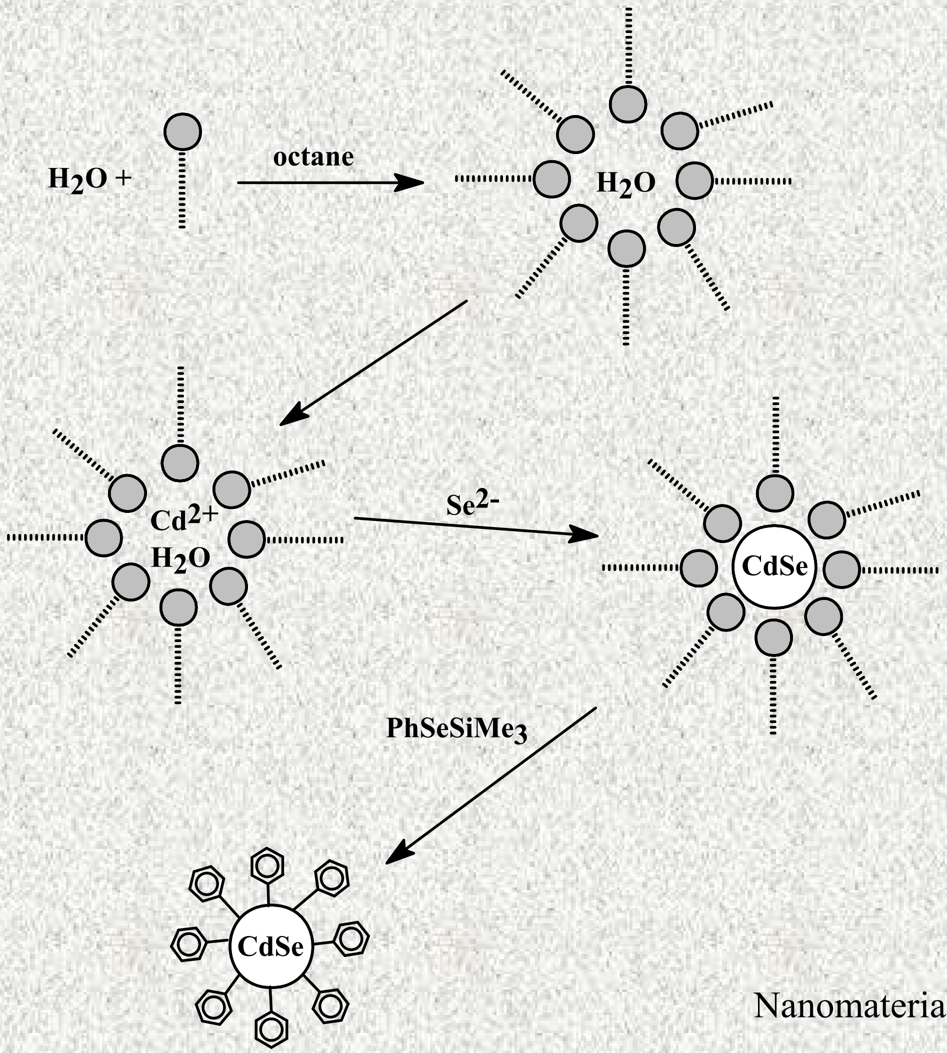

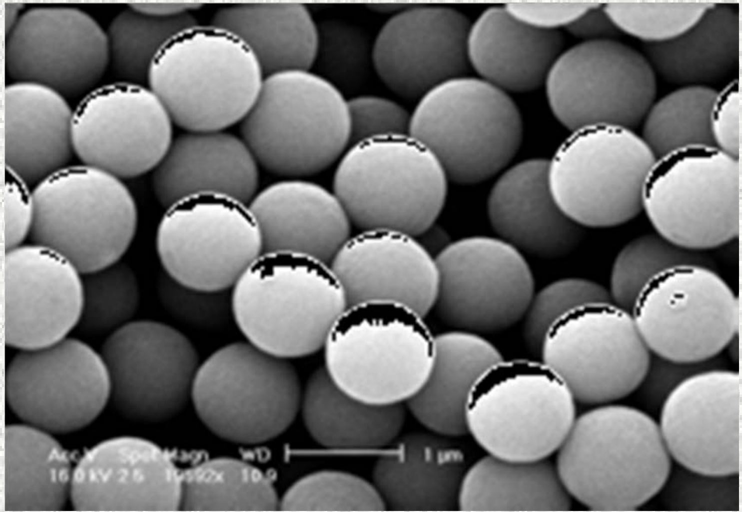

Bottom-up Synthesis

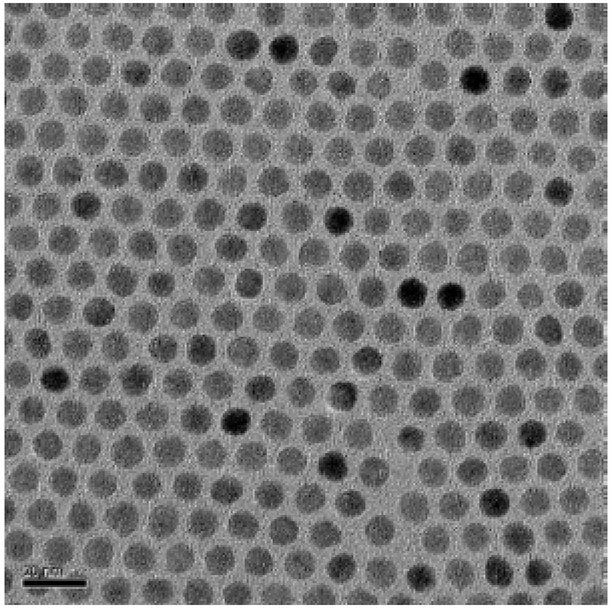

Number of counted particles: 204
Average size: 9.04 nm
Standard deviation: 0.33 nm (3.7%)

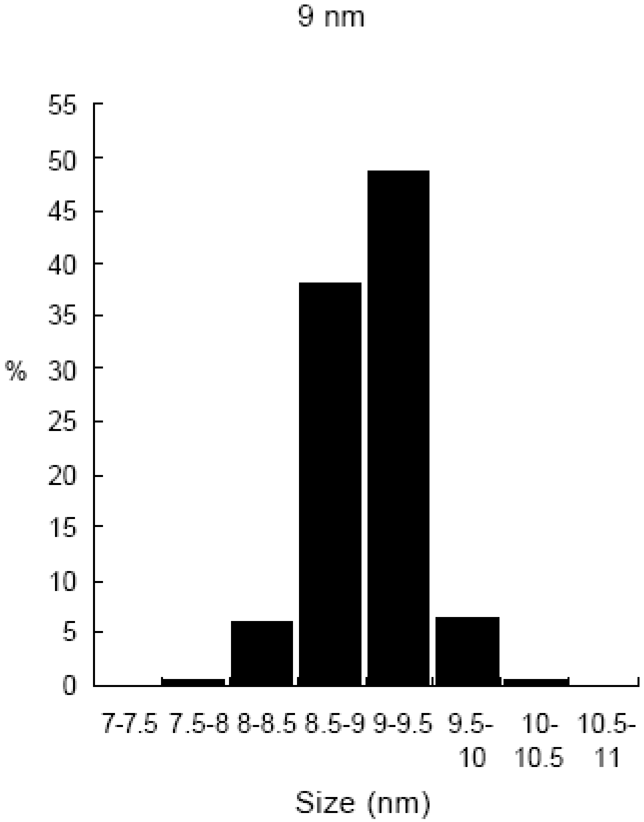

Bottom-up Synthesis

Phase Control

$[N^{n}Bu_4]_2[Fe_4S_4(SPh)_4]$

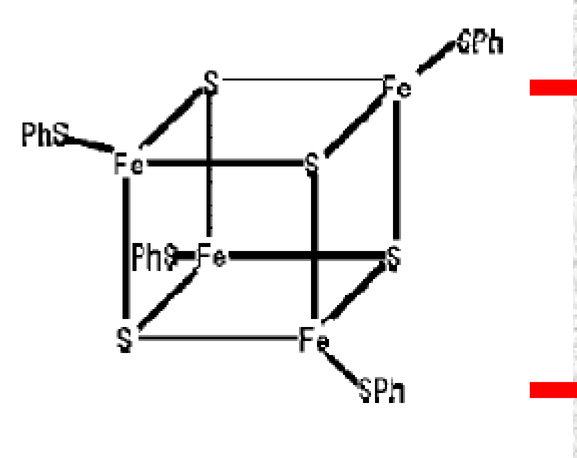

180 °C in octylamine

pyrrhotite Fe_7S_8

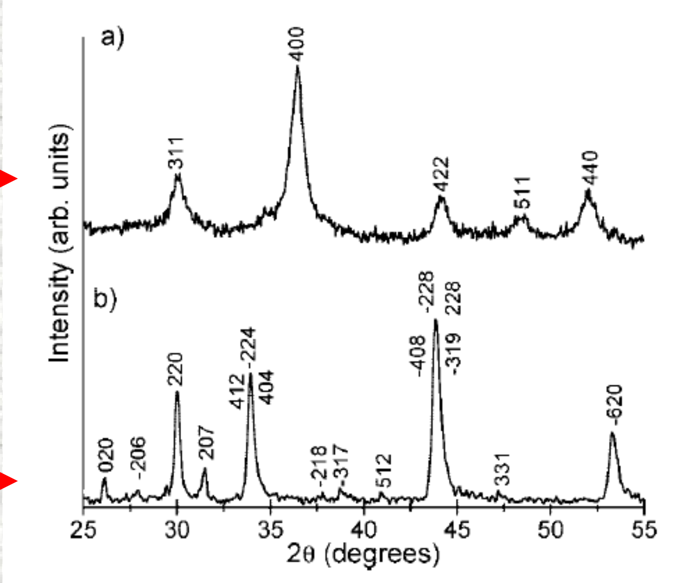

200 °C in dodecylamine

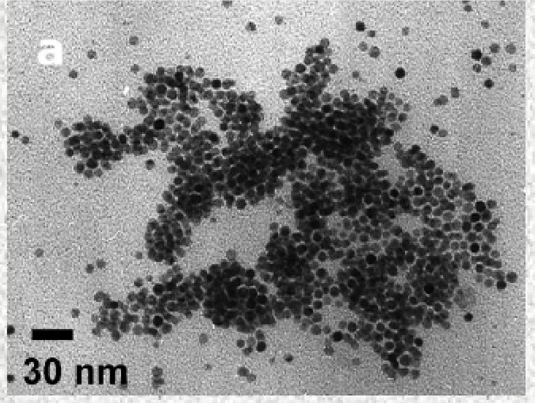

greigite Fe_3S_4

thiospinel, the sulfide analogue of magnetite

Polymeric Nanoparticles from Rapid Expansion of Supercritical Fluid Solution

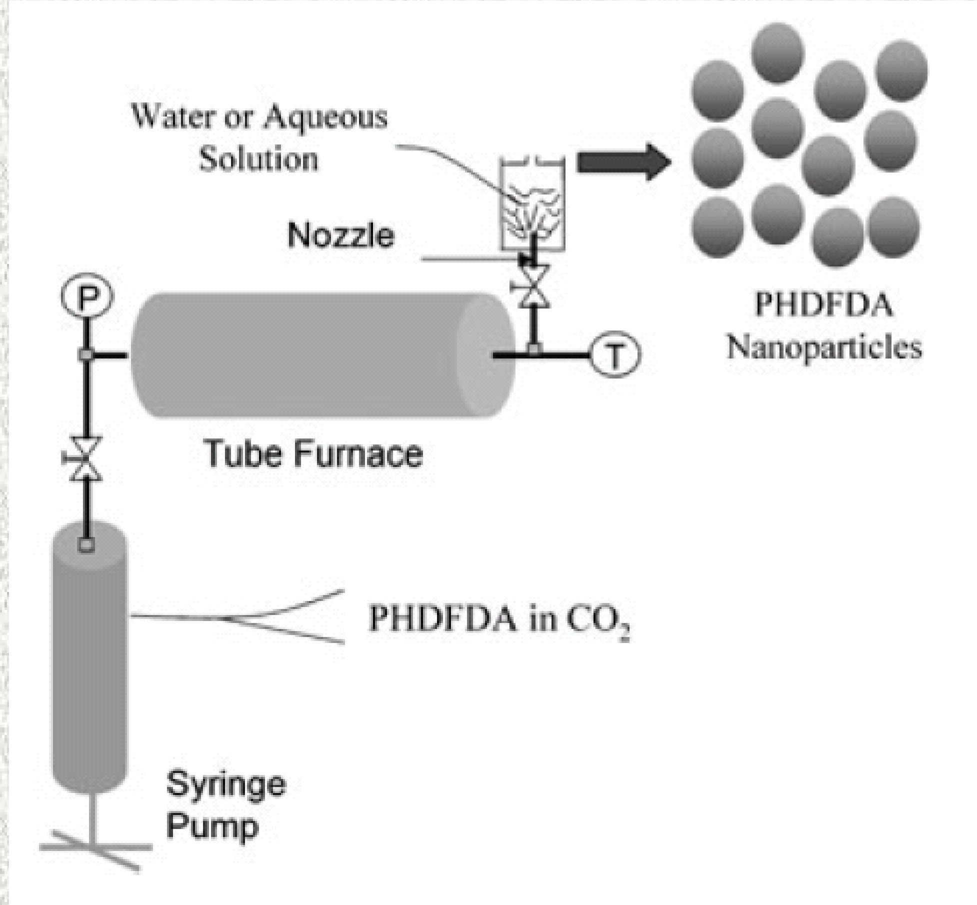

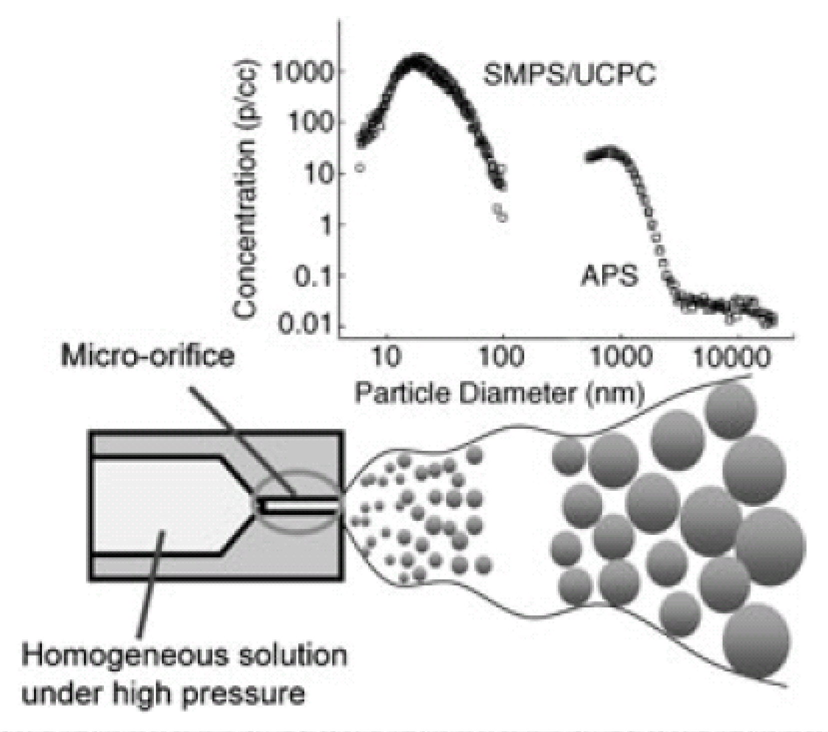

Polymeric Nanoparticles from Rapid Expansion of Supercritical Fluid

Solution

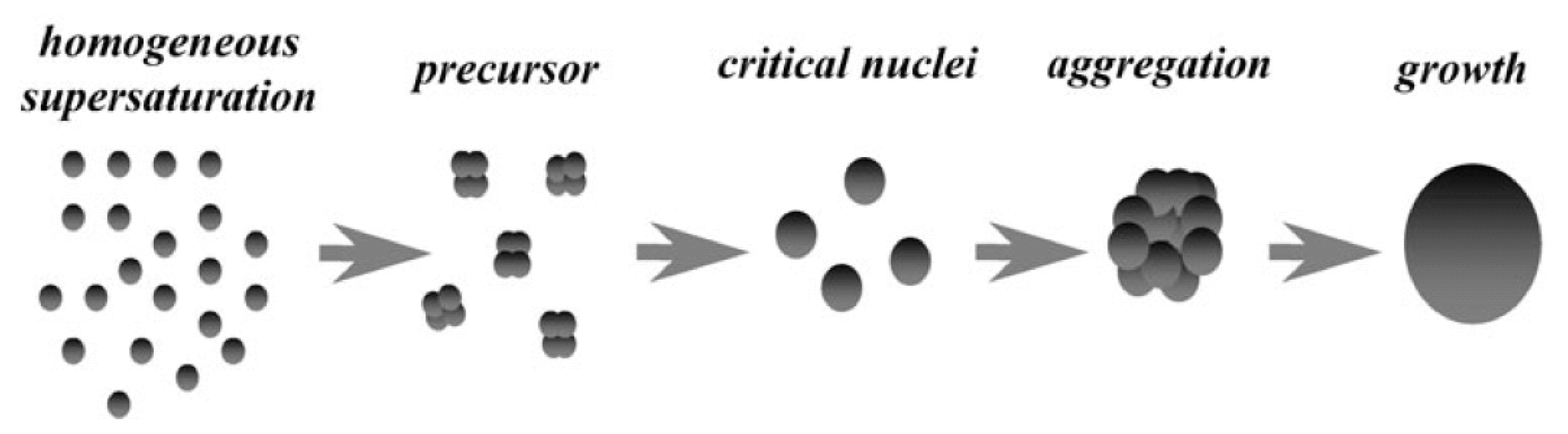

Nanoparticles *via* Spray-drying

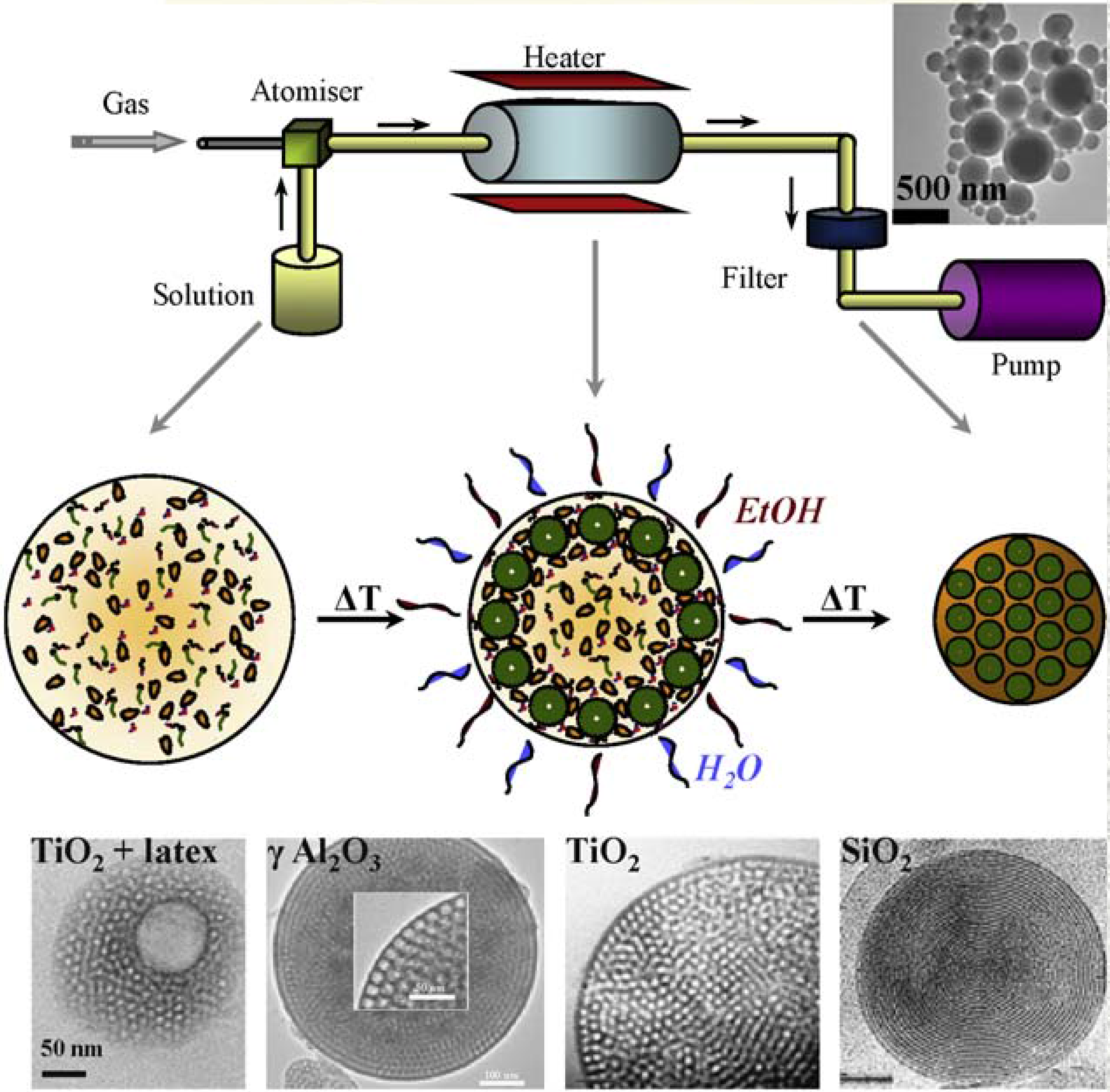

Spinning Disc Processing (SDP)

A rapidly rotating disc (300-3000 rpm)
Ethanolic solutions of $Zn(NO_3)_2$ and NaOH, polyvinylpyrrolidone (PVP) as a capping agent
Very thin films of fluid (1 to 200 μm) on a surface
Synthetic parameters = temperature, flow rate, disc speed, surface texture influence on the reaction kinetics and particle size

Intense mixing, accelerates nucleation and growth,
affords monodispersed ZnO nanoparticles with controlled particle size down to a size of 1.3 nm and polydispersities of 10%

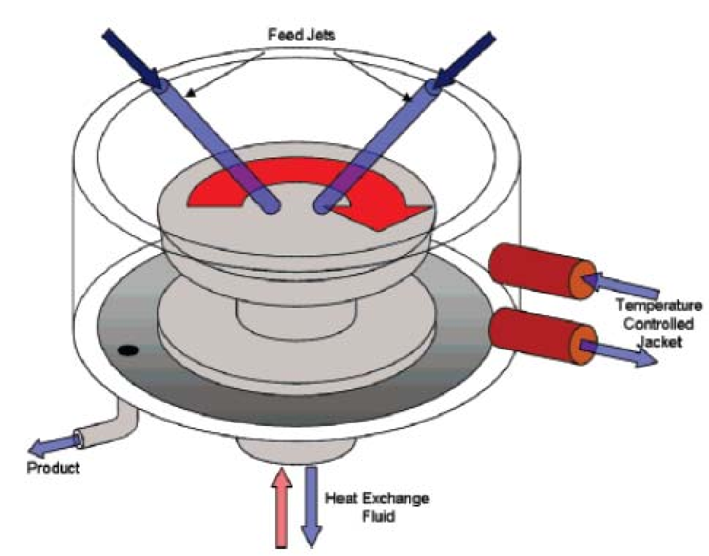

NANOSTRUCTURAL MATERIALS

Properties on Nanostructured Materials

Ⓟ Metallic behavior
Single atom cannot behave as a metal
nonmetal to metal transition : 100-1000 atoms

Ⓟ Magnetic behavior
Single domain particles, large coercive field

Ⓟ Depression of melting points in nanocrystals
bulk Au mp 1064 °C 10 nm Au 550 °C

LaMer mechanism

Supersaturated solution

Burst of nucleation

Slow growth of particles without additional nucleation

Separation of nucleation and growth

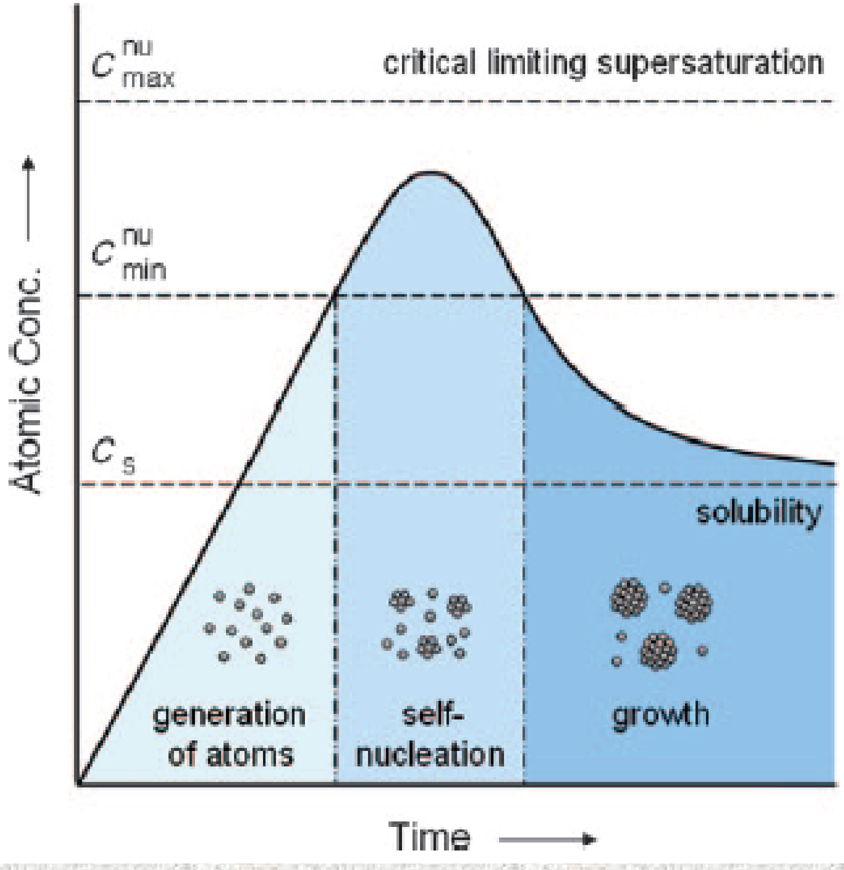

Watzky-Finke mechanism

Slow continuous nucleation

Fast autocatalytic surface growth

Seed-mediated mechanism

Au nanoclusters as seeds

Bi, Sn, In, Au, Fe, Fe_3O_4

Other mechanisms

Digestive rippening

Surfactant exchange

Thermal Decomposition of Precursors

$$Fe(CO)_5 \xrightarrow[\text{oleic acid, trioctylamine}]{350\ ^{o}C,\ 1\ h} Fe \xrightarrow[Me_3NO]{350\ ^{o}C,\ 1\ h} Fe_2O_3$$

6 nm

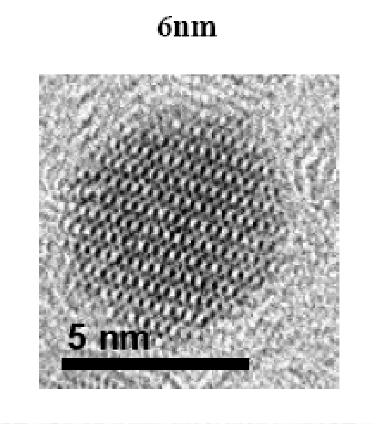

Separation of nucleation and growth

$Fe(CO)_5$ thermal decomposition at 100 ^{o}C contributes to nucleation

Fe(oleate) thermal decomposition at 350 ^{o}C contributes to growth

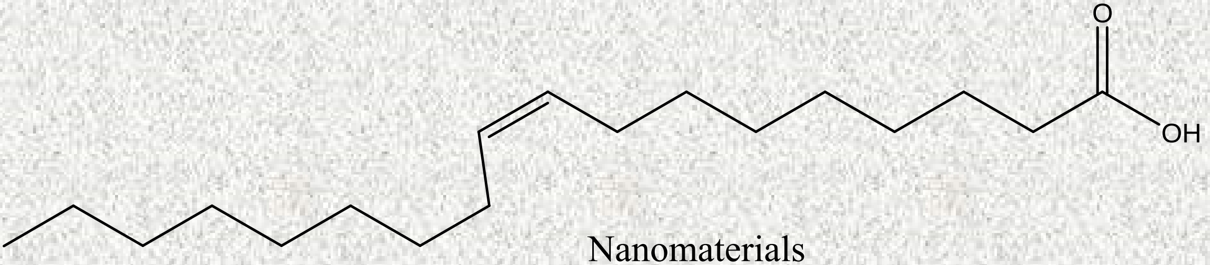

Surface Modification

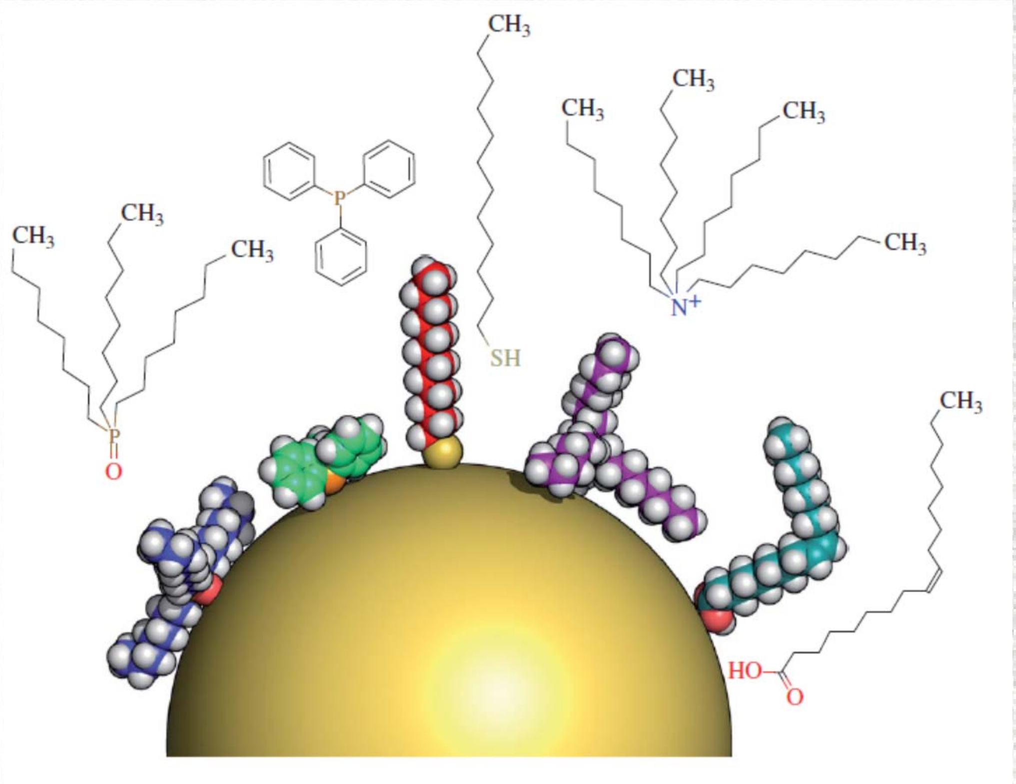

A nanoparticle of 5nm core diameter with different hydrophobic ligand molecules both drawn to scale.

The particle is idealized as a smooth sphere.

trioctylphosphine oxide (TOPO)
triphenylphosphine (TPP)
dodecanethiol (DDT)
tetraoctylammonium bromide (TOAB)
oleic acid (OA)

Top-down Synthesis: Bulk Down

🛠 **Introduction of Crystal Defects (Dislocations, Grain Boundaries)**

✧**High-Energy Ball Milling**

final size only down to 100 nm, contamination

✧ **Extrusion, Shear, Wear**

✧**High-Energy Irradiation**

✧ **Detonative Treatment**

🛠 **Crystallization from Unstable States of Condensed Matter**

✧ **Crystallization from Glasses**

✧**Precipitation from Supersaturated Solid or Liquid Solutions**

Top-down Synthesis: Bulk Down

🛠Lithographic Techniques

✧electron beam and focused ion beam (FIB) lithography

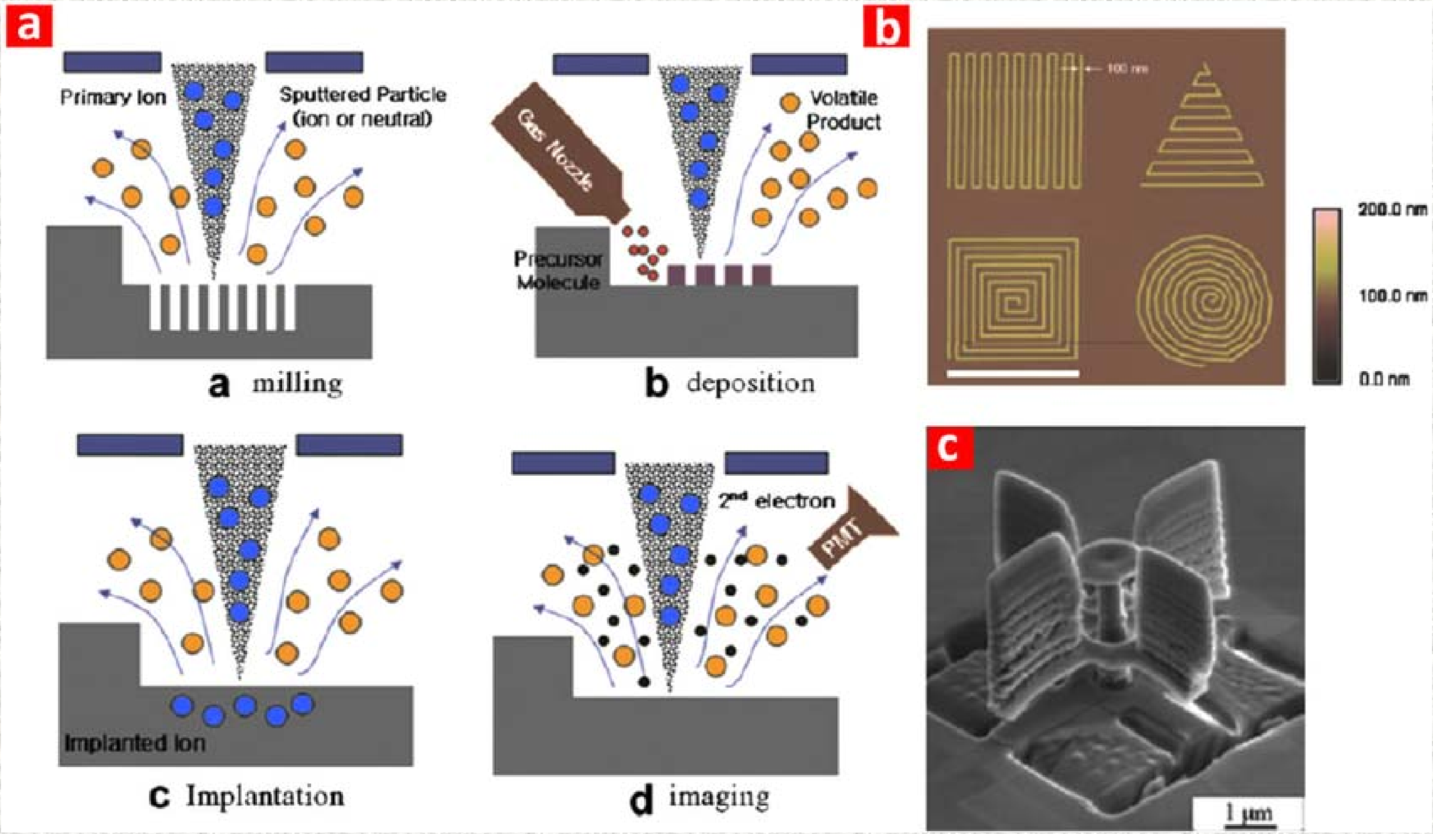

Top-down Synthesis: Bulk Down

🛠**Lithographic Techniques**

✧electron beam and focused ion beam (FIB) lithography

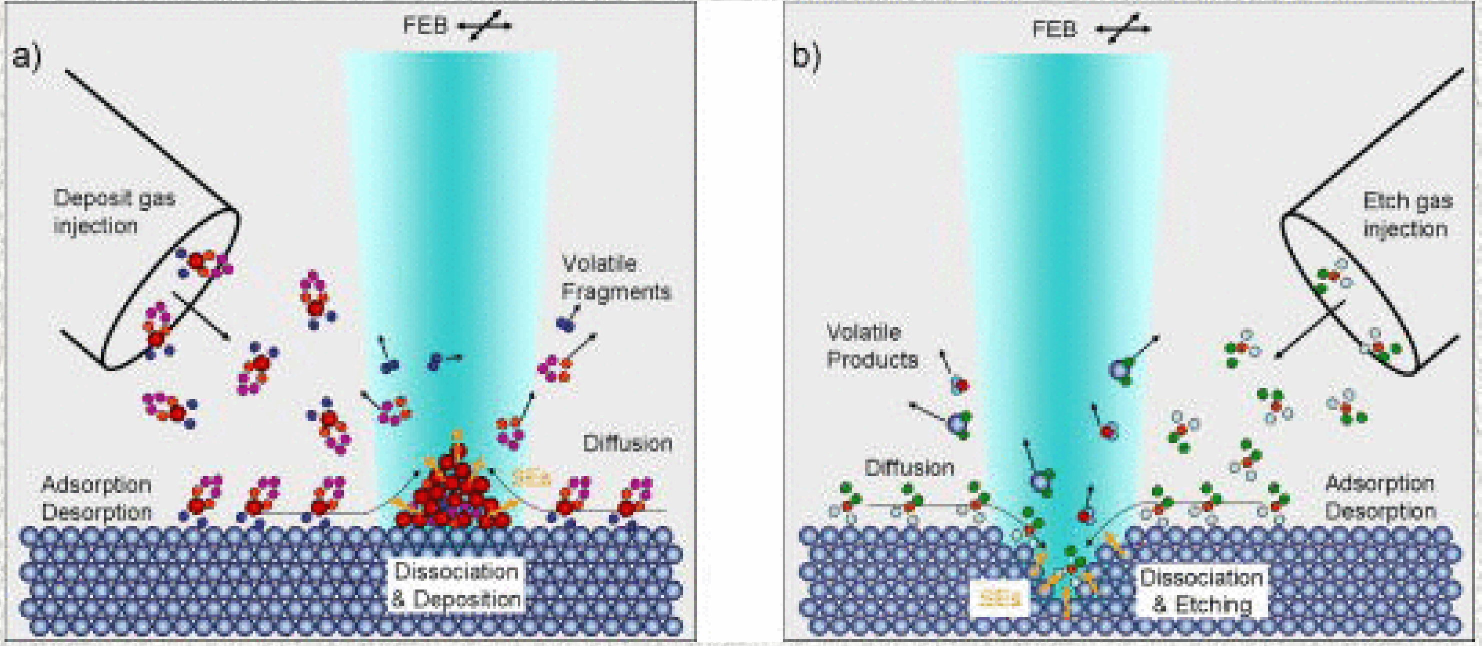

Nanocatalysis

Morphologies of bimetallic nanoparticles

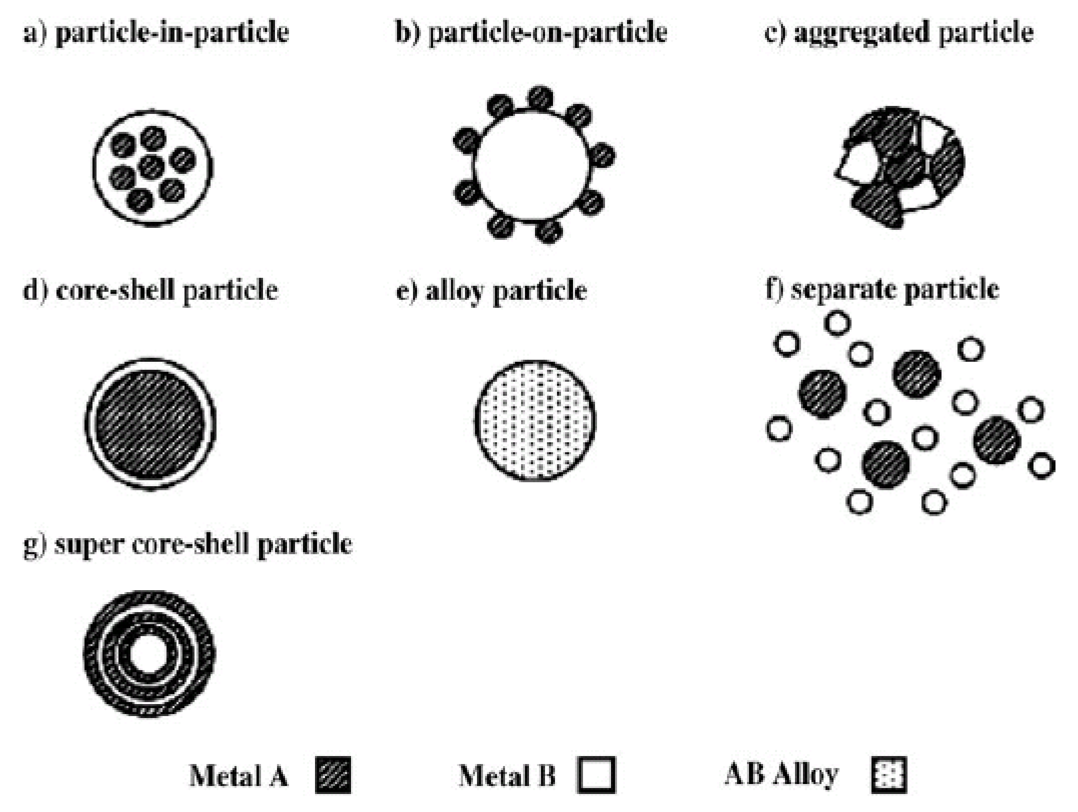

Nanocatalysis

Polymers used as metal NP supports for catalysis

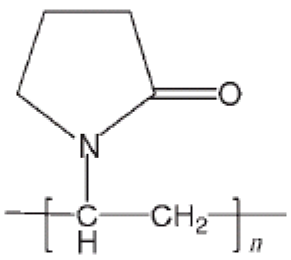

PVP

poly(vinylpyrrolidone)

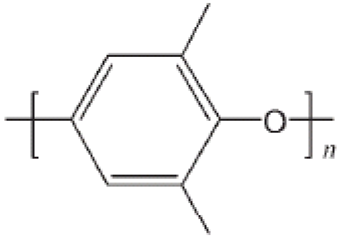

PPO

poly(2,5-dimethylphenylene oxid

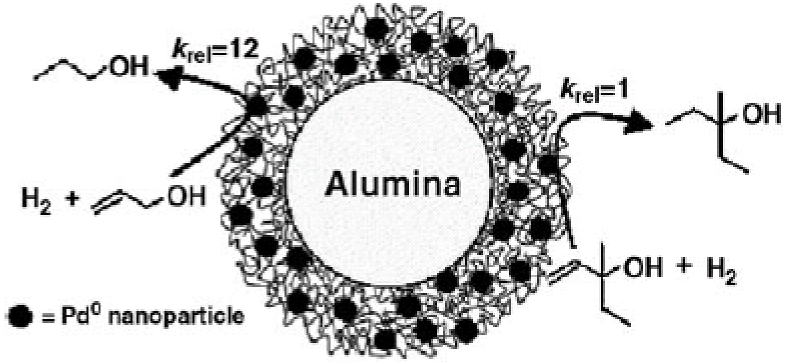

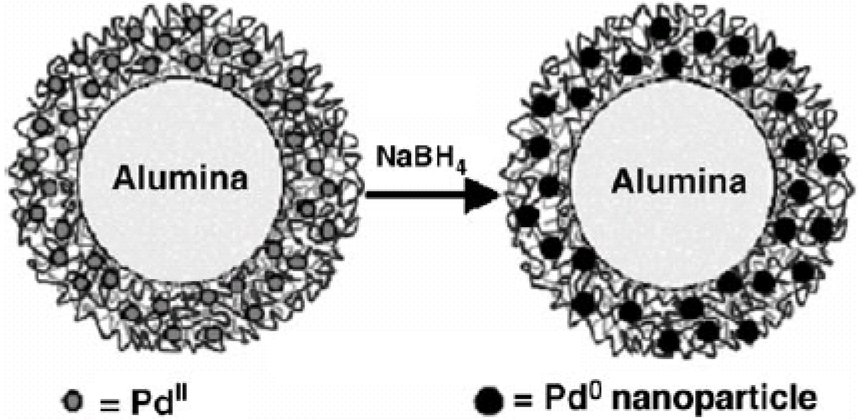

Nanocatalysis

Catalysis by nanoparticles encapsulated in PAMAM or PPI dendrimers

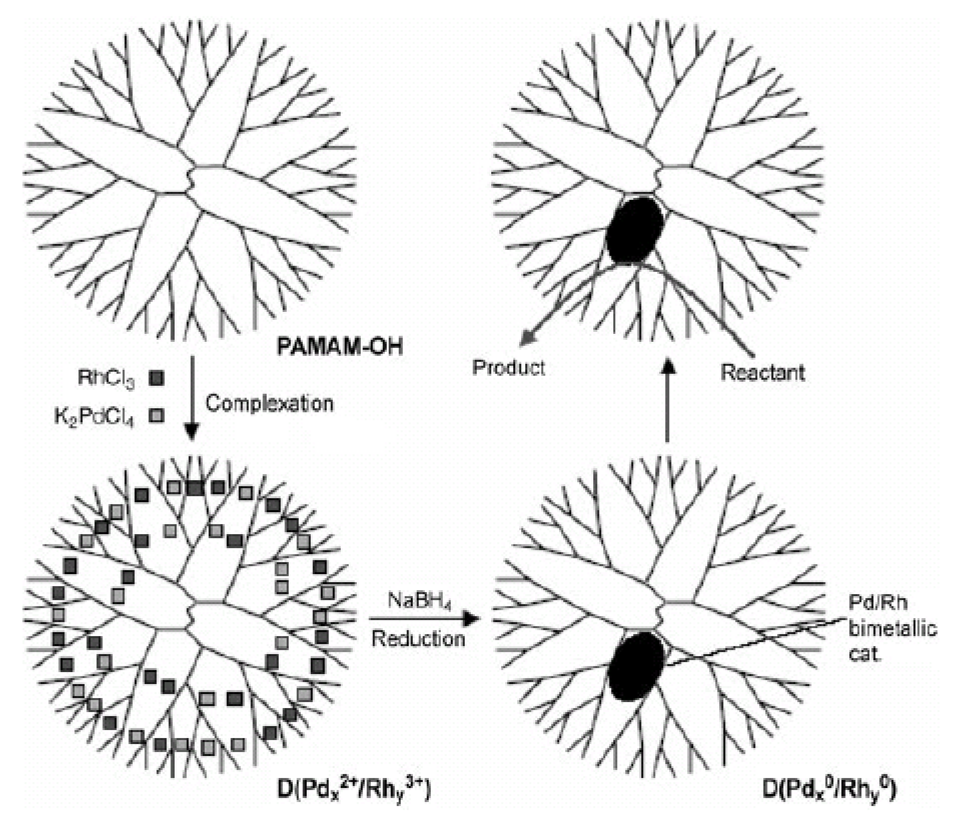

Nanocatalysis

Asymmetric heterogeneous catalysis on nanoparticles

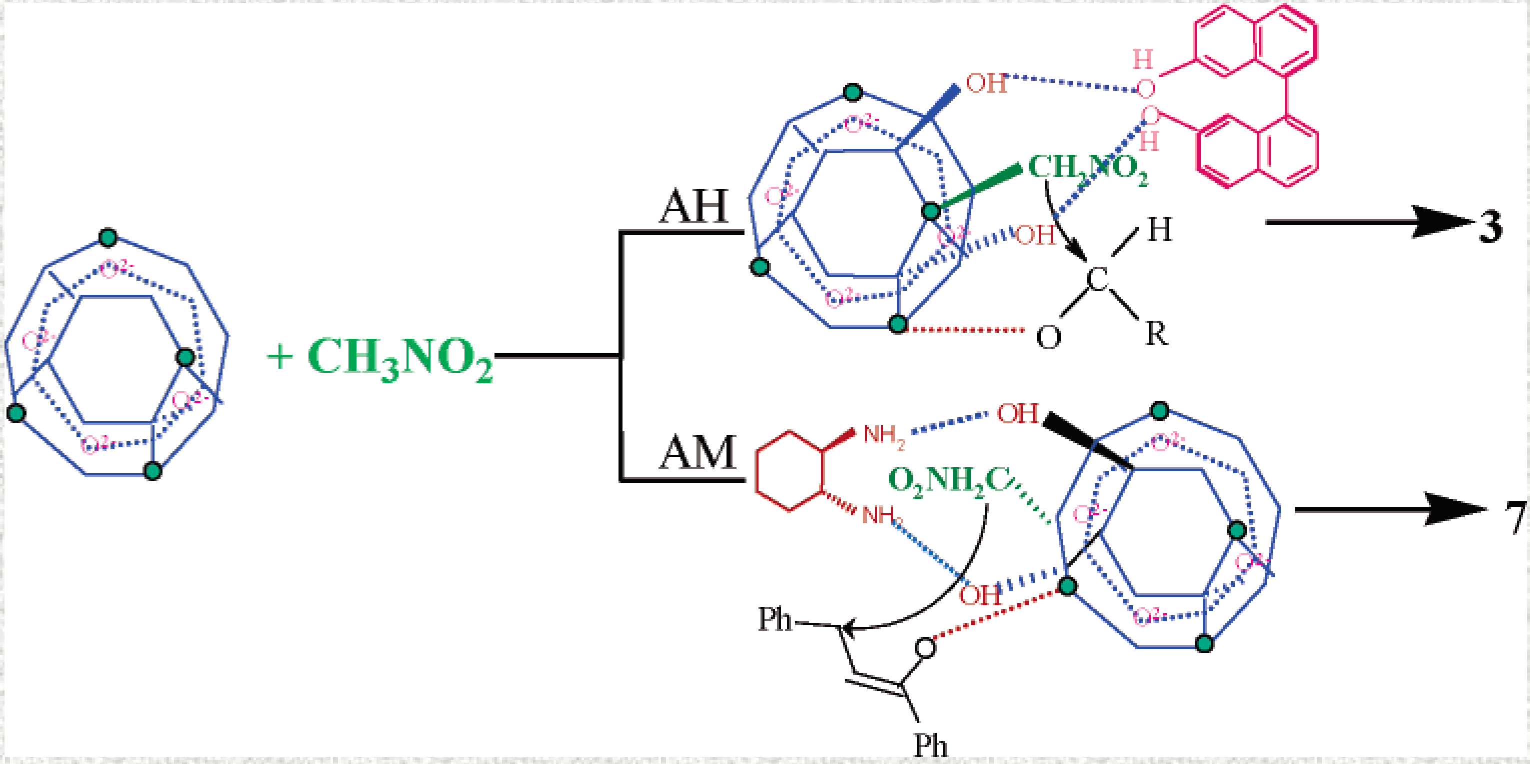

Hollow Nanoparticles

formation of hollow spheres

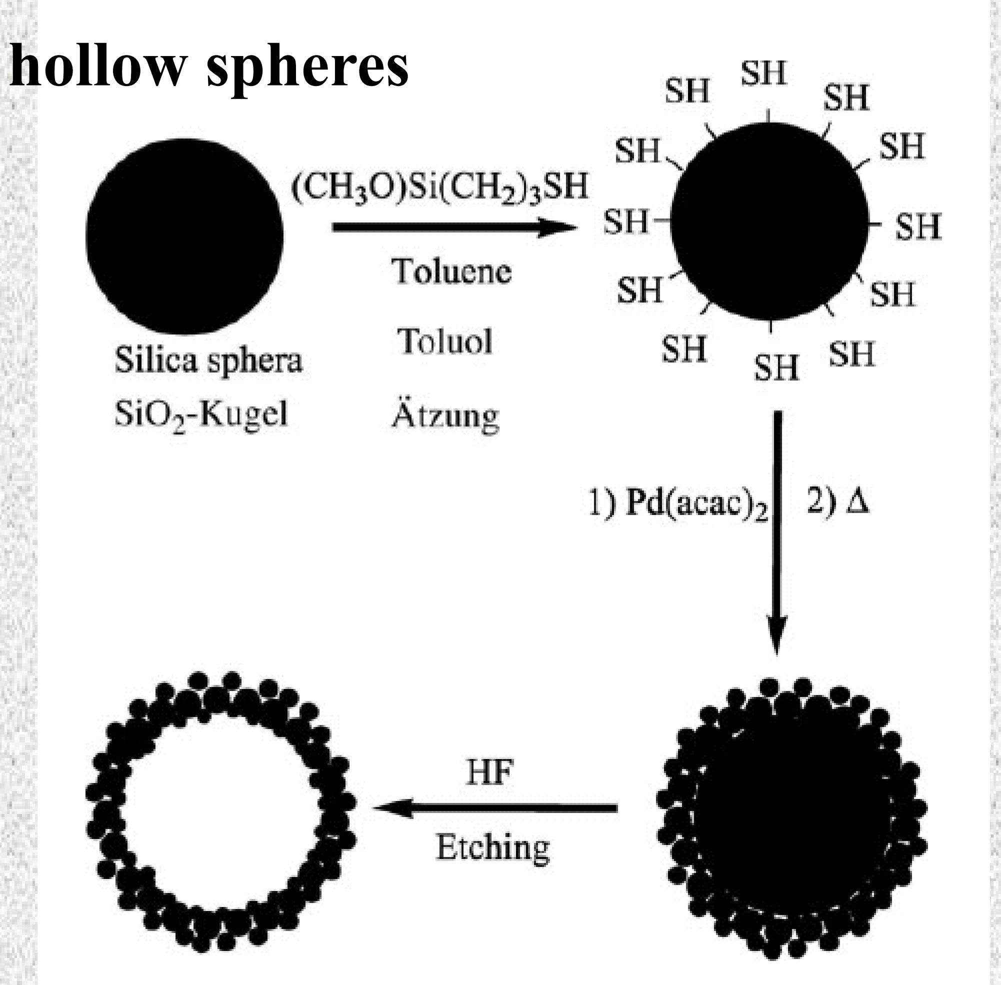

Applications

Destruction of dangerous organic compounds (organophosphates - VX, chlorinated - PCB)

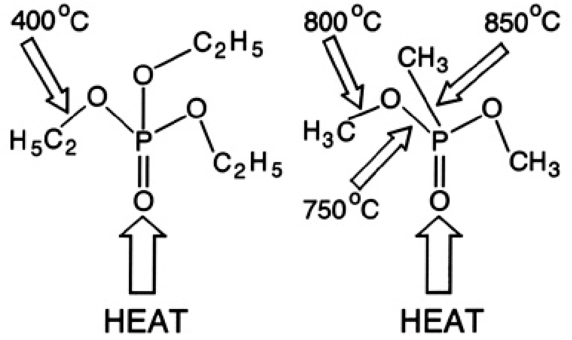

Figure 3. Cleavages of bonds in $(C_2H_5O)_3P(O)$ and DMMP under thermal decomposition condition.

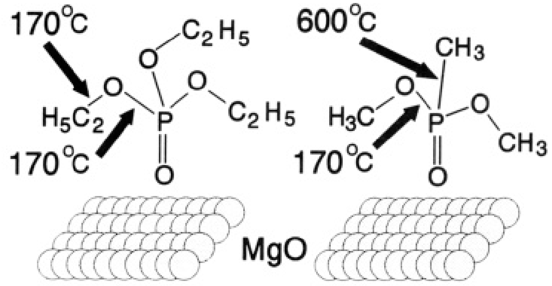

Figure 4. Cleavages of bonds of $(C_2H_5O)_3P(O)$ and DMMP on MgO.

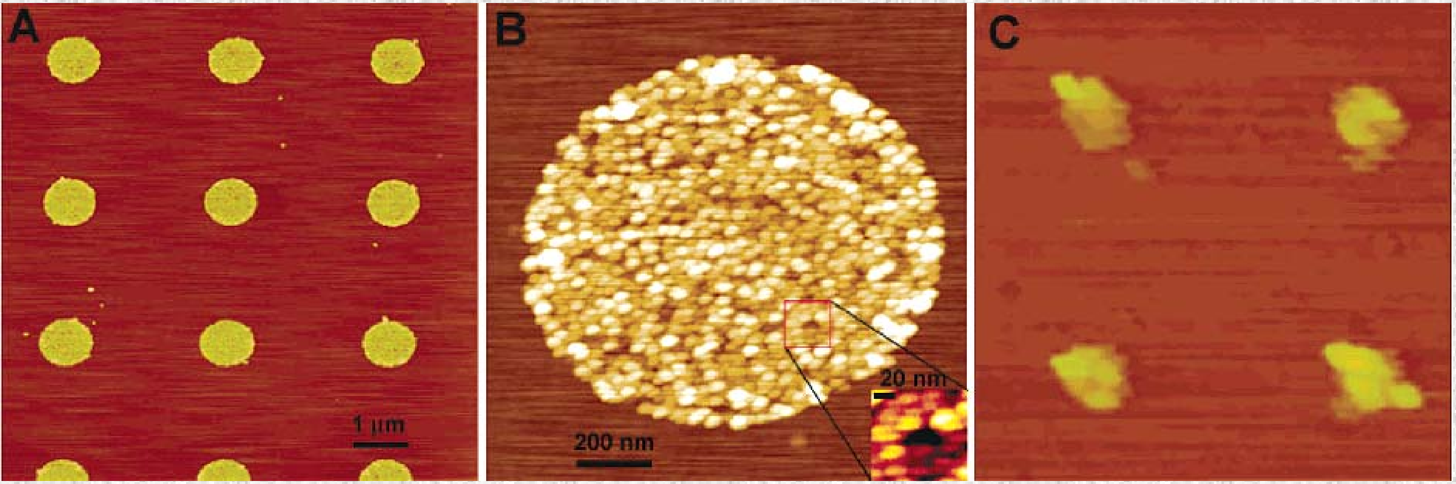

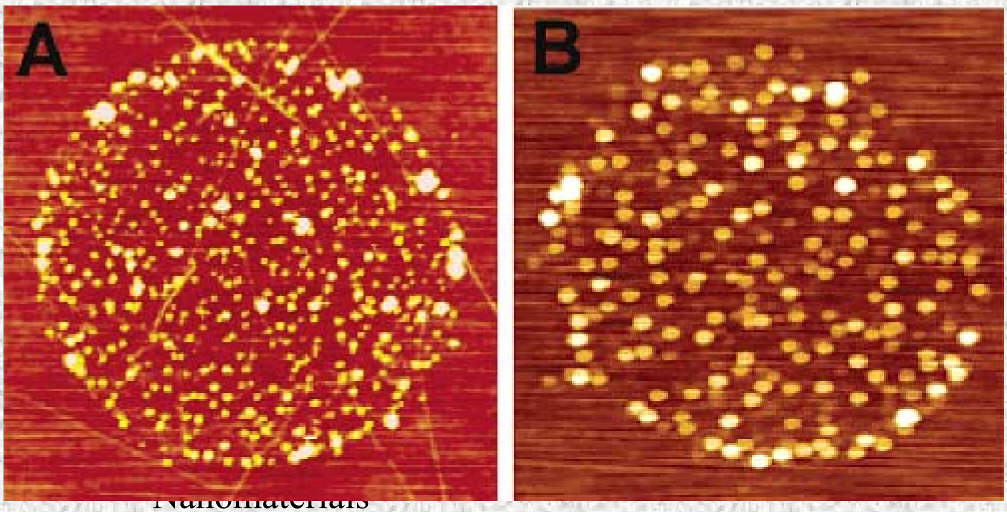

CNT growth

Nanoengine

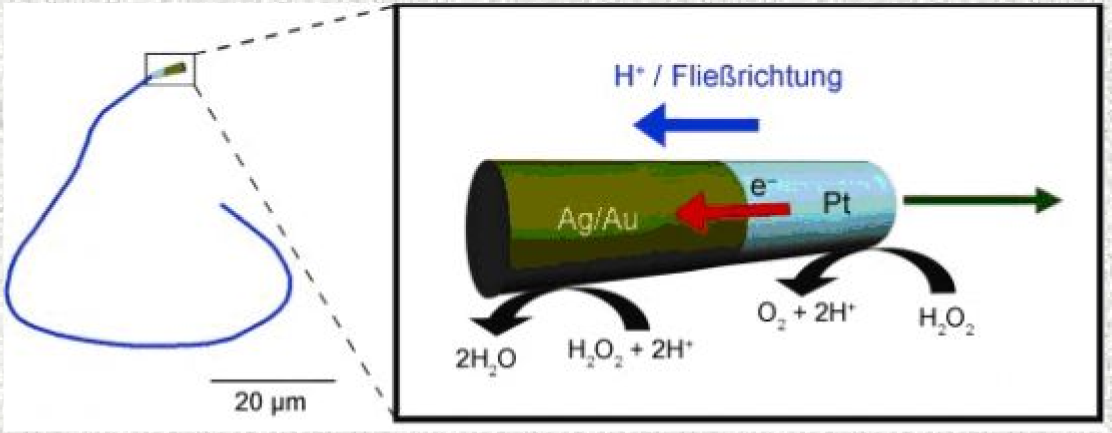

Nanoengine runs on catalytic reactions:

Pt part splits H_2O_2 to O_2 and protons H^+.

Excess electrons move to Ag/Au, reduce H_2O_2 and protons to water.

Release of O_2 causes streaming that propels the engine through the liquid

150 micrometers per second

Joseph Wang UC San Diego and Arizona State

Growth twinning in gold nano-particle

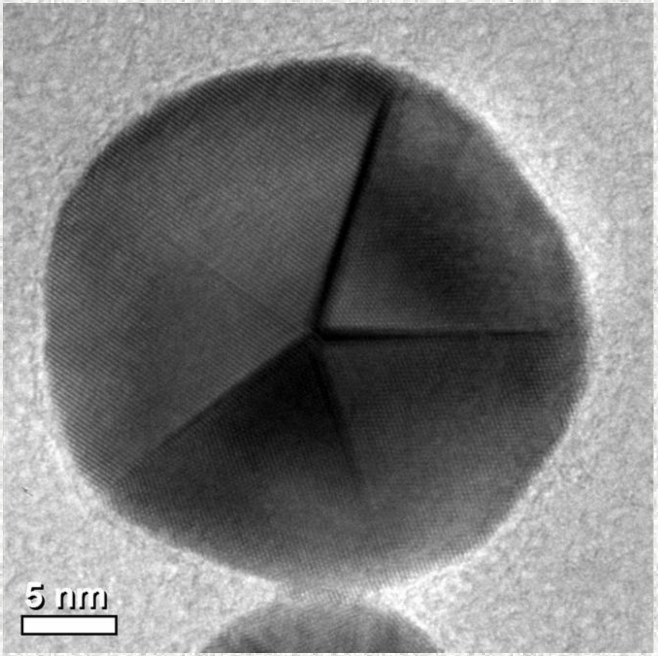

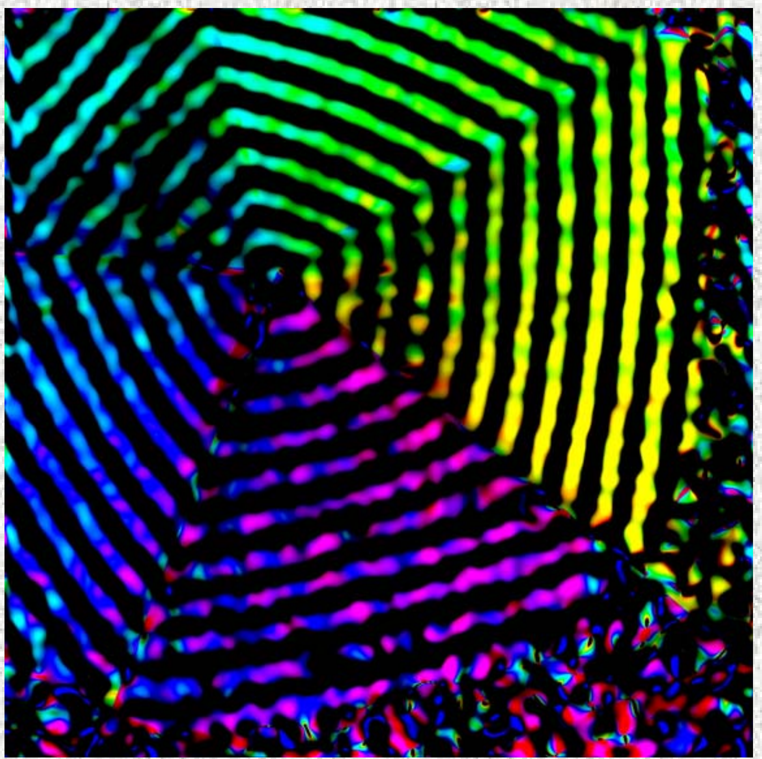

The Moiré-fringe image of a 30 nm decahedral gold nanoparticle shows five-fold rotational symmetry (black fringes) that results from serial twinning and shows the internal distortion of the atomic structure (indicated by the gradual change of the color fringes) that accommodates this unique geometry. The Moiré-fringe image was extracted from the original TEM image taken on the spherical-aberration-corrected Tecnai F20 at the CEMES-CNRS in Toulouse, France. Such particles have tremendous potential as components of nanoscale plasmonic devices for imaging, cancer therapy, and biosensing among other applications.